DESIGN AND CHARACTERIZATION OF SHELL STRUCTURE OF MICROBUBBLES USED IN ULTRASOUND IMAGING

A Thesis Submitted to
the Graduate School of Engineering and Sciences of
İzmir Institute of Technology
in Partial Fulfillment of the Requirements for the Degree of

MASTER OF SCIENCE

in Chemical Engineering

by
Elif Şeniz BÖLÜKÇÜ

December 2012
İZMİR

We approve the thesis of **Elif Şeniz BÖLÜKÇÜ**

Examining Committee Members:

_____

Assist. Prof. Dr. Sevgi KILIÇ ÖZDEMİR
Department of Chemical Engineering
İzmir Institute of Technology

_____

Prof. Dr. Mehmet POLAT
Department of Chemical Engineering
İzmir Institute of Technology

_____

Prof. Dr. Salih OKUR
Department of Materials Science and Engineering
İzmir Katip Çelebi University

13 December 2012

_____

Assist. Prof. Dr. Sevgi KILIÇ ÖZDEMİR
Supervisor, Department of Chemical Engineering
İzmir Institute of Technology

_____

Prof. Dr. Mehmet POLAT
Head of the Department of
Chemical Engineering

_____

Prof. Dr. R. Tuğrul SENGER
Dean of the Graduate School of
Engineering and Sciences

ACKNOWLEDGEMENTS

I would like to express my gratitude to all those who gave me the possibility to complete this thesis. I am grateful to my supervisor Assist. Prof. Dr. Sevgi Kılıç Özdemir whose experience, stimulating suggestions and encouragement helped me in all the time of research and writing of this thesis. I am also grateful to Assoc. Prof. Dr. Ekrem Özdemir for inspiring this thesis and for providing support and guidance. I would also like to acknowledgement Assist. Prof. Dr. Hadi M. Zareie for his all kind of support and help. I want to thank to Prof. Dr. Salih Okur for his help. I would also like to thank Tübitak for the financial support throughout the study.

I want to thank to Hasan Aydın for his help and spending his time for this study. I wish to express my thanks to my friends from the Department of Chemical Engineering sharing lovely time and their intimate behaviors. Especially, I would like to thank E. Aysu Sağdıç, Derya Köse, Sezen D. Alıcı, Tuğba Toker for all their help, warm friendship and encouragement.

Also, I am most grateful to Onur Gökbulut for his great love, infinite confidence and continuous support, thank you being in my life.

Lastly and most importantly, I would like to give my special thanks to my family whose absolute love enabled me to complete this work and unconditional support since the day I was born have made me come this far.

ABSTRACT

DESIGN AND CHARACTERIZATION OF SHELL STRUCTURE OF MICROBUBBLES USED IN ULTRASOUND IMAGING

The main goal of the study is to redesign the microbubble (MB) shell structure and investigate the interactions between the shell components in the mixed monolayers treated as a model for MBs' shell in order to improve the stability. To examine effects of emulsifier type (DSPC/PEG40 St, DSPC/DSPE-PEGn) and additional components (DSPC/PEG40 St/DSPG, DSPC/PEG40 St/DSPA, DSPC/PEG40 St/DSPE) on stability, molecular interactions and morphological properties, mixtures having various compositions were investigated by Langmuir Blodgett (LB) method and Atomic Force Microscope (AFM) and Brewster Angle Microscope (BAM).

For DSPC/PEG40 St monolayers thermodynamically analysis indicated that the attractive forces between the components in the monolayer of 30% PEG40 St were very strong. It was observed that addition of large amount of peg-grafted phospholipids (lipopolymer) increased the attractive forces between molecules in DSPC/DSPE-PEG1000 and DSPC/DSPE-PEG350 monolayers unlike DSPC/DSPE-PEG2000 monolayers. Additionally, the use of different phospholipid as an additional component such as DSPG, DSPE and DSPA in DSPC/PEG40 St mixture signified that intermolecular forces were influenced by the monolayers' compositions and polar headgroups differences. It was noticed that among the ternary mixtures consisting 70% DSPC, DSPC/PEG40 St/DSPE monolayers exhibited stronger molecular interaction than DSPC/PEG40 St/DSPG and DSPC/PEG40 St/DSPA monolayers while DSPC/PEG40 St/DSPA mixtures showed stronger interaction for mixtures composed of 50% PEG40 St. However, phase separations detected at some regions for these monolayers by BAM and AFM may affect the stability negatively. Therefore, thermodynamically analysis, BAM and AFM results should be evaluated together to assess potential MBs' shell structures.

ÖZET

ULTRASON GÖRÜNTÜLEMEDE KULLANILAN MİKROKÖPÜKCÜKLERİN ZAR YAPISININ TASARIMI VE KARAKTERİZASYONU

Bu çalışmada, mikroköpükcükleri oluşturan monotabaka zar yapısının yeniden tasarlanması ve bu yapıyı oluşturan bileşenler arasındaki etkileşimleri inceleyerek mikroköpükcüklerin stabilitesine katkı sağlanması amaçlanmıştır. Emülsiyonlaştırıcı tipinin (DSPC/PEG40 St, DSPC/DSPE-PEGn) ve zar yapıya ilave edilen üçüncü bileşenlerin (DSPC/PEG40 St/DSPG, DSPC/PEG40 St/DSPA, DSPC/PEG40 St/DSPE) stabiliteye, moleküller arası etkileşimlere ve faz davranışlarına etkileri değişik formulasyonlarda karışımlar hazırlanarak Langmuir Blodgett (LB) metodu, Brewster Açı Mikroskobu (BAM) ve Atomik Kuvvet Mikroskobu (AFM) ile incelenmiştir.

DSPC/PEG40 St karışımlarının termodinamik analizleri, molce 30% PEG40 St içeren karışımdaki moleküller arası çekici kuvvetlerin oldukça güçlü olduğunu göstermiştir. DSPC/DSPE-PEG1000 ve DSPC/DSPE-PEG350 karışımlarında, peg-bağlanmış fosfolipid miktarının arttırılmasıyla moleküller arası çekici kuvvetlerin etkisinin arttığı gözlemlenmişken, DSPC/DSPE-PEG2000 karışımları için bu durum söz konusu olmamıştır. DSPG, DSPE ve DSPA fosfolipidlerinin, DSPC/PEG40 St karışımına ilave bileşen olarak eklenmesiyle, moleküller arası itici ve çekici kuvvetlerin hem karışımın bileşiminden hem de bu fosfolipidlerin polar baş grup bölgelerindeki farklılıklardan etkilendiği gözlemlenmiştir. Molce 70% DSPC içeren üçlü karışımlar kıyaslandığında DSPC/PEG40 St/DSPE karışımı, DSPC/PEG40 St/DSPG ve DSPC/PEG40 St/DSPA karışımlarına kıyasla daha kuvvetli moleküler etkileşim göstermişken, molce 50% PEG40 St içeren karışımlarda ise DSPC/PEG40 St/DSPA karışımındaki moleküller arası ilişkiler daha kuvvetlidir.Ayrıca, BAM ve AFM ile yapılan analizlerde bu karışımların yüzeylerinde faz ayrılıkları gözlemlenmiştir.Bu farklılıklar monotabakanın stabilitesini olumsuz yönde etkileyebilir. Bu sebepten dolayı mikroköpükcüklerin zar yapısının stabilitesini arttırmak için hem termodinamik analiz sonuçları hem de BAM ve AFM görüntülerinin sonuçları dikkate alınmalıdır.

TABLE OF CONTENTS

LIST OF FIGURES

Figure **Page**

LIST OF TABLES

Table **Page**

CHAPTER 1

INTRODUCTION

Ultrasound (US) is the most widely used medical imaging technique in the world and in recent years the use of ultrasound as a diagnostic imaging method has continued to grow (Klibanov 1999, Schutt, Klein et al. 2003).For instance in the United State only 7000 computed tomography and 5000 magnetic resonance imaging instruments are installed compared with 75000 ultrasound instruments installed. Nearly 100 million ultrasound scan of the heart, vascular system and abdominal organs are obtained worldwide each year (Schutt, Klein et al. 2003). Ultrasonography is non-invasive, low risk, low cost, portable and real-time imaging technique and it abstains hazardous ionizing radiation. Medical ultrasound imaging is based on the pulse-echo principle. The working principle of this technique is that an ultrasound transducer is placed on the skin and it broadcasts ultrasound pressure wave pulses partially reflected or scattered by the interfaces between different tissues or structures in the body, then the transducer captures some of the reflected sound which return to the transducer. Finally these signals are converted to electrical pulses and digitized by imaging system (Hernot and Klibanov 2008). Although the imaging of blood and blood flow within organs is important to observe differences between healthy and abnormal tissues, blood which is liquid phase material with low compressibility does not scatter ultrasound strongly. Moreover, the normal spleen, liver and kidney have similar acoustic properties to many tumors. The ultrasound distinctness of normal and abnormal tissues is not detected clearly due to these limitations (Wang, Moser et al. 1996, Schutt, Klein et al. 2003, Hernot and Klibanov 2008).Therefore ultrasound imaging can be improved by the use of contrast agents which are injected intravenously and reflect ultrasound waves powerfully. Ultrasonic contrast agents can be characterized as colloidal particles composed of biocompatible materials. Gas-liquid emulsions (microbubbles), liquid-liquid emulsions (nanodrops), liposomes have been used as ultrasound contrast agents. The quality of acoustic backscatter depends on the intrinsic properties of the biocolloid. Also, the density distinctions between the biocolloid and surrounding tissue and the compressibility of the biocolloid contribute to the acoustic backscatter. The commonly

used nanoparticles used as ultrasound contrast agents are composed of a solid of a liquid. Solid and liquid nanoparticles are incompressible materials which produce much less backscattered signal to transmitted ultrasound and do not oscillate strongly with passing acoustic wave, so they are less echogenic than gas microbubbles (Sirsi and Borden 2009, Borden, Qin et al. 2010).

Small gas filled microspheres with a size range of 1-8 μm, so-called microbubbles (MBs), are used commonly as contrast agents (Hernot and Klibanov 2008).Their specific acoustic properties make microbubbles excellent contrast agents for ultrasound imaging. Microbubbles are extremely echogenic, biocompatible and economical thus they are an ideal ultrasound contrast agent. The gas core of microbubble has low density and is highly compressible. Due to gas core properties microbubbles can shrink and expand with applying acoustic wave and generate a very strong echo. Recently, MBs consisting of a gaseous core coated by a thin shell are preferred as effective ultrasound contrast agents, because they can move unobstructed through the vasculature and are highly echogenic and improve the diagnostic capabilities of ultrasound imaging. They react strongly to ultrasonic pressure waves and are highly reflective when exposed to an ultrasound field. Materials have characteristic acoustic impedances defined as the product of the speed of the sound in material and its physical density. The degree of reflection at interface and the intensity of the sound wave rely on the distinctions in acoustic impedance between the two adjacent materials. The acoustic impedances of gases are lower than water, soft tissue and bone. The higher differences of acoustic impedances create the stronger reflected sound wave. Therefore the acoustic backscatter of MBs are greater than other structures, MBs generate good signals and a contrast media in the entire blood pool. Moreover, at moderate excitation pressures they exhibit a non-linear response which enables their scattered signal to be clearly distinguish from tissue (Sirsi and Borden 2009). It makes the MBs useful as contrast agents for ultrasound imaging (Albrecht and Hohmann 2004, Hernot and Klibanov 2008).The use of these contrast agents enhance the quality of the images and increase the contrast between pathologic and normal tissues, so it provides the meaningful information (Klibanov 1999, Hernot and Klibanov 2008).

Apart from their ultrasound imaging utility, MBs has become excellent potential as ultrasound-facilitated drug and gene delivery vehicles (Dijkmans, Juffermans et al. 2004, Unger, Porter et al. 2004, Lentacker, De Smedt et al. 2009, Sirsi and Borden 2009). For this purpose ideal MBs which are suitable to drug and gene targeting should

be obtained. The ideal MBs ought be highly echogenic, nontoxic, stable for a long time and avoid the risk of embolism (Wang, Moser et al. 1996, Liu, Miyoshi et al. 2006) In addition to bubble size is critical parameter that must be controlled because the resonance frequency of bubbles is directly related to its size. Although larger bubbles show better scattering intensity, the current accepted sizes are in the range of 1-8 μm and they shouldn't exceed 8 μm to pass the capillaries (Schutt, Klein et al. 2003).

Ultrasound applications by using these contrast agents needs continuous infusion of stable MBs over several minutes. The stability of MBs' shell structure is very important, from the point of view of MBs to persist during both store and in vivo applications obviously (Klibanov 1999). Encapsulation of MBs with a shell which enhances stability against gas loss and prevents microbubble coalescence is essential to prolong their lifespan. Furthermore, this shell enables more standard size distribution and the thickness of the shell is crucial for microbubbles acoustic backscattered signal, thin shell can increase the acoustic properties of microbubbles (De Jong, Hoff et al. 1992, Hernot and Klibanov 2008). The hardness of the bubbles, their resistance to rupture in the ultrasound pressure field is determined by the nature of the shell.

The MBs' shell can be manufactured from biocompatible materials, such as protein, biocompatible polymer or phospholipid .However, previously studies exhibited that MBs coated with polymer shells demonstrated gas loss due to formation of cracks on the shell. Additionally, it was observed that the protein coated MBs tend to adhere into vasculature (Borden, Kruse et al. 2005, Hernot and Klibanov 2008).Conversely to these behaviors, phospholipid coated MBs did not exhibit any cracking during ultrasound pulsing and increased the stability of MBs .Therefore, phospholipids are commonly preferred as shell component for current biomedical applications (Kim, Kim et al. 2004, Lozano and Longo 2009, Tinkov, Bekeredjian et al. 2009).

Although microbubbles' shell structure is very crucial for currently ultrasound applications and promising applications a few study has been applied about the effect of shell composition and their phase behavior. Microbubbles' shells need to be redesigned and characterized in order to improve the microbubbles stability because the stability depends on molecular interaction between the components in the shell structure (Xing, Ke et al. 2010). Therefore, the objective of our study to investigate the molecular interactions of microbubble shell components and obtain new insight about shell stability. For this purpose phospholipids having same hydrocarbon chain length were added to the traditional MB formulation composed of DSPC and PEG40 St. DSPE-

PEGn lipopolymers (DSPE-PEG350, DSPE-PEG2000, DSPE-PEG1000) were also used as emulsifier in lieu of PEG40 St. The effect of emulsifier type (DSPC/PEG40 St, DSPC/DSPE-PEGn) and the effect of additional phospholipid capable of H-bonding component in the shell structure (DSPC/PEG40 St/DSPG, DSPC/PEG40 St/DSPA, and DSPC/PEG40 St/DSPE) on microbubble stability were examined. The reason behind choosing phospholipids for main shell component is that biocompatibility of microbubbles is not an issue since phospholipids are the main constituents of our cell membrane. In addition, PEG40 St and lipopolymers were preferred because they prevent microbubbles from coalescence, undesirable adsorption of blood plasma proteins, phagocytosis and also promote the shell formation.

A monolayer at the gas-liquid interface is similar to the gas-liquid interface in the microbubbles and the monolayer phase properties can be examined the best by measuring the surface pressure as a function of the area of the water surface available to each molecule using Langmuir Blodgett (LB) method (Moghaddam, Ali et al. 2011). Therefore, in present study, monolayer behaviors of the shell components and interactions between them were investigated by Langmuir Blodgett (LB) method which can provide important information on molecular interactions between microbubble shell components and this information may be used to improve microbubble stability (Wang, Moser et al. 1996, Shen, Powell et al. 2008, Xing, Ke et al. 2010). In addition, BAM and AFM were used as the techniques complementary to the surface pressure-area isotherm measurements to investigate the monolayer characteristics of microbubble shell. (Deleu, Nott et al. 2001, Takamoto, Lipp et al. 2001, Connell and Smith 2006). Also, Brewster Angle Microscope (BAM) which is based on Brewster Angle principle at the air-water interface and non-impurity method unlike Fluorescent Microscope was used to observe morphological properties and phase behavior of the monolayers in micro level (Kubo, Adachi et al. 2001, Arnold, Cloutier et al. 2005, Brandal, Viitala et al. 2007, Lucero, Rodríguez Nino et al. 2008, Risovic, Frka et al. 2011).On the other hand, AFM gives information about the organization of molecules in nano level (Deleu, Nott et al. 2001, Takamoto, Lipp et al. 2001, Connell and Smith 2006)

This thesis contains five chapters. In chapter one, addition to general introduction for ultrasound imaging technique, limitations of this method, microbubbles used as ultrasound contrast agents and also the aim of this thesis are introduced. In chapter two, a literature survey on microbubbles and Langmuir Blodgett (LB) monolayers are presented. In chapter three, the chemicals used in this study, sample

preparation procedure and characterization methods for these samples, such as Langmuir Blodgett (LB), Brewster Angle Microscope (BAM), Atomic Force Microscope (AFM) are explained in details. In addition, the analysis of the surface pressure-molecular area isotherms obtained by LB method is declared. In chapter four, the effect of emulsifier type and the effect of additional component on microbubble shell stability are presented and discussed. Finally, the conclusions are given in chapter five.

CHAPTER 2

LITERATURE SURVEY

2.1. Microbubbles as Ultrasound Contrast Agent

Microbubbles (MB) are small gas filled microspheres having specific acoustic properties which made them useful as a contrast agent in ultrasound imaging (Dijkmans, Juffermans et al. 2004, Hernot and Klibanov 2008, Tinkov, Bekeredjian et al. 2009).The development of microbubble ultrasound contrast agent began as the result of an accidental discovery by Dr Claude Joyner in the late 1960's. An M-mode echocardiogram was being carried out at the same time as a study of cardiac output was being made, using injection of indocyanine green dye into the patient's left ventricle. A temporary increment in the ultrasound signal from the ventricle was detected, after each injection of dye. In the beginning, it was thought that the contrast enhancement was because of the nature of dye. However, it was found that the same effect was noticed with other fluids, including saline (Feigenbaum, Stone et al. 1970). Gramiak and Shah showed that agitated saline improved the ultrasound echo signal in the human ascending aorta and cardiac chambers, probably minibubbles present in the medium reflected the ultrasound. Since this first breakthrough, microbubbles have developed as an ultrasound contrast agent for clinical use (Dijkmans, Juffermans et al. 2004, Stride and Edirisinghe 2008).

The first generation microbubbles were simple air bubbles. However, they disappeared in only a few seconds after intravenous administration since the solubility of air in blood is high. In addition, these MBs could not pass capillaries due to their large size. Therefore, if they injected intravenously, they could not reach the left heart and these first generation MBs were not useful to opacify the left cardiac chamber. The improvement of air bubbles was achieved by stabilizing them with a thin shell. These second generation MBs had smaller size distribution due to effect of thin shell, so they were able to pass through the lungs and reached the left heart and other organs following intravenous application. Further, to increase stability of MBs, the air core was replaced by gases having heavy molecular weight and low solubility in blood such as

perfluorocarbons or sulfur hexafluoride. The lifespan of microbubbles within circulation was prolonged to more than 15 minute with this change (Dijkmans, Juffermans et al. 2004, Tinkov, Bekeredjian et al. 2009).The development of more stable MBs and specific physical characteristic of MBs broadened the scope of MB application beyond ultrasound imaging and ultrasound also became an interest as a therapeutic tool. High quality ultrasound images can be obtained with effective stable microbubbles, so as diagnostic performance and confidence will increase and needed time for diagnosis will decrease. Additionally, ultrasound irradiation destroys MBs and this destruction phenomenon can be used for targeted drug and gene delivery. The ultrasound field can be focused at the targeted tissues and organs, so selectively treatment can be enhanced. The drug can be either attached or included in the shell and circulation of the microbubbles can be monitored by ultrasound imaging. When the microbubbles reach to the target side, the bubbles are burst into fragments by increasing ultrasound intensity. The applied acoustic energy converts to cavitation energy and the cavitation energy makes the cells and tissues permeable to the drug. After this treatment, the cells and tissues recover (Lentacker, De Smedt et al. 2009, Tinkov, Bekeredjian et al. 2009, Tinkov, Coester et al. 2010).Drug-loaded microbubbles will help to increase the benefit of drug action in the diseased site while reducing undesirable side effects in the healthy tissues and improve the therapeutic efficient compared with free drugs. Currently, the potential use of MBs in gene and drug delivery has been studied by research groups worldwide (Schutt, Klein et al. 2003, Tinkov, Bekeredjian et al. 2009).

2.1.1. The Ideal Microbubble

Ideality of microbubbles is very important for efficiency of ultrasound imaging and future applications mentioned above. For ideality, MBs' size is a critical parameter which must be controlled during ultrasound applied. The larger MBs scatter the ultrasound strongly, because the intensity of scattered ultrasound is proportional to the sixth power of the radius of the bubble. Nevertheless, for in vivo applications the acceptable upper size limit is determined by the need for MBs to pass through capillaries. Therefore, their accepted sizes are in the range of 1-8 μm. Also, the bubbles tend to growth with aggregation and the aggregation in the circulation must be avoided. For effective and convenient examination of a patient, the MBs should be stable enough

in the systematic circulation and in vivo half life of bubbles is a major requirement. In addition to these, elasticity is needed to maximize resonance and ideal MBs should be nontoxic for intravenous injection (Schutt, Klein et al. 2003, Liu, Miyoshi et al. 2006, Pancholi, Farook et al. 2008).

As mentioned that a typical microbubble consists of a gaseous core that is coated by a thin shell. Air, perfluorocarbons or sulfur hexafluoride can be used as gaseous core while the thin shell which plays important role to obtain ideal microbubble can be composed of protein, surfactant, polymer or lipid (Borden and Longo 2002, Hernot and Klibanov 2008).The microbubble shell forms a protective layer to prevent gas escaping from the core as well as to avoid coalescence of microbubbles, so encapsulation of MBs with a shell is required to stabilize the MBs. In addition, the resistance of MBs to rupture in the ultrasound field and their stiffness are improved by the composition of shell. The backscatter ultrasound signals from MBs are dependent on the size and the thickness of microbubbles. Therefore, to obtain good signal for ultrasound applications, appropriate microbubble shell can produce a more standard size distribution and flexible thin shell which enables resonance of microbubble under acoustic field. Obviously, the stability of the shell is crucial to for appropriate stability of microbubbles on the shelf and in vivo applications (Klibanov 1999, Hernot and Klibanov 2008).

2.1.2. The Types of Microbubbles

2.1.2.1. Protein Coated Microbubbles

The shell components of microbubbles determine the type of microbubbles. The albumin protein was used for coating of early produced microbubbles which could pass the lung capillaries and provide contrast in the left ventricle of the heart. The first commercial albumin coated microbubble formulation was Albunex. Albunex was stable upon refrigeration for at least two years. Following Albunex, another albumin formulation named as Optison was developed encapsulating a perfluorocarbon gas core. The low solubility of the perfluorocarbon gas provides much longer circulation persistence in vivo (Sirsi and Borden 2009).Currently, several proteins different from albumin have been used for coating microbubbles, because the amphipathic nature of many proteins makes them highly surface active. For instance, *Cavalieri and coworkers*

(Cavalieri, Ashokkumar et al. 2008) were used lysozyme to form microbubbles while a mixture of albumin and avidin were preferred by *Korpanty et al* (Korpanty, Grayburn et al. 2005). However, the protein shells tend to be rigid and less stable under ultrasound, because it was not a good barrier against gas diffusion. Therefore, protein coated microbubbles disappeared from the bloodstream within seconds after application and their lifespan are low. Moreover, the protein coated MBs tend to adhere into capillary which is also disadvantage for in vivo applications (Hernot and Klibanov 2008, Sirsi and Borden 2009).

2.1.2.2. Polymer Coated Microbubbles

The polymer microbubbles are stabilized by a thick shell composed of cross-linked or entangled polymeric species. In the literature, the microbubbles coated by a polymer shell were studied by some of authors. A new polymer shelled microbubble was reported by *Wheatley et al*, the shell formed by using the ionotropic gelation of alginate but the microbubble diameters were too large for intravenous injection (Wheatley, Schrope et al. 1990). Although later microbubbles formed by biodegradable copolymers poly(D,L-lactide-co-glycolide) (PLGA) showed smaller diameter, their lifetime were short (Cui, Bei et al. 2005). Also, *Bjerknes et al* produced microbubbles encapsulated by a proprietary double-ester polymer with ethylidene units and the polymer shell was thick (Bjerknes, Braenden et al. 2001). Unlike expected for polymeric shell that may increase bubble resistance to pressure, the nature of polymer shell stiffer than either protein and lipid coatings reduces the echogenicity of the MBs. The polymer coated microbubbles can not oscillate actively due to their thickness, so even at low ultrasound intensity the shell cracks and encapsulated gas escapes (Schutt, Klein et al. 2003, Hernot and Klibanov 2008, Stride and Edirisinghe 2008, Chlon, Guédon et al. 2009).

2.1.2.3. Surfactant Coated Microbubbles

To generate stabilized microbubbles, Span-type and Tween-type surfactants were employed by *Wang et al and by Singhal et al* (Singhal, Moser et al. 1993, Wang, Moser et al. 1996). Some mixtures of Span-type and Tween-type surfactants at certain

conditions were able to form stable microbubbles after the Span/Tween solutions were sonicated in the presence of air. Span-type surfactant alone can not form stable microbubbles without an anticoalescence agent and also Tween-type surfactants alone are not able to form stable microbubbles due to insufficient surface activity to reduce surface tension. It was established that Span60/Tweeen80 and Span40/Tweeen40 mixtures can be used to produce stable microbubbles whereas Span80/Tweeen40 mixtures were not suitable to form stable microbubbles as Span80 has insufficient surface activity and the hydrocarbon chain exhibits large steric effects owing to an ethylene group in the hydrocarbon chain (Singhal, Moser et al. 1993, Wang, Moser et al. 1996). Additionally, stable microbubbles formed from sucrose stearate (mono-and di-ester) formed by a blending process in 75%wt glucose syrup were reported by *Dressaire et al* (Dressaire, Bee et al. 2008). These microbubbles were stable in suspension for over a year and remarkable polygonal domains were noticed on their surface. However, these microbubbles were not stable upon dilution, so their biomedical utilities were limited. The study demonstrated that the importance of surface heterogeneity with regard to microbubble stability (Sirsi and Borden 2009).

2.1.2.4. Lipid Coated Microbubbles

For biomedical imaging and drug delivery lipid coated microbubbles are the most interesting and useful formulations. The lipid shell of a microbubble is bioinspired, because it can mimic the stability and compliance of lung surfactant. In worldwide there are several commercial lipid coated microbubbles including are approved for clinical use (Sirsi and Borden 2009). Definity was the first phospholipid-shelled fluorocarbon gas filled microbubble received FDA (Food and Drug Administration) approval. These bubbles' shell were composed of methyl-poly(ethyleneglycol) dipalmitoylphosphatidylethanol amine (MPEG5000DPPE), (DPPC) dipalmitoyl phosphatidylcholine and a small amount of negatively charged dipalmitoylphosphatidic acid (DPPA). Sonovue was developed as a contrast agents and sulfur hexafluoride was used in the gas core. The shell materials of Sonovue were distearoyl-sn-glycero-3-phosphocholine (DSPC), palmitic acid (PA) and dipalmitoylphosphatidylglycerol (DPPG). Sonovue microbubbles have a shelf life of two years at room temperature (Schutt, Klein et al. 2003, Tinkov, Bekeredjian et al.

2009, Borden, Qin et al. 2010). Currently, lipids are used as the main components to make bubbles, since use of phospholipids as shell component increases biocompatibility of microbubbles due to the cells consisting of phospholipids and they can decrease the surface tension stabilizing the microbubbles (Xing, Ke et al. 2010). Also, lipid shells have several advantages due to specific structural properties of phospholipids. Phospholipids have two hydrocarbon chains (acyl chains) and a polar headgroup attached to the glycerol. They spontaneously are able to self-assemble into highly ordered monolayer at the air/water interface, such that their hydrophilic headgroups contact with the water while the hydrophobic parts face to the gas (Petty 1996, Sirsi and Borden 2009). Therefore, the lipid can build up spontaneously a shell around gas core. In addition to these, the attractive hydrophobic and van der Waals interactions between the tightly packed acyl chains made the lipid monolayer highly cohesive. Hence, stability of the shell can be provided by high cohesiveness and rapid dissolution is prevented. Additionally, the lipid molecules are held together by weak physical forces without chain entanglement and the physical forces make the shell compliant to expansion and compression under ultrasound field. For that reason, lipid MBs do not exhibit sonic cracking during the ultrasound pulse and reduce the gas permeability which made them highly echogenic and ideal for clinical applications compared to polymer coated microbubbles. Also, by incorporating different lipid headgroup species or post-production bioconjugation lipid coated microbubbles can be easily functionalized for drug delivery. Therefore, the lipid coated microbubbles have great potential for versatile platform technologies (Borden, Kruse et al. 2005, Hernot and Klibanov 2008, Sirsi and Borden 2009). In the literature, some of authors studied about microbubbles' shell structure to improve the stability of microbubbles for future applications. Generally, saturated diacyl phosphatidylcholine (DinPC; where n equals to the number of carbons per acyl chain) is preferred as main component in the shell, since the endothelial cells are mainly composed of these phospholipids and zwitterionic phosphatidylcholine modified surfaces resistive to cell adhesion and are able to reduce the clot formation under physiological conditions (Kim, Kim et al. 2004, Kyun Kim, Kim et al. 2005, Pu, Borden et al. 2006). Although it lowers interfacial tension, adds rigidity and impedes gas escape, a second component also called as anticoalescence agent is necessary to form microbubble and to prevent the microbubbles from coalescence. This component should be surface active material that participate in the interfacial region of microbubbles and consist of hydrophillic groups which remain in

the aqueous environment outside the microbubbles to prevent microbubbles interaction (Wang, Moser et al. 1996). Commonly, PEG 40 St (Polyethylene glycol 40 stearate) comprising a hydrophilic poly-ethylene glycol and that is covalently bound to a hydrophobic stearate anchor is used as anticoalescence agent for lipid coated microbubbles, because it prevents the bubbles against coalescence, undesirable adsorption of blood plasma proteins and phagocytosis, and improves blood compatibility and microbubble stability. Therefore, lipid coated microbubble production has been performed mostly using DinPC and PEG40 St components (Kim, Kim et al. 2000, Borden and Longo 2002, Borden, Pu et al. 2004, Borden, Martinez et al. 2006, Swanson, Mohan et al. 2010).

The length of hydrocarbon chain of phosphatidylcholine affects the stability of microbubbles. The oxygen permeation resistance of microbubbles composed of phospholipids with different hydrocarbon chain length (DinPC; n=16, 18, 20, 22, 24) and PEG40 St were examined by *Borden et al* and *Pu et al*. It was detected that with increasing the chain length resistance of the microbubles to gas permeation increased (Borden and Longo 2004, Pu, Longo et al. 2005).Similarly, *Swanson et al* compared oxygen filled microbubbles encapsulated using mixtures of DSPC(n=18)/PEG40 St and DPPC(n=16)/PEG40 St at 9:1 molar ratio. Over the three week testing period the DPPC-based microbubbles lost almost all of their gas while DSPC kept its gas for a far longer period of time and still contained more than 30 vol % gas at the end of testing suggesting that the stability of DSPC coated microbubbles were higher than that of DPPC (Swanson, Mohan et al. 2010). Longer chains enhance van der Waals and hydrophobic interactions between constituent lipids in the monolayer shell and thus increase the overall cohesiveness of the shell. This increment in cohesiveness provides greater stability for microbubbles during ultrasound applied, so stiffness of the shell increases and gas permeability from the shell decreases (Borden and Longo 2002, Borden, Kruse et al. 2005, Borden, Qin et al. 2010). Also, *Cox et al* studied about the effect of unsaturated hydrocarbon chain on stability. DOPC-coated and DSPC-coated microbubbles were examined under different ultrasound pulses. DOPC-coated microbubbles ultimately vanished whereas DSPC coated microbubbles persisted even at higher pulses (Cox and Thomas 2010).

The study of monolayer behaviors of microbubbles' shell components by Langmuir Blodgett (LB) method can provide important information on molecular interactions between the shell components, since the lipid shell has a similar structure to

a Langmuir monolayer at gas/liquid interface. Thus, this information extracted from the measurements may be used to redesign MB shell (Wang, Moser et al. 1996, Shen, Powell et al. 2008, Xing, Ke et al. 2010). The monolayer behaviors of phospholipids having different hydrocarbon chain in the shell were investigated with LB method and it was observed that collapse pressures of phospholipids which indicate deformation pressure of monolayer raised with increasing hydrocarbon chain length up to phospholipid having 18 carbons in acyl chain, then they decreased (Borden and Longo 2002). In another work, the effect of PEG40 St on the phase behavior of mixed monolayers including expanded or condensed phase lipid and interactions between the shell components was studied *by Borden et al* (Borden, Pu et al. 2004).The pure phospholipids having 12 ($Di_{12}PC$) and 14 ($Di_{14}PC$) carbon in acyl chains and pure PEG40 St displayed expanded phase behavior, $Di_{16}PC$ showed both of expanded and condensed phase while only condensed phase behavior was noticed for $Di_{18}PC$, $Di_{20}PC$, $Di_{24}PC$. Therefore, their mixed monolayers with PEG40 St behaved differently at the air/water interface. Moreover, generally it was assumed that shell components of microbubbles uniformly distributed over the microbubble surface. On the contrary, they detected that there were phase separation over MBs' surfaces which consist of PEG40 St and condensed phase monolayer-forming lipids (Borden, Pu et al. 2004).

The microbubble shell can have a dramatic effect on microbubble properties. The concentration changes of MBs' shell components which were DSPC and PEG40 St were investigated *Talu et al.* It was detected that increasing the concentration of lipid and emulsifier or emulsifier alone reduced the coalescence of the microbubbles, thus the coalescence of the microbubbles strongly depended on the concentration of the lipid and emulsifier (Talu, Lozano et al. 2006). Also, *Kim et al* examined mixed monolayer of DPPC/ PEG lipid and they observed that the adhesion of platelet decreased when the concentration of PEG lipid was above 3 mol% (Kim, Kim et al. 2000). Span60/ PEG40 St mixed monolayers were investigated at different molar ratios to get information on interactions between the two MBs' shell components in another study. It was found that behavior of the mixed monolayers at the air/water interface depended on the molar fraction of PEG40 St due to interactions between the interfacial components of Span60 and PEG40 St and low amount of PEG40 St could interact sufficiently with Span60 molecules (Xing, Ke et al. 2010).

During past years lipopolymer (polyethyleneglycol grafted lipid) received considerable attention due to their special physical and chemical properties which make

them useful for a broad range of medical and technical applications. A lipopolymer composed of a lipid anchor covalently linked by the headgroup to a hydrophilic polymer moiety such as polyethyleneglycol. The lipopolymer encourages self-assembly of the monolayer shell and it prevents microbubble coalescence and adsorption of protein owing to steric barrier created by polyethyleneglycol moiety, so it promotes biocompatibility (Winterhalter, Bürner et al. 1995, Bianco-Peled, Dori et al. 2001, Tsukanova and Salesse 2003, Tanwir and Tsoukanova 2008, Lozano and Longo 2009). For that reasons, lipid coated microbubbles stability is enhanced by the incorporation of lipopolymer (Borden, Qin et al. 2010). *Borden et al* investigated microbubbles coated with DSPC(n=18)/DSPE-PEG2000, DBPC(n=22)/DSPE-PEG2000 lipid and lipopolymer having different chain length mixtures and DBPC/PEG40 St, DSPC/PEG40 St. They observed that the acyl chain length of main component (phospholipid) influenced the rate of acoustic dissolution and the fragmentation propensity of the microbubbles. The cohesiveness of shell monolayer increased with increasing chain length and the fragmentation was strongly dependent on the cohesiveness, so the fragmentation tendency reduced. Also, the double chain lipopolymer emulsifier created more intermolecular forces and more cohesive shell (Borden, Kruse et al. 2005) Additionally, lateral phase separation in phosphatidylcholine lipid (PC) and lipopolymer (DSPE-PEG2000) coated microbubbles were studied. It was found that phase heterogeneity existed in microbubble shells, ordered lipid rich domains were surrounded by disordered lipopolymer-rich regions and the degree of phase separation increased with increasing lipopolymer content (Borden, Martinez et al. 2006). In another study, also PC/DSPE-PEG2000 and PC/PEG40 St coated microbubbles were compared. The resistance and dissolution rate of microbubbles encapsulated by PC/DSPE-PEG2000 which limits microbubbles circulation time in the blood pool were found to be higher than PC/PEG40 St coated microbubbles due to acly chain condensation in DSPE-PEG2000 (Lozano and Longo 2009). Also, same authors investigated miscibility and phase behaviors of mixtures composed of phosphatidylcholine lipid (PC) and DSPE-PEG2000 lipopolymer with forming Langmuir monolayer. It was noticed that DMPC(n=14)/DSPE-PEG2000 mixtures formed a single condensed phase, DPPC(n=16)/DSPE-PEG2000 formed a single expanded or condensed phase with respect to amount of lipopolymer in mixture whereas DSPC(n=18)/DSPE-PEG2000 displayed two phase coexistence. Hence, the phase behavior of the shell monolayer changed by altering the chain length of

phosphatidylcholine lipid and this monolayer study might provide good information for microbubble applications (Lozano and Longo 2009).

2.2. Langmuir-Blodgett (LB) Monolayers

The scientist has been interested in behavior of oil films residing on top of water for many hundreds of years. In 1774, Benjamin Francklin wrote the first documented experiment on the effect of oily films on a water surface. However, a method to manipulate oily films at the air-water interface by means of movable barriers was described by Agnes Pockels in 1891. A few years later Raleigh suggested that the films prepared by Pockels at the air-water interface were one molecule thick. Langmuir built up the experimental (surface balance) and theoretical concepts that underlie modern understanding of the behavior of molecules in a monolayer at the air-water interface in 1917.Then Katherine Blodgett developed a method to transfer the monolayer on solid substrates in 1929 and this technique has been called as Langmuir-Blodgett (LB) methods. The scientists all around the world started to realize the opportunities of this method after the pioneering studies done by Langmuir and Blodgett In 1979, the first international conference on LB monolayer was held and then the use of this method has been increased. The early investigations have been mostly related to the interfacial phenomena, but currently the interest of LB films with potential applications in thin film optics, as sensors and transducers, as protective layers, as patternable materials for surface preparation and modification, for chemically modified electrodes and as models for biological membranes has been growing (Fuller 2003, Chatterji and Rajdev 2008).

2.1.3. The LB Monolayer Formation

Certain organic molecules can oriented themselves at the interface between a gaseous and a liquid phase. The resulting surface film is called as a monolayer. The molecules of monolayer forming materials consist of two parts: one that hydrophilic head group and hydrophobic chain. These molecules are amphiphiles and also known as surfactants, the most important type of which is phospholipids composed of two hydrocarbon chains and polar headgroup (Petty 1996).To form a monolayer at the air/water interface, also called as Langmuir monolayer, insoluble surfactants can be

spread on a water surface with the help of a volatile and water insoluble solvent. The amphiphilic nature of the surfactants orients the molecules at the interface. The polar head group is immersed in the water and the hydrophobic chain is pointing towards air as seen in Figure 2.1. The association behavior of the surfactants in solution and on the interface is determined by the physical and chemical properties of the hydrophobic and hydrophilic groups. The shape and size of hydrocarbon part and the size, charge and hydration of the hydrophilic head group are very important in this respect (Chatterji and Rajdev 2008). Moreover, to form insoluble monolayer at the interface the hydrocarbon chain of the substance used for monolayer studies has to be long enough. If the chain is smaller than 12 hydrocarbons, it is still insoluble in water and tends to form micelles which are water soluble and prevents the build-up of a monolayer at the interface. On the other hand, the substances having too long hydrocarbon chain length tend to crystallize on the water surface and consequently do not form a monolayer (Gaines 1966).

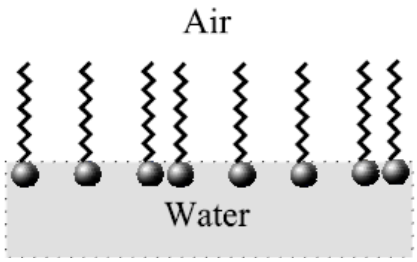

Figure 2.1. Monolayer formation at the air/water interface

2.1.4. Fundamental Properties of Langmuir Blodgett (LB) Technique

Langmuir Blodgett monolayers are generated on a LB trough shown in Figure 2.2. The setup of LB technique consists of a Teflon trough that contains subphase solution, a Wilhelmy plate and two movable barriers (Moghaddam, Ali et al. 2011). The surfactant dissolved in a suitable solvent is spread on the surface with help of a microsyringe. After that the solvent evaporates and a monolayer formed on the surface. The arrangement of a monolayer on the surface can be controlled by varying the position of the barriers. The monolayer can be compressed by barrier system and the available surface area per molecule in monolayer decreased (Fuller 2003, Chatterji and

Rajdev 2008, Moghaddam, Ali et al. 2011).This causes the different surface tensions between the surface with surfactant present and pure surface.

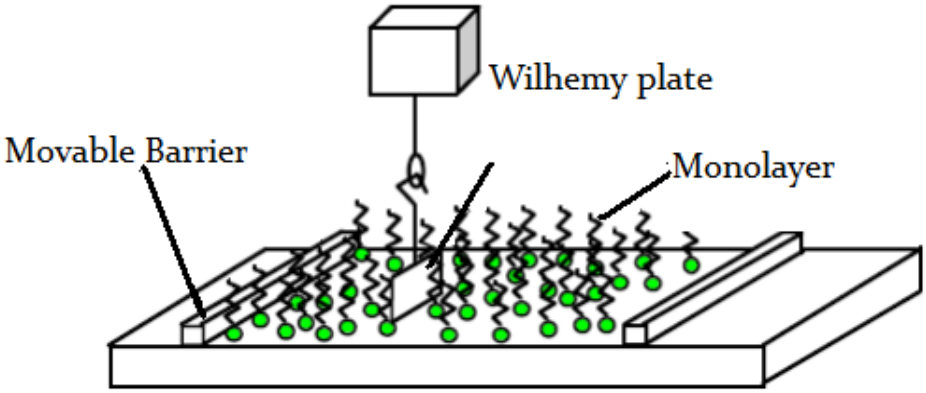

Figure 2.2. Langmuir Blodgett trough

The differences of the surface tension of the subphase in the absence and in the presence of the surfactant are called as surface pressure which is calculated by the following equation:

$$\pi = \gamma - \gamma_0 \qquad (2.1)$$

where π represents surface pressure (mN/m), γ is the surface tension of the subphase in the absence of a monolayer and γ_0 is surface tension in presence of a monolayer (Moghaddam, Ali et al. 2011). Prior to spreading of the surfactant on the surface, a Wilhelmy plate is dipped into the subphase solution and the plate measures the surface pressure of the system during compression which is important property for the characterization of LB monolayer. Various forces which are downward forces such as gravity and surface tension and upward forces such as buoyancy due to the displacement of the water act on the this plate, when this plate is partially immersed in the subphase. Generally, a sensitive elector balance measures these forces converted into surface tension (mN/m) with the help of the dimensions of the plate and the changes of the plate in the absence and presence of the monolayer were determined. The surface pressure can be related to the average area per molecule and surface pressure isotherms can be plotted during compression by measuring the surface pressure against the molecular area (Chatterji and Rajdev 2008, Moghaddam, Ali et al. 2011).

2.1.5. Information Gained from LB Monolayer Studies

A range information which are the orientation and conformation of molecules in the monolayer, their dimensional properties and molecular interactions between mixed surfactant monolayers can be gathered from the surface pressure (π) - mean molecular area (A) isotherms plotted by using LB technique (Chatterji and Rajdev 2008, Moghaddam, Ali et al. 2011).Therefore, the Langmuir Blodgett technique is a useful method for two-dimensional model systems since surface pressure-mean molecular area isotherms reflect the intermolecular interactions operating in 2D arrangements of molecules and provide information on molecular packing (Degen, Rehage et al. 2005). An isotherm is recorded by compressing the monolayer with the barriers at constant rate while continuously recording surface pressure. The distinct regions indicated the phase behavior of the monolayer apparent on the isotherm during compression as shown in Figure 2.3.

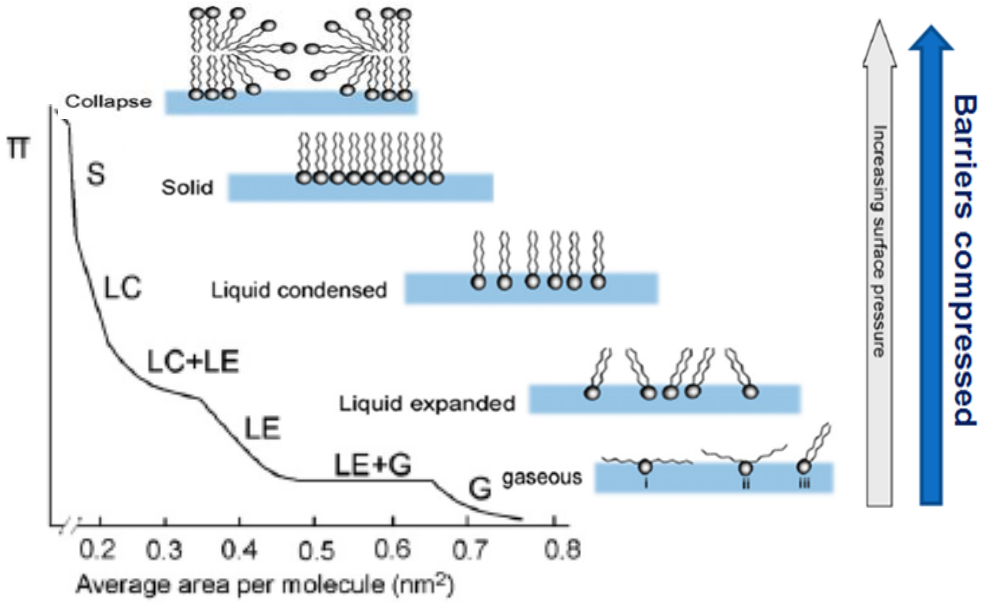

Figure 2.3. Schematic illustration of π-A isotherm exhibiting various phases

In the gaseous (G) phase, the molecules are far enough apart on the surface and they can not interact each other, so the surface pressure is nearly zero. As the gaseous

phase is compressed on the subphase surface, in the isotherm a constant pressure region is detected, in which the floating films consists of a mixture of gaseous and liquid expanded (LE) phases. Generally, the phase change is thought as a first-order thermodynamic transition. The molecules come closer and there is some interaction between the molecules with further compression. This state represents the liquid expanded (LE) phase. As the molecular area is gradually reduced, the molecules get oriented and liquid condensed phase (LC) appears. A constant pressure region which is characteristic of a first transition thermodynamic transition appears between LE and LC phases similar to G-LE transition region. Upon further compression, finally the molecules are closely packed and reach the solid phase. The interaction between the molecules is highest in this phase and if the monolayer further compressed after reaching solid phase, molecules break out the monolayer and .This is referred to as collapse. At this maximum surface pressure the monolayer packing is no longer controlled and 2D structure does not exist anymore. The monolayer will collapse into three-dimensional structures and it is generally seen as a rapid reduction in the surface pressure or as a horizontal break in the isotherm (Petty 1996, Chatterji and Rajdev 2008, Moghaddam, Ali et al. 2011).

2.1.6. Deposition of LB Films

The amphiphilic molecules at the air-subphase interface can be transferred onto a solid substrate by using Langmuir-Blodgett technique. This is carried out by successively dipping a solid substrate up or down through the monolayer, at the same time the surface pressure is kept constant by a computer feedback system between the barrier moving mechanism and electrobalance measuring the surface pressure. These coated monolayers are commonly called as Langmuir-Blodgett (LB) films. In this deposition technique, the solid substrate is placed in the subphase before the sample is spread. Then the sample is spread on surface of the subphase and compressed to selected surface pressure for coating and the monolayer is deposited onto the solid substrate by raising the substrate from the interface as shown in Figure 2.4. Moreover, different types of multilayer LB films can be obtained by various deposition methods. The transfer of the monolayer may occur only during the downstroke (X-type deposition), only during the upstroke (Z-type deposition) or both during down- and

upstroke (Y-type deposition) which are demonstrated in Figure 2.4 (Petty 1996, Chatterji and Rajdev 2008).Atomic force microscopy (AFM) that is nondestructive and high resolution method is used to investigate LB film structure and can provide a wealth of information on the structure of molecules with nanometer resolution (Zasadzinski, Viswanathan et al. 1994).

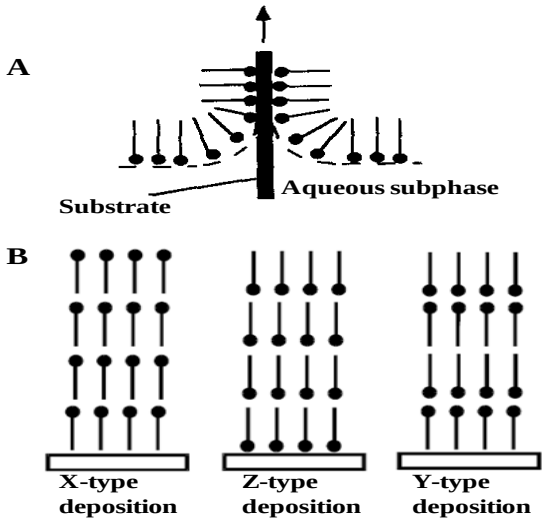

Figure 2.4. A) Deposition of a monolayer on a solid substrate B) Different types of deposited LB films

2.1.7. Characterization of LB Monolayers by Brewster Angle Microscopy

Brewster Angle Microscopy (BAM) the most informative method for analysis of monolayers is used to investigate monolayer morphology (Degen, Rehage et al. 2005). Although fluorescent microscopy is a popular method for observation of monolayers, previously it was reported that fluorescent probe which emits fluorescence and is necessary to obtain images of the monolayer affected the formation of domains in the monolayer and this probe served as an impurity. Therefore, observation of the monolayer without impurities is important and Brewster Angle Microscopy is preferred as a non-impurity method (Meunier 2000, Kubo, Adachi et al. 2001).

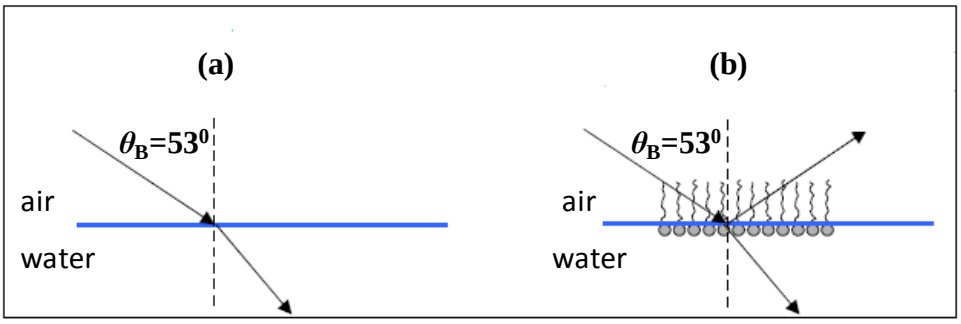

Figure 2.5. Schematic illustration of the change in reflectivity due to a thin film on air/water interface

The microscope is mounted on the Langmuir Blodgett trough, so it provides information on homogeneity, phase behavior and morphological properties of the monolayer at the air/subphase interface. The method of investigation of monolayer on surface with BAM is based on the Brewster Angle principle at the air/subphase interface. When an incident light encounters a boundary between two media, some of the light reflects. However, if p-polarized light incidents at the Brewster Angle, the light does not reflect from the interface as seen in Figure 2.5 (a). The Brewster angle of incident light is determined by the equation:

$$\theta_B = \arctan\{\frac{n2}{n1}\} \quad (2.2)$$

where n_2 ,n_1 is the refractive indexes of the two media at the interface and θ_B is calculated Brewster angle for these media. For example, the ratio of refractive indexes for air/water interface is 1.333 and the Brewster Angle is 53^0 at air/water interface. However, as illustrated in Figure 2.5 (b) that the addition of a monolayer (thin film) changes the refractive index of the interface, so the incident light is reflected from the surface (Hénon and Meunier 1991, Hernández 2010).

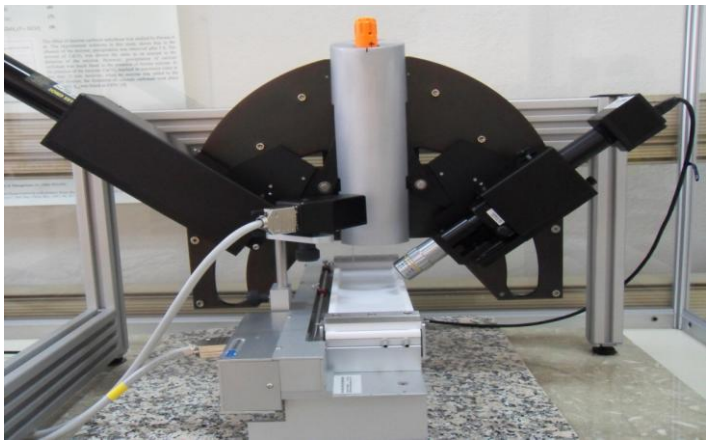

Figure 2.6. Brewster Angle Microscopy (BAM) mounted on the Langmuir Blodgett trough

Figure 2.6 shows Brewster Angle Microscopy consisting of a HeNe laser, two polarizer and a CCD camera. The laser was polarized in the plane of incidence by a polarizer. The reflected light from surface pass through a second polarizer and the CCD camera received the light. Before the images of monolayers were taken, a black glass plate is placed on the Langmuir trough to absorb any incident light that pass the subphase, the trough was filled with ultra pure water and the microscope was adjusted to the incident beam fixed at Brewster angle of water (53^0) for no reflection from the surface. When the samples were spread on the water, the reflected beams were recorded with CCD camera. The BAM images of the samples are taken at different surface pressure while the compression continued and the image are stored digitally. Using the Brewster Angle Microscope changes in monolyer can be observed in real time during the measurement (Hernández 2010).

CHAPTER 3

MATERIALS AND METHODS

3.1. Materials

All the compounds used in this study, namely:1,2-distearoyl-sn-glycero-3-phosphocholine %99 (DSPC), 1,2-distearoyl-sn-glycero-3-phosphate (sodium salt) %99 (DSPA), 1,2-distearoyl-sn-glycero-3-phosphoethanolamine (DSPE), Polyethylene glycol 40 stearate (PEG 40 St) were purchased from Sigma Aldrich (St. Louis, MO). 1,2-distearoyl-sn-glycero-3-phospho-(1'-rac-glycerol) (sodium salt) %99 (DSPG) and the poly(ethylene glycol)-grafted phospholipids having different PEG chain length, 1,2-distearoyl-sn-glycero-3-phosphoethanolamine-N-(methoxy (polyethylene glycol)-2000) (ammonium salt) (DSPE-PEG2000), 1,2-distearoyl-sn-glycero-3-phosphoethanolamine-N-(methoxy(polyethylene glycol)-1000) (ammonium salt) (DSPE-PEG1000), 1,2-distearoyl-sn-glycero-3-phosphoethanolamine-N-(methoxy (polyethylene glycol)-350) (ammonium salt) (DSPE-PEG350) were purchased from Avanti Polar Lipids (Alabaster, Alabama).The chemical structures of these components are presented in Table 3.1. In addition chloroform and methanol were obtained from Sigma Aldrich and Merck (Darmstadt, Germany) respectively were used as solvents.

3.2. Methods

3.2.1. Sample Preparation Procedure

The solutions of pure phospholipids, mixtures containing pure poly(ethylene glycol)-grafted phospholipids and pure PEG 40 St were prepared by dissolving predetermined amounts of materials in chloroform and homogenous samples were obtained by using ultrasonic bath. These binary mixtures were prepared at the predetermined molar ratios of 9:1; 8:2; 7:3; 6:4 and 5:5 respectively for DSPC/PEG40 St and at molar ratios of 9:1 and 5:5 for DSPC/DSPE-PEG. The same procedure was

applied for DSPC/PEG 40 St/DSPG, DSPC/PEG 40 St/DSPE, DSPC/PEG 40 St/DSPA ternary mixtures at 7:2:1; 7:1.5:1.5; 7:1:2 and 4:5:1; 2:5:3; 0:5:5 molar ratios prepared by dissolving in the mixture of chloroform and methanol (2:1, v/v).

3.2.2. Characterization of the Samples

Langmuir Blodgett isotherms were obtained for the binary system and pure components using Langmuir minitrough (KSV Instruments Ltd., Helsinki, Finland) enclosed in a cabinet to eliminate surface contamination. A teflon trough with two barriers was used for compression isotherms. The trough was filled with ultra pure water and impurities were controlled before solution spread. The spreading solutions were deposited onto the water subphase with Hamilton micro syringe. Chloroform was allowed to evaporate for 20 minutes, before the compression was initiated with barrier speed of 5 mm/min. The compression was continued until the monolayer collapsed. During the compression surface pressure was measured via filter paper plate. To ensure the reproducibility of the isotherms measurements, isotherms of each monolayer were run at least in triplicate.

The cycle experiments of the isotherms were carried out by periodic expansions followed by recompressions. For these experiments, a monolayer was compressed to until surface pressure reached targeted pressure, then the monolayer was waited 20 minutes for per compression and expansion while the surface pressure was held constant.

Langmuir trough was mounted with Brewster Angle Microscope (BAM) manufactured by KSV. The Brewster Angle Microscope (KSV Optrel BAM300) was used to investigate monolayer morphology. The instrument consists of a 10mW HeNe laser, two polarizer and a CCD camera. The laser was polarized in the plane of incidence by a polarizer. The reflected light from surface pass through a second polarizer and the CCD camera received the light. Before the images of monolayers were taken, the microscope was adjusted to the incident beam fixed at Brewster angle of water (53^0) for no reflection from the surface. When the samples were spread on the water, the reflected beams were recorded with CCD camera. The BAM images of the samples were taken at different surface pressure while the compression continued and

the images were stored digitally. All experiments were carried out at 20 ± 2^0 C controlled with circulating water system.

To obtain information about surface topography, phase contrast and interactions of lipids Atomic Force Microscope (AFM) was employed. Freshly cleaved mica was used for film deposition. Firstly, the trough was filled with ultra pure water. Then the barriers were compressed to selected surface pressure. Before the film deposition, the monolayers were waited for equilibrium 20 minutes. Using a vertical dipping method the monolayers were transferred to the mica surface at selected surface pressure. The LB films were prepared with 1 mm/min deposition rate.AFM images of these films were obtained using Scanning Probe Microscopy Instruments (Solver Pro 7 from NT-MDT, Russia and NanoMagnetics Instruments, Ankara) in the tapping mode that gave topographical and phase contrast images. The AFM images were taken by using silicon tip with 75 kHz resonance frequency.

Table 3.1. Chemical structures of materials used in the experiments

Chemicals	**Chemical Structure**
DSPC	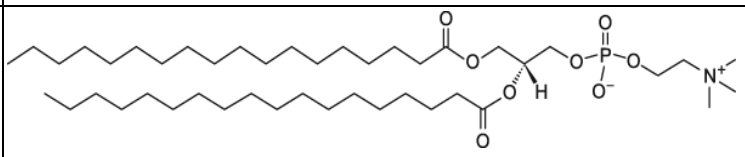
DSPG	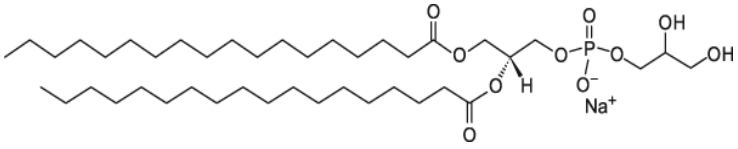
DSPA	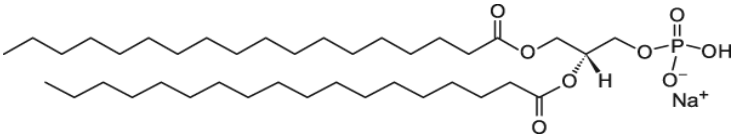
DSPE	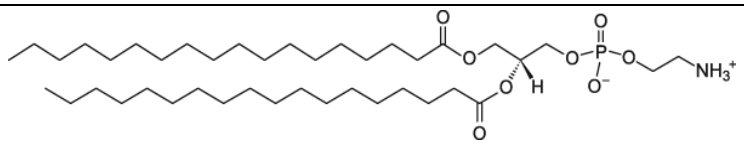
DSPE-PEG350	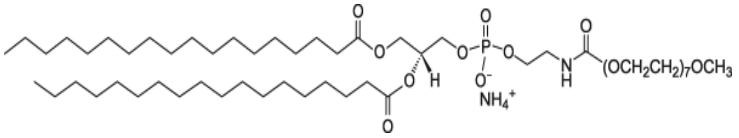
DSPE-PEG1000	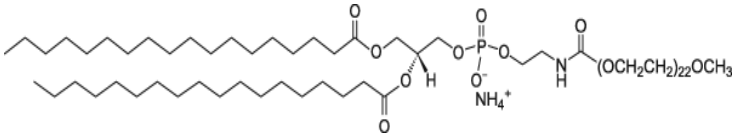
DSPE-PEG2000	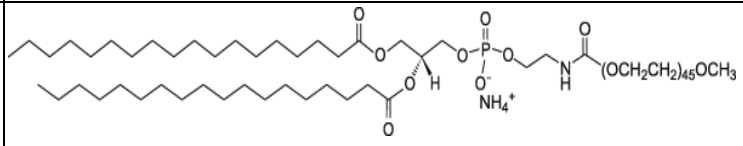
PEG40 Stearate	

3.2.3. The Analysis of the Langmuir Blodgett Isotherms

The analysis of the parameters calculated from π-A isotherms give information on the molecular organization and molecular interaction of the components in mixed monolayer. The interactions and the miscibility between molecules in the mixed monolayers can be investigated according to additivity rule (Wydro and Witkowska 2009).

$$A_{ideal} = x_1A_1 + x_2A_2 \quad (3.1)$$

where A_{ideal} is mean molecular area of ideal mixture and,x_1, x_2 are mol fractions of the components, A_1 and A_2 are molecular areas of the pure components at given surface pressure. The excess area (A_{exc}) and excess Gibbs energy of mixing (ΔG_{exc}) can be calculated to obtain more information on the behavior of intermolecular interaction in the mixed monolayer (Chou and Chu 2003, Wydro and Witkowska 2009).

$$A_{exc} = A_{12} - (x_1A_1 + x_2A_2) \quad (3.2)$$

wherein A_{12} is mean molecular area of real mixed monolayer gained from the isotherms at different surface pressures. The excess free energy of mixing ΔG_{exc} is defined as,

$$\Delta G_{exc} = N \int_{\pi 1}^{\pi 2} A_{12} - (x_1A_1 + x_2A_2)\, d\,\pi \quad (3.3)$$

where N is the Avogadro number and π is the surface pressure, so ΔG_{exc} is obtained directly by π-A isotherms (Gaines 1966, Deleu, Paquot et al. 1999, Chou and Chu 2003, Wydro and Witkowska 2009, Wydro, Knapczyk et al. 2011).Also, the compression modulus known as incompressibility (C_s^{-1}) provides information on molecular ordering of molecules in monolayer and this parameter is used to examine monolayer fluidity correlated with phase behaviors(Pavinatto, Caseli et al. 2007, Wydro and Witkowska 2009).The compression modulus can be estimated by the following equation (Wydro and Witkowska 2009, Wydro, Knapczyk et al. 2011),

$$C_s^{-1} = -A(\, d\,\pi\, /dA) \quad (3.4)$$

where A is mean molecular area and π is the surface pressure.

CHAPTER 4

RESULTS AND DISCUSSION

4.1. The Effect of Emulsifier Type on Microbubbles' Shell Structure

4.1.1. The Effect of PEG40 St on Shell Structure of Microbubbles

As it is known that commonly, lipid coated microbubble production has been performed using DSPC and PEG40 St mixture at a molar ratio of 9:1 (Borden, Pu et al. 2004, Talu, Lozano et al. 2006, Borden, Feshitan et al. 2009),but it has been observed that microbubble shell prepared with this formulation is not stable for long time (Mulvana, Stride et al. 2010). Although the microbubble shell composition have a dramatic effect on microbubble properties, to date a few studies have been applied about the effect of shell composition and their phase behavior. For instance, microbubbles having different concentrations from current formulation were investigated by *Talu et al* and they showed that the coalescence of the microbubbles reduced with increasing PEG40 St concentration (Talu, Lozano et al. 2006). In another study, Span60/PEG40 St mixtures which were used to produce microbubble were investigated by changing concentration of components in order to obtain optimum interaction between the components (Xing, Ke et al. 2010).Herein, in this part of our study we examined the effect of PEG40St content on microbubble shell stability, molecular interaction and monolayer phase behavior. For this aim, the mixtures composed of DSPC and PEG40St at various molar ratios (9:1, 8:2, 7:3, 6:4 and 5:5) were investigated by Langmuir–Blodgett (LB) method and Brewster Angle Microscopy (BAM).

The surface pressure (π) versus mean area per molecule (A) isotherms were obtained for pure components and DSPC/PEG40 St binary mixtures at different molar ratios. Figure 4.1 shows π-A isotherms of pure DSPC, pure PEG40 St and their mixed monolayers. Pure DSPC monolayer exhibited liquid-condensed (LC) phase at the air-water interface upon spreading, the collapse pressure was nearly 63 mN/m and the

isotherm of DSPC was good agreement with the literature (Kubo, Adachi et al. 2001, Chou and Chu 2003, Borden, Pu et al. 2004, Hollinshead, Harvey et al. 2009). As described previously DSPC monolayer showed strong cohesive interactions between C_{18} aliphatic chains on aqueous subphase exhibiting liquid-condensed (LC) phase (Kubo, Adachi et al. 2001, Tanwir and Tsoukanova 2008, Wydro, Knapczyk et al. 2011). Unlike DSPC, pure PEG40 St monolayer showed liquid-expanded (LE) phase at air-water interface and its collapse pressure was observed around a surface pressure of 35 mN/m, which is in a good agreement with the literature(Borden, Pu et al. 2004, Xing, Ke et al. 2010).The mean area per molecule of pure PEG40 St is large due to repulsive interactions between the large hydrophilic PEG chains, so that pure PEG40 St remains in the expanded phase at all compression states (Shen, Powell et al. 2008). As seen from Figure 4.1, the isotherms of the mixed monolayers of DSPC/PEG40 St at various molar ratios (9:1, 8:2, 7:3, 6:4, 5:5 mixtures of DSPC/PEG40 St) showed more expanded behavior than pure DSPC as their isotherms fell between the isotherms of two pure components at surface pressures up to 35 mN/m. For mixed monolayers initial mean molecular area increased with increasing of the mol fraction of PEG40 St because the molecular areas were expanded by the bulky hydrophilic head group of PEG40 St. The isotherms of mixed monolayers showed a plateau nearly at 35 mN/m which signified that conformational changes of PEG chains like detected for lipopolymers (Luna, Falcão et al. 2011). The length of the plateau broadened with rising molar fraction of PEG40 St. Moreover, an additional smaller plateau which indicated gradually reorientation of molecules was observed after 35 mN/m (nearly at 42 mN/m) for these isotherms and the extent of second plateau increased again with increasing amount of PEG40 St as reported by *Xing et al* for mixture of Span60 and PEG40 St (Xing, Ke et al. 2010).

A_{ideal} and A_{exc} values for mixed monolayers were calculated based on Equation 3.1 and Equation 3.2 respectively. The zero value for A_{exc} indicates that the components form an ideal mixed monolayer or are immiscible. On the other hand, deviation from ideality can signify that miscible and non ideal mixed monolayers (Chou and Chu 2003, Tanwir and Tsoukanova 2008, Wydro and Witkowska 2009).Negative deviation from ideality prove that the interactions between components in mixed monolayer more attractive than the interactions in pure monolayers, whereas positive deviation indicates that interactions between monolayer components are less attractive (Wydro and

Witkowska 2009). In our experiments A_{exc} values didn't exhibit zero values, in this case mixed monolayer proved non ideal behavior and the components were miscible.

Figure 4.2 demonstrates that the deviation of measured mean molecular area (A_{12}) of mixed monolayer from ideality at different surface pressures. A_{12} values are given as a function of mol fraction of PEG40 St and dashed lines represent the calculated area assuming ideal mixture A_{ideal}. As seen in Figure 4.2 that DSPC/ PEG40 St mixed monolayer illustrated negative deviation from ideality which signified that the interactions between molecules in mixed monolayer are more attractive (or less repulsive) than the interactions in pure monolayer. Furthermore maximum deviation was observed for the mixed monolayer of DSPC/PEG40 St at 7:3 molar ratio.

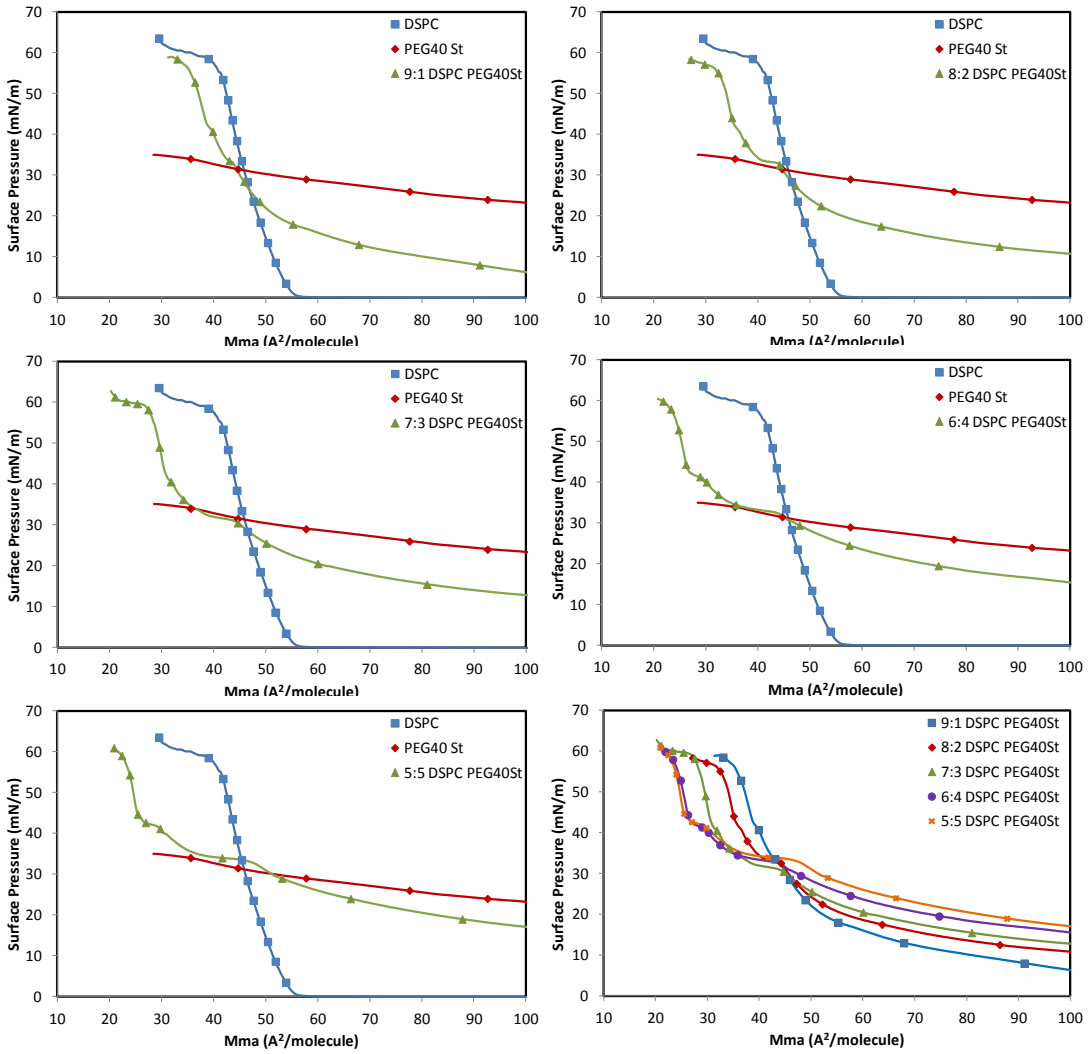

Figure 4.1. The surface pressure –mean molecular area (π-A) isotherms for pure and DSPC/PEG40 St mixed monolayers at the air/water interface

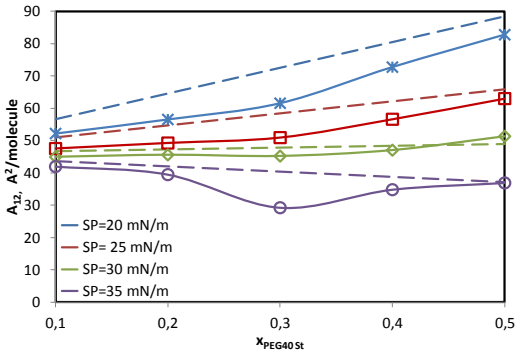

Figure 4.2. The mean molecular area (A_{12}) vs. $x_{PEG40\ St}$ plots for DSPC/PEG40 St mixed monolayers

To gain more information on the interactions of the components, excess free energy of mixing ΔG_{exc} was calculated by using Equation 3.3. If ΔG_{exc} is negative, that means attractive forces between molecules are dominant, while if ΔG_{exc} is positive it indicates that repulsive forces between molecules are dominant. (Gaines 1966, Deleu, Paquot et al. 1999, Chou and Chu 2003, Nakamura, Nakahara et al. 2007, Wydro and Witkowska 2009, Wydro, Knapczyk et al. 2011).

Figure 4.3 illustrates that the excess free energy of mixed monolayers (ΔG_{exc}) at different surface pressure. The values of the excess free energy for all mixed monolayers were negative which indicated that the interactions between monolayer components were more attractive than interactions in one component. In addition, magnitude of ΔG_{exc} showed maximum when the molar ratio of PEG40 St raised to 30%. But after that ΔG_{exc} shifted to less negative values. This indicated that the intermolecular interaction was stronger at $x_{PEG40\ St}$=0.3.Simiarly the minimum of ΔG_{exc} values was observed at x_{Chol}=0.3 for DSPC/Cholesterol mixed monolayer (Wydro, Knapczyk et al. 2011).

The properties of monolayer phases and phase transitions in amphiphilic monolayers can be obtained from incompressibility plots. The occurrence of discontinues minimum can be interpreted as phase transition. The increase of surface pressure cause a rapid increase of compressibility modulus because of an order-disorder transition of molecules until the collapse occurs (Keller 2003, Risovic, Frka et al. 2011). The compression modulus (C_s^{-1}) values of pure and mixed monolayers are given in Figure 4.4. We observed that the compression modulus of pure DSPC monolayer was high and increased with increasing surface pressure until collapse was approach meaning that there are higher order interactions between DSPC molecules. Moreover,

any changes in molecular conformation and orientation was not detected during compression for DSPC monolayer due to high compression modulus (Hollinshead, Harvey et al. 2009). Although DPPC and DSPC have different hydrocarbon chain length, C_s^{-1} values of DPPC raised with surface pressure up to collapse point similar to DSPC (Lucero, Rodríguez Nino et al. 2008). C_s^{-1} values for PEG40 St monolayer were lower because of expanded behavior of PEG40 St molecules. The C_s^{-1} plots of mixed monolayers were situated between the C_s^{-1} plots for pure components. In comparison with pure DSPC, mixed DSPC/ PEG40 St monolayers exhibited reduction of compression modulus. At low surface pressures, C_s^{-1} values of mixed monolayer reduced with increasing mol fraction of PEG40 St and the minimums of mixed plots were detected at nearly 35 mN/m which indicated that the change of molecular orientation. Unlike at low surface pressures, C_s^{-1} values for mixed monolayers tend to be higher after 35 mN/m due to order of the molecules. However the second minimum points were observed at around 42 mN/m that pointed to gradually reorientation of molecules to reach more condensed state. Furthermore, the maximal values of the compression modulus for mixed monolayers were noticed after 42 mN/m and C_s^{-1} values of DSPC/PEG40 St mixed monolayers at molar ratios of 8:2 and 7:3 were higher than the others. The incorporation of PEG40 St into DSPC monolayers affected the compressibility of mixed monolayer and made the monolayer more flexible as described previously for DSPC/DSPE-PEG2000 mixed monolayers (Chou and Chu 2003).

Langmuir isotherms of compression-expansion cycles are carried out to investigate that the emulsifier molecules after plateau region observed at 35 mN/m and recompression of the molecules in monolayer (Borden, Pu et al. 2004, Xing, Ke et al. 2010). It was reported in the literature that the shifting of compression isotherm to the left signifies that loss of molecules from monolayer and the plateau observed after cyclic compression indicates that reincorporated reversibility into the monolayer (Lipp, Lee et al. 1998, Takamoto, Lipp et al. 2001, Saad, Policova et al. 2009). In this study, the compression-expansion cycles were performed at two surface pressures which were 30 mN/m (below the collapse surface of PEG40 St) and 50 mN/m (above the collapse surface of PEG40 St) to obtain more information on respreading behavior of the mixed monolayers. Figure 4.5 exhibits that compression-expansion cycles pure DSPC and pure PEG40 St. The second and third compression of pure DSPC shifted slightly to the left compared to first compression whereas successive compressions of pure PEG40 St demonstrated larger shifting to the left. This suggested that conformational change of

PEG chain part of PEG40 St molecules. The compression-expansion cycles of DSPC/PEG40 St mixed monolayers were also examined as seen from Figure 4.6. When the mixed monolayers were compressed to 50 mN/m, degree of shifting of second compression was larger compared to the compression to 30 mN/m. This suggested that incomplete molecular orientation at 30 mN/m .Moreover, the plateaus detected nearly 35 mN/m during first compressions was not observed through second and third compressions due to irreversibility of the molecules. The area per molecules at the end of compressions to 50 mN/m intersected at the same point which indicated no loss of material from surface after first compression as interpreted in literature (Baekmark, Elender et al. 1995). The same surface pressures were reached at lower area per molecules in the subsequent cycles for the compressions to 30 mN/m. This situation may be arising from conformational rearrangements of molecules in each compression-expansion cycles.

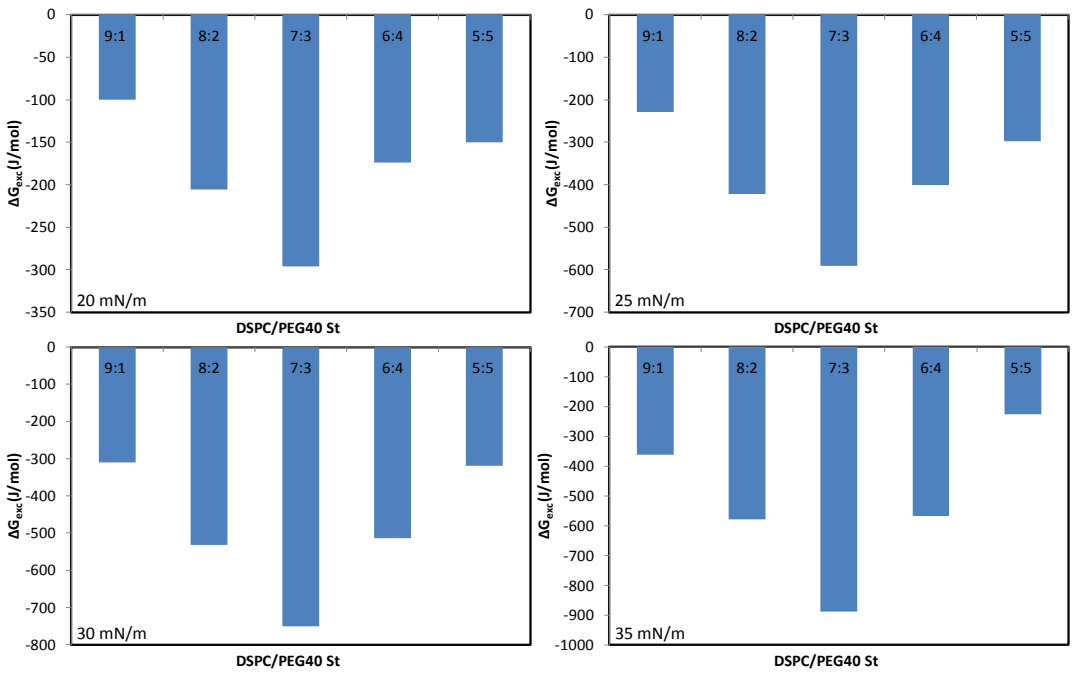

Figure 4.3. The excess free energy of mixing (ΔG_{exc}) values of DSPC/PEG40 St mixed monolayers at different surface pressures

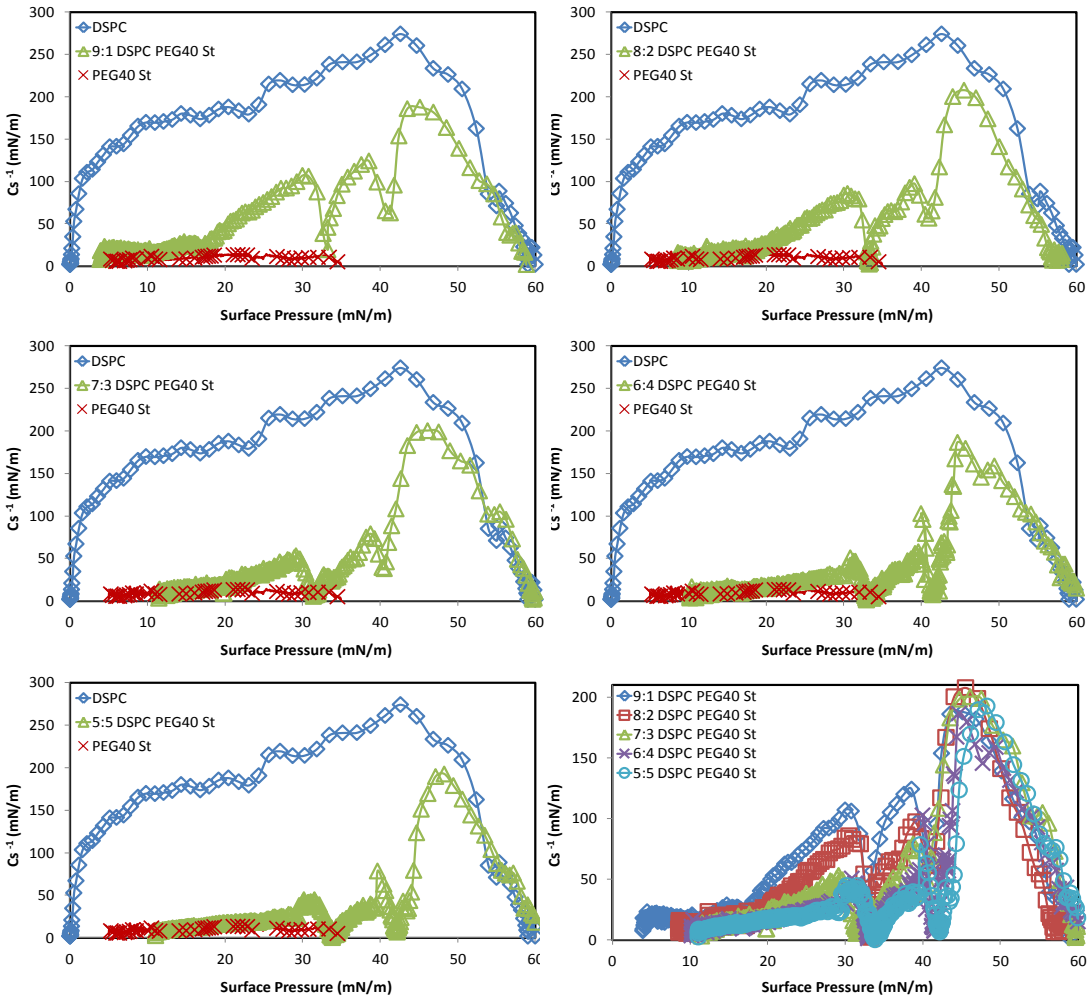

Figure 4.4. The compression modulus (C_s^{-1}) values of DSPC/PEG40 St mixed monolayers at different surface pressures

BAM images of the mixed monolayers at 9:1 and 5:5 molar ratios were taken to obtain more information on the variations of the morphology during compression-expansion cycles to 30 mN/m and to 50 mN/m respectively. As seen in Figure 4.6 that any plateau was not noticed up to 30 mN/m in the compression isotherms. However, BAM images of the mixed films taken during second and third compressions at low surface pressure and shown in Figure 4.7 and Figure 4.8 displayed change of the morphologies compared to first compressions. The gradually conformational change in PEG chain known as pancake-to-mushroom transition (Naumann, Brooks et al. 1999, Jebrail, Schmidt et al. 2008) was observed for lipopolymers might cause to these variances. Possibility, PEG40 St could not revert to first conformation due to this alteration of PEG chains and differences between the compressions' images were noticed. As seen in Figure 4.9 and Figure 4.10 though some differences were detected,

the images taken at the same surface pressures were similar for the following compressions and different from pure DSPC. These results presented an evidence for some PEG40 St molecules stay in the monolayer due to hydrophobic interactions between components.

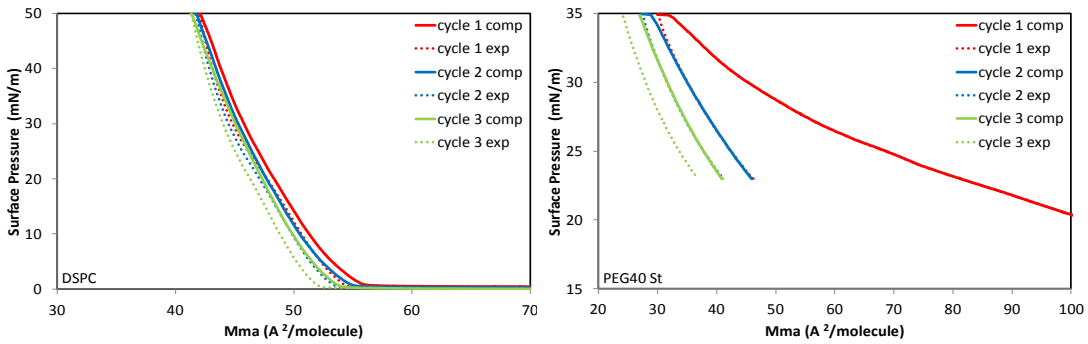

Figure 4.5. The compression-expansion cycles of pure DSPC and pure PEG40 St

In this study, the phase behavior of shell structure was investigated in molecular level with Brewster Angle Microscope (BAM) and Atomic Force Microscopy (AFM) at micro-meter and nano-meter scale, respectively. As shown in Figure 4.11, pure DSPC displayed the patches of the condensed phase at low surface pressure and these patches fused together with the compression of the monolayer and covered the surface completely which was in good agreement with the current literature (Kubo, Adachi et al. 2001, Sanchez and Badia 2008, Tanwir and Tsoukanova 2008, Hollinshead, Harvey et al. 2009, Stepniewski, Pasenkiewicz-Gierula et al. 2011, Wydro, Knapczyk et al. 2011). This uniform film of DSPC molecules indicates the presence of a single condensed phase (Kubo, Adachi et al. 2001, Tanwir and Tsoukanova 2008, Wydro, Knapczyk et al. 2011).The distance of PEG40 St molecules were very large and these molecules more tilted to the surface than DSPC molecules formed liquid-expanded (LE) phase. Therefore BAM images of PEG40 St monolayer were darker and in some regions these molecules aggregated together as illustrated in Figure 4.12. Figure 4.13 shows the results of BAM experiments of the mixed monolayer of DSPC/PEG40 St at 9:1 molar ratio. At low surface pressures, small domains and phase separations were noticed. As reported before, dark regions in the BAM images denote that expanded phase while bright regions signify that condensed phase (Minones, Rodríguez Patino et al. 2002, Nakamura, Nakahara et al. 2007, Nakahara, Krafft et al. 2011). By

incorporation of PEG40 St molecules the size of condensed domain of DSPC patches were reduced as reported for DSPC/DMPC mixed monolayer (Kubo, Adachi et al. 2001).After surface pressure was 15 m N/m the monolayer became more homogeneous with compression. Figure 4.14 indicated that the mixed monolayer of DSPC/PEG40 St at 8:2 molar ratio demonstrated bigger domains and phase separation, this monolayer exhibited homogeneous surface after 15 mN/ m like the mixed monolayer of DSPC/PEG40 St at 9:1 molar ratio. The mixed monolayer of DSPC/PEG40 St at 7:3 molar ratio showed similar behavior but the size of condensed parts increased as seen from Figure 4.15, also at 35 mN/m small bright spots indicated conformational change of molecules were detected.

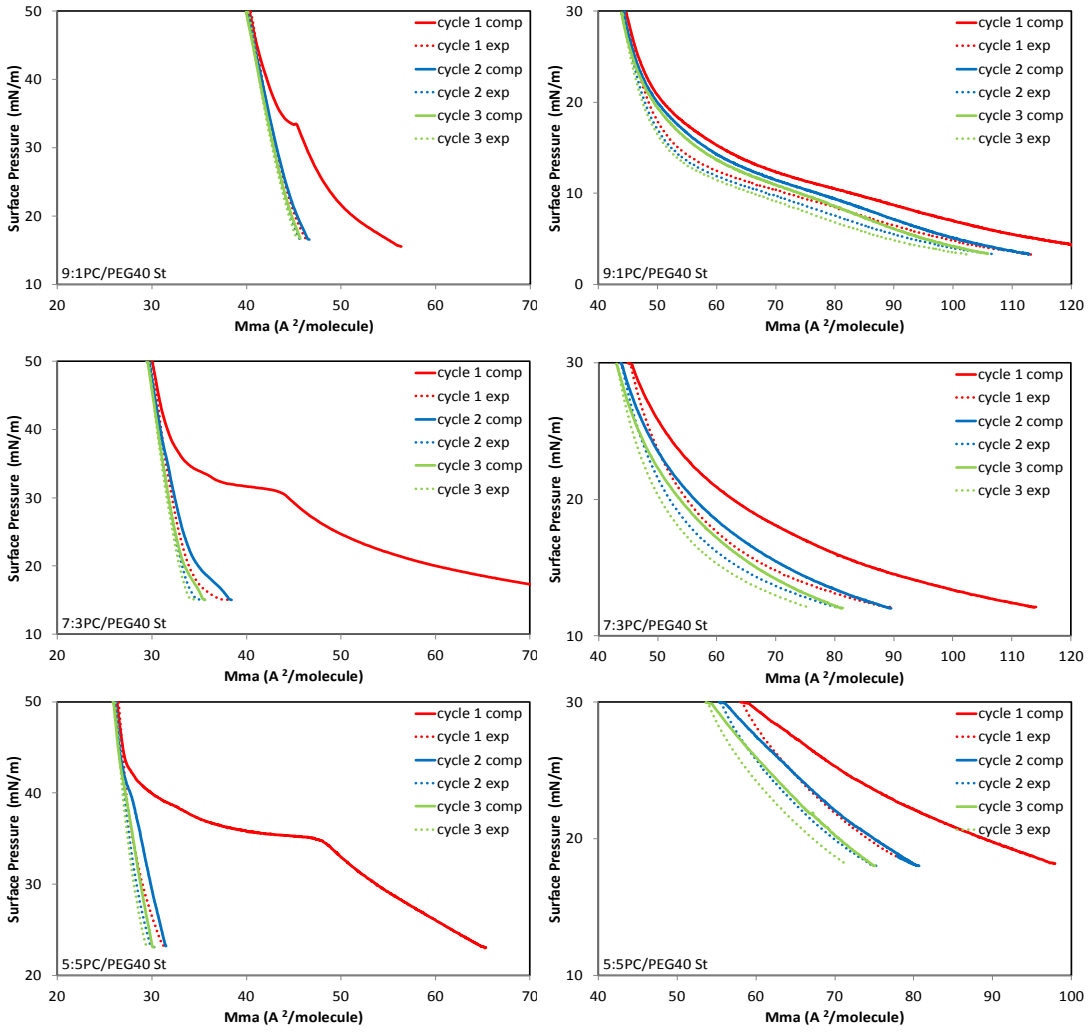

Figure 4.6. The compression-expansion cycles of DSPC/PEG40 St mixed monolayers

As illustrated in Figure 4.16, the molecules of the mixed monolayer of DSPC/PEG40 St at 6:4 molar ratio were far away from each other at low surface pressure and the size of condensed domain were the largest. Upon further compression, density of these bright condensed patterns as well as their size increased so that they become clearly resolved in BAM images at π=15 mN/m. Eventually these islands fused together forming a big one at π=20 mN/m. Moreover, the bright spots were observed at surcafe pressures of 35 mN/m and at 42 mN/m at which isotherm of this mixed monolayer exhibited plateaus. The BAM images of the mixed monolayer of DSPC/PEG40 St at 5:5 molar ratio in Figure 4.17 pointed to large circular domains and larger molecular distance due to PEG chains in PEG40 St. Although these circular domains fused together with raising surface pressure, smaller domains remained at high surface pressures unlike other mixed monolayers which might indicate that phase separations continued at higher surface pressure. Also, brightness appeared at 35mN/m and at 42 mN/m as similarly observed for 6:4 molar ratio.

Although a featureless bright phase was observed for DSPC monolayers at all compression states, a noticeable change in monolayer morphology was detected for the mixtures even at lower surface pressures as can be seen in the BAM images. This suggested that the observed features in the BAM images of the mixtures in resulting from the presence of the PEG40 St in the monolayer. As can be seen in BAM images of the mixed monolayers, the phase separations were noticeably increased and the sizes of condensed domains were bigger with increasing the mol fraction of PEG40 St. In addition to this, the small bright spots suggested that transition to more ordered state were observed at 35 mN/m and at 42 mN/m, when mol fraction of PEG40 St was higher than 0.2. According to these results PEG40 St and DSPC molecules were incompletely miscible in some regions at surface pressures lower than 35 mN/m and two coexisting phases which were the condensed lipid-rich phase and less condensed emulsifier-rich phase were detected. At higher surface pressures the molecules exhibited ordered condensed phase with compression and homogeneous surface was detected up to collapse pressure.

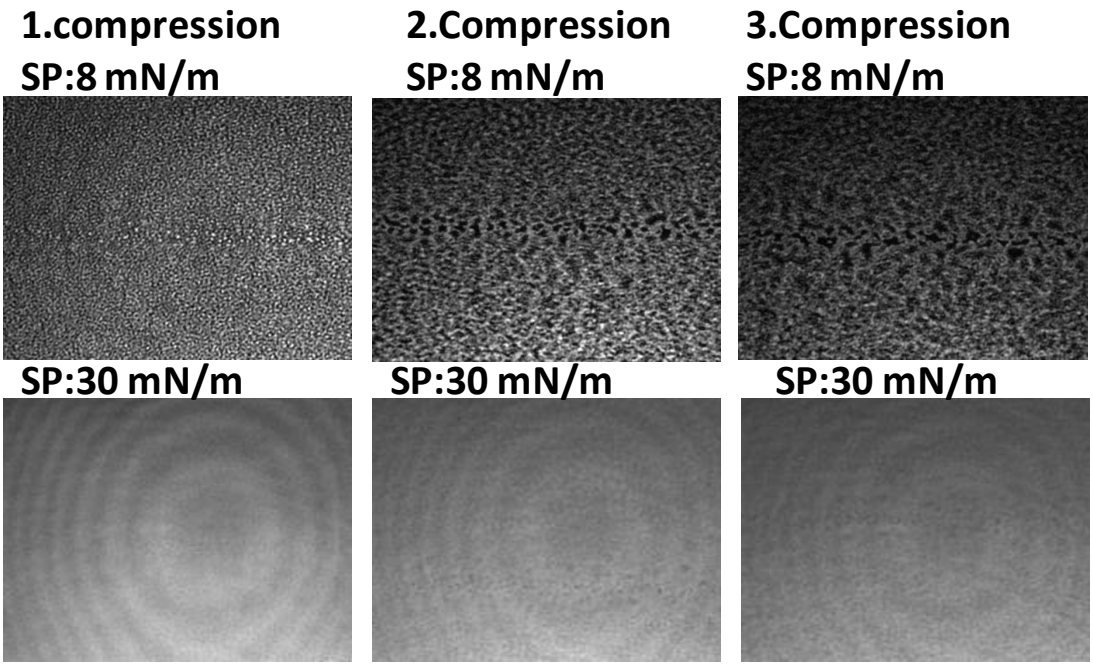

Figure 4.7. BAM images of the compression-expansion cycle up to 30 mN/m of 9:1 DSPC/PEG40 St mixed monolayer at the air/water interface

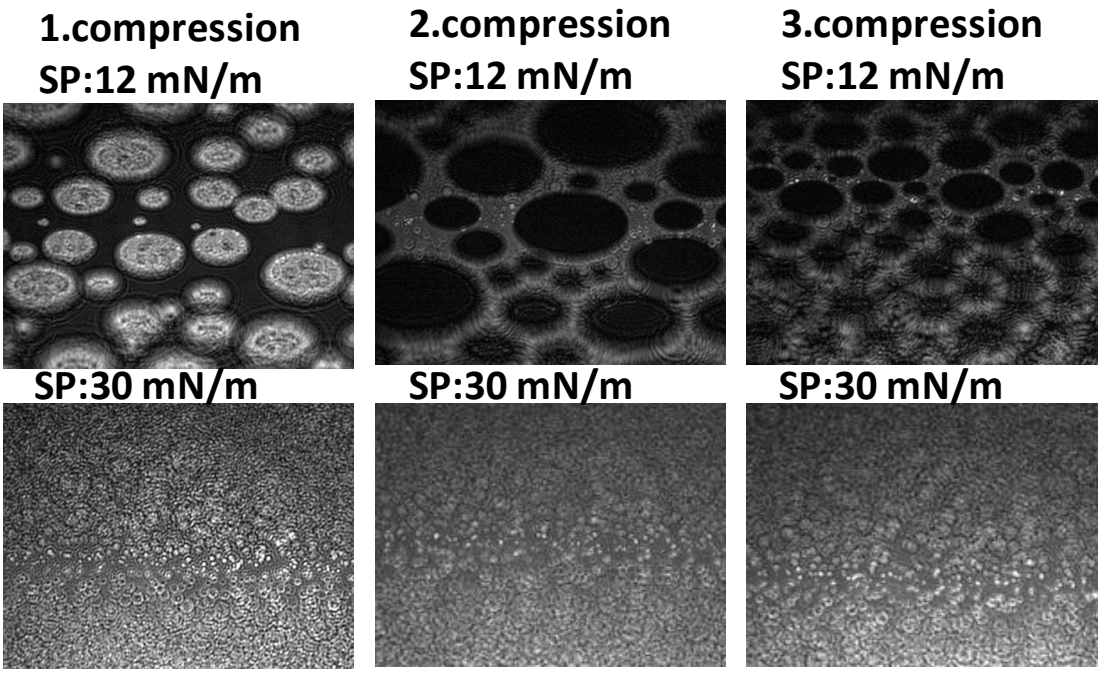

Figure 4.8. BAM images of the compression-expansion cycle up to 30 mN/m of 5:5 DSPC/PEG40 St mixed monolayer at the air/water interface

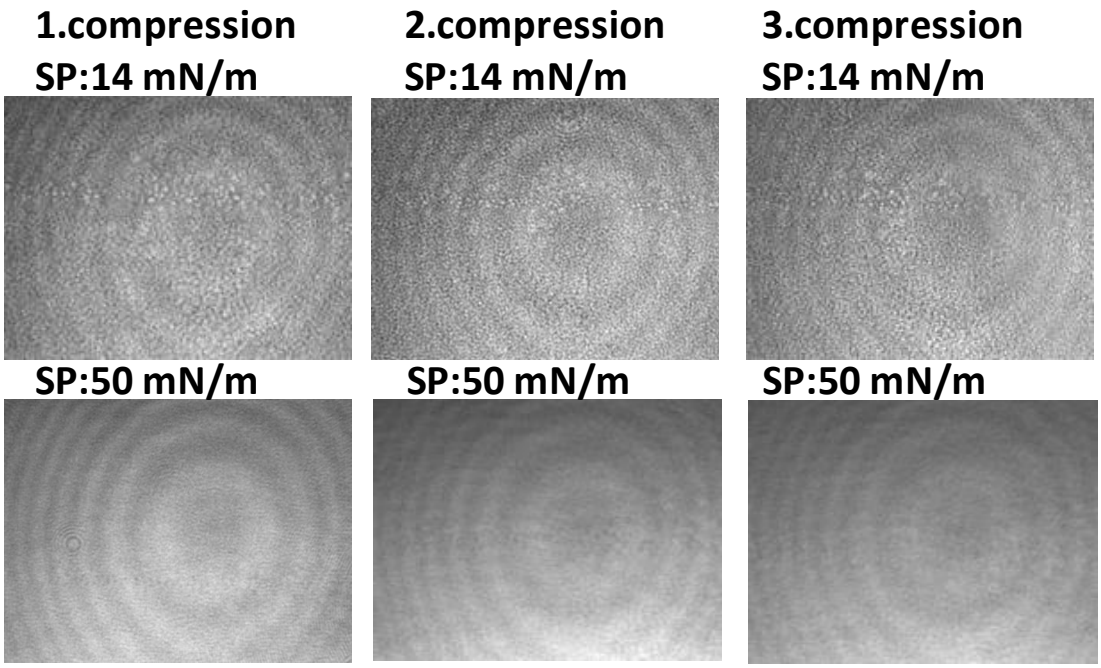

Figure 4.9. BAM images of the compression-expansion cycle up to 50 mN/m of 9:1 DSPC/PEG40 St mixed monolayer at the air/water interface

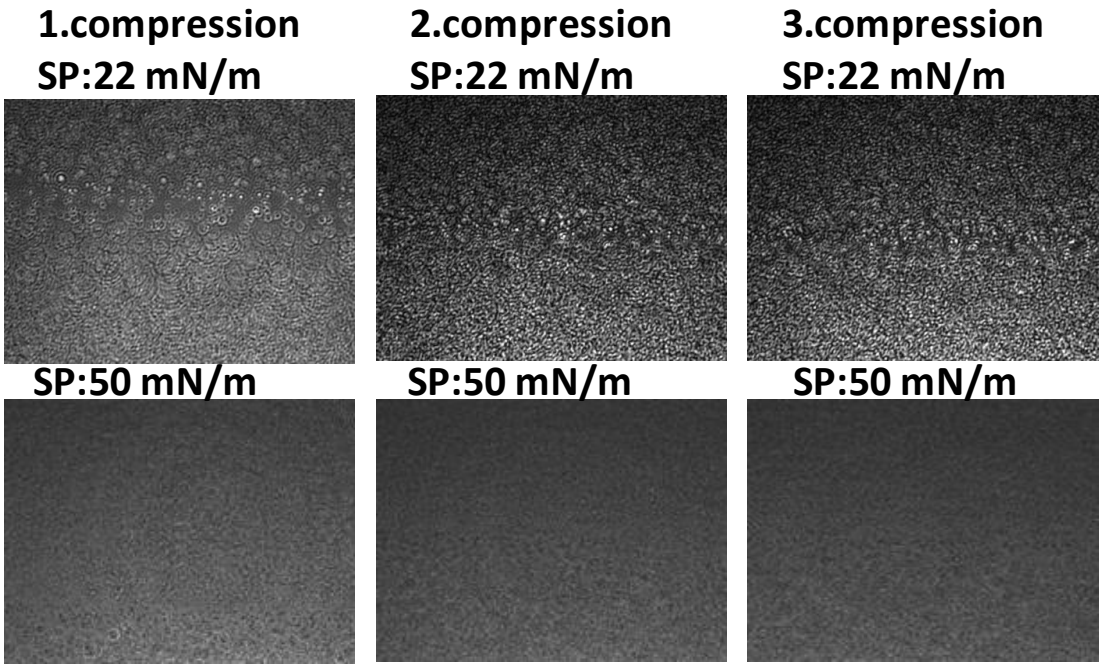

Figure 4.10. BAM images of the compression-expansion cycle up to 50 mN/m of 5:5 DSPC/PEG40 St mixed monolayer at the air/water interface

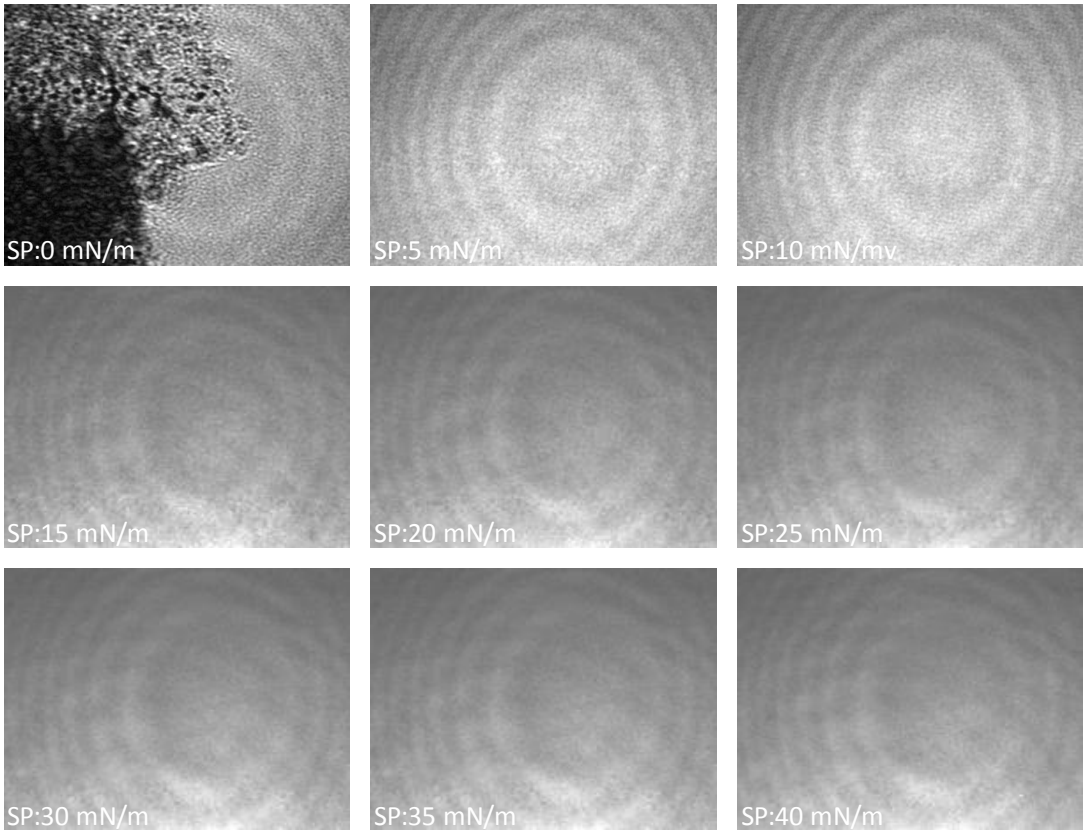

Figure 4.11. BAM images of DSPC at the air-water interface

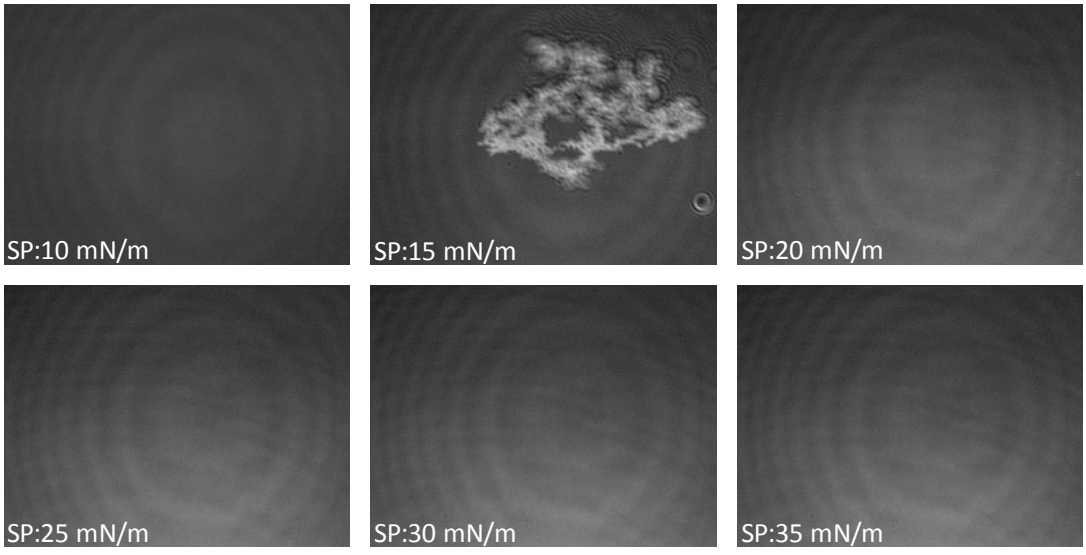

Figure 4.12. BAM images of PEG40 St at the air-water interface

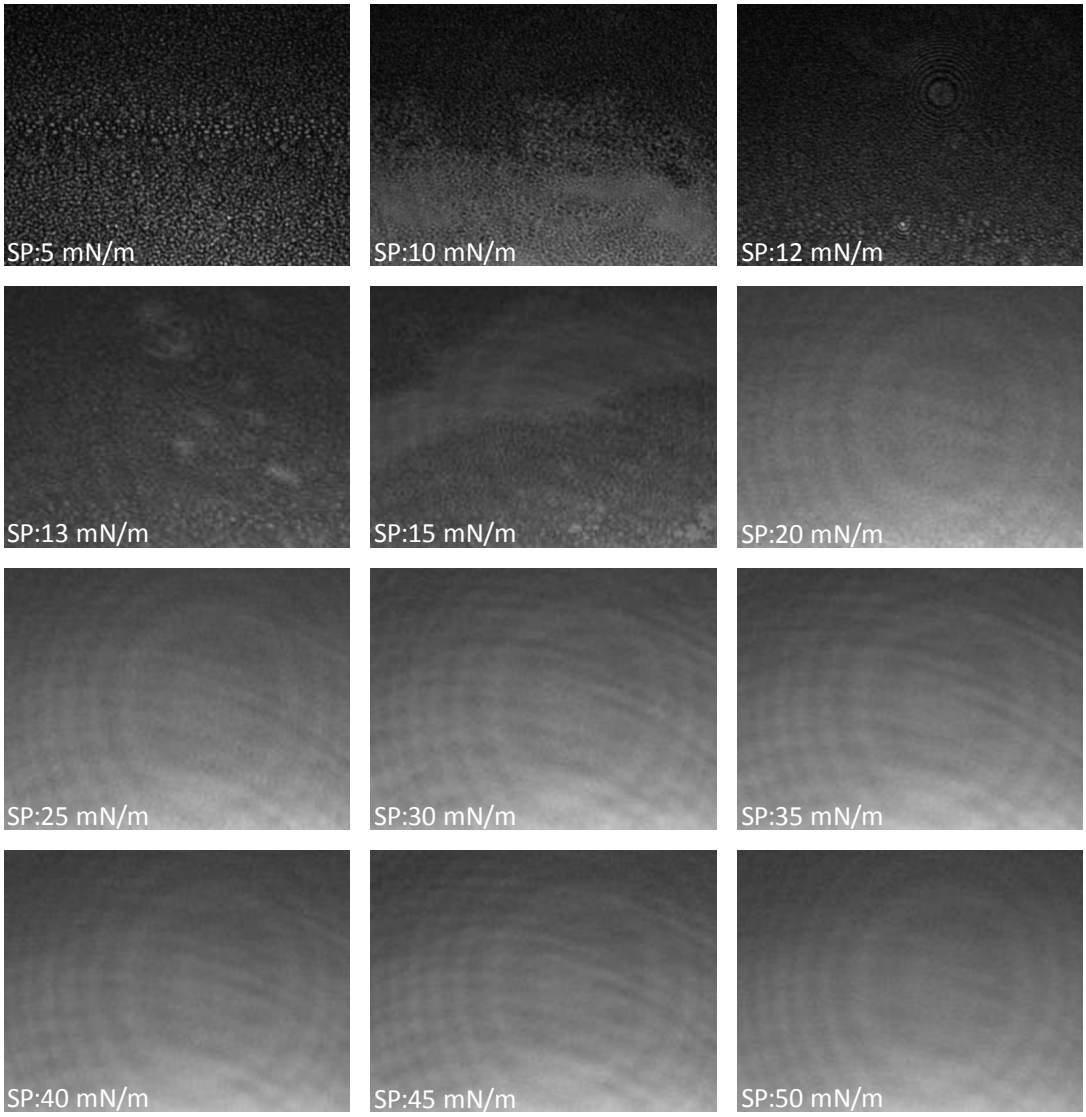

Figure 4.13. BAM images of 9:1 DSPC/PEG40 St mixed monolayer at the air-water interface

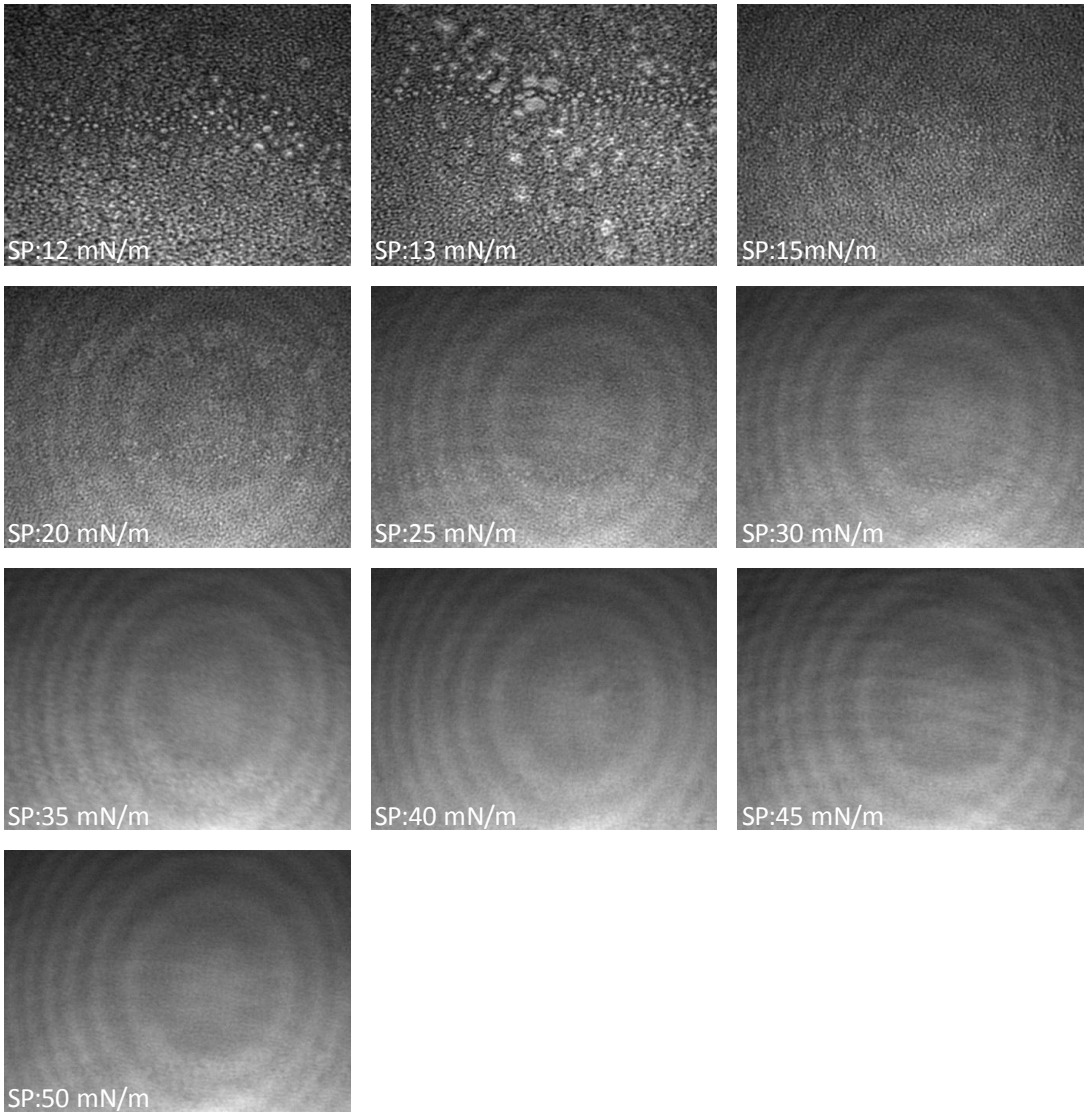

Figure 4.14. BAM images of 8:2 DSPC/PEG40 St mixed monolayer at the air-water interface

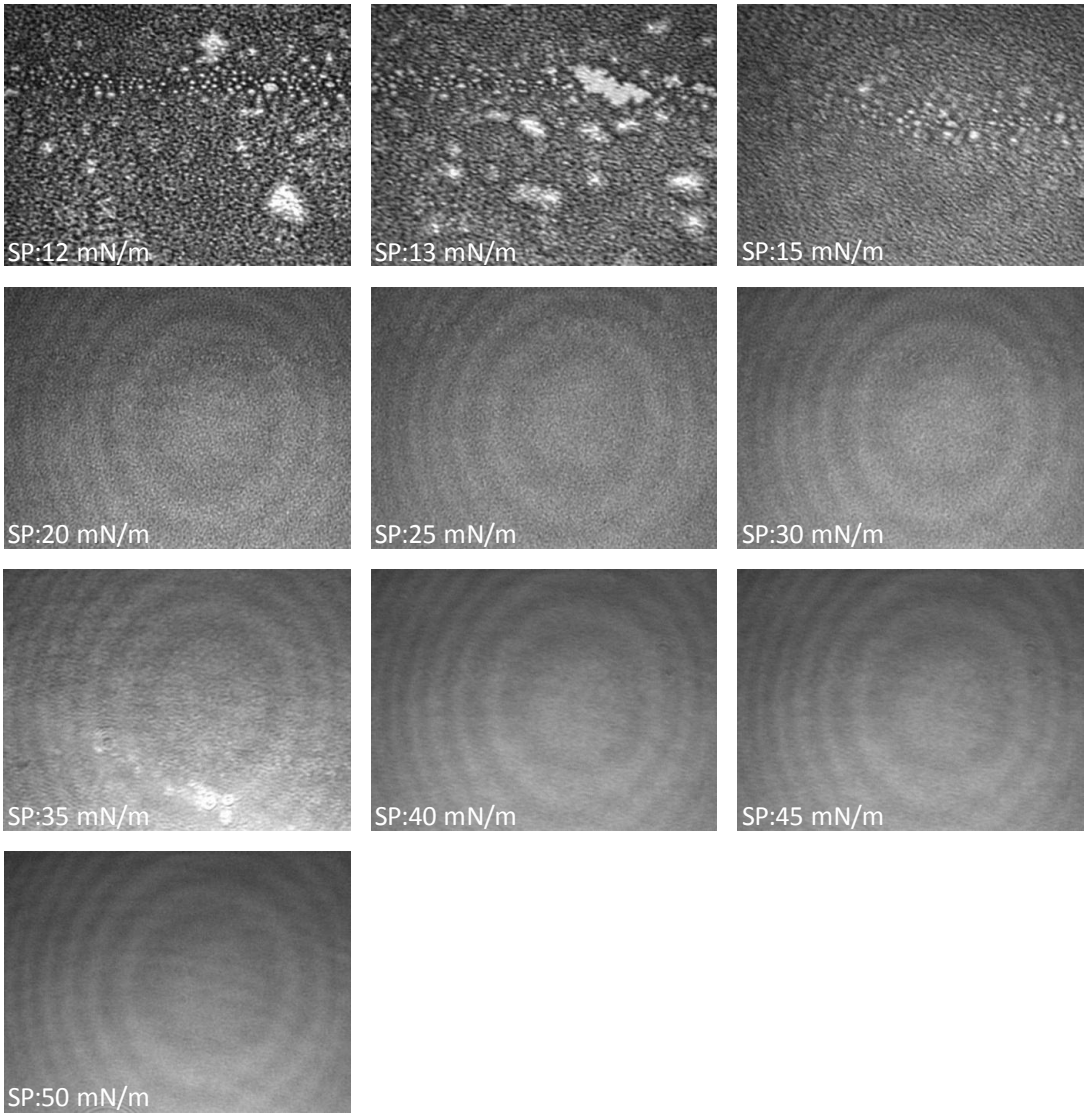

Figure 4.15. BAM images of 7:3 DSPC/PEG40 St mixed monolayer at the air-water interface

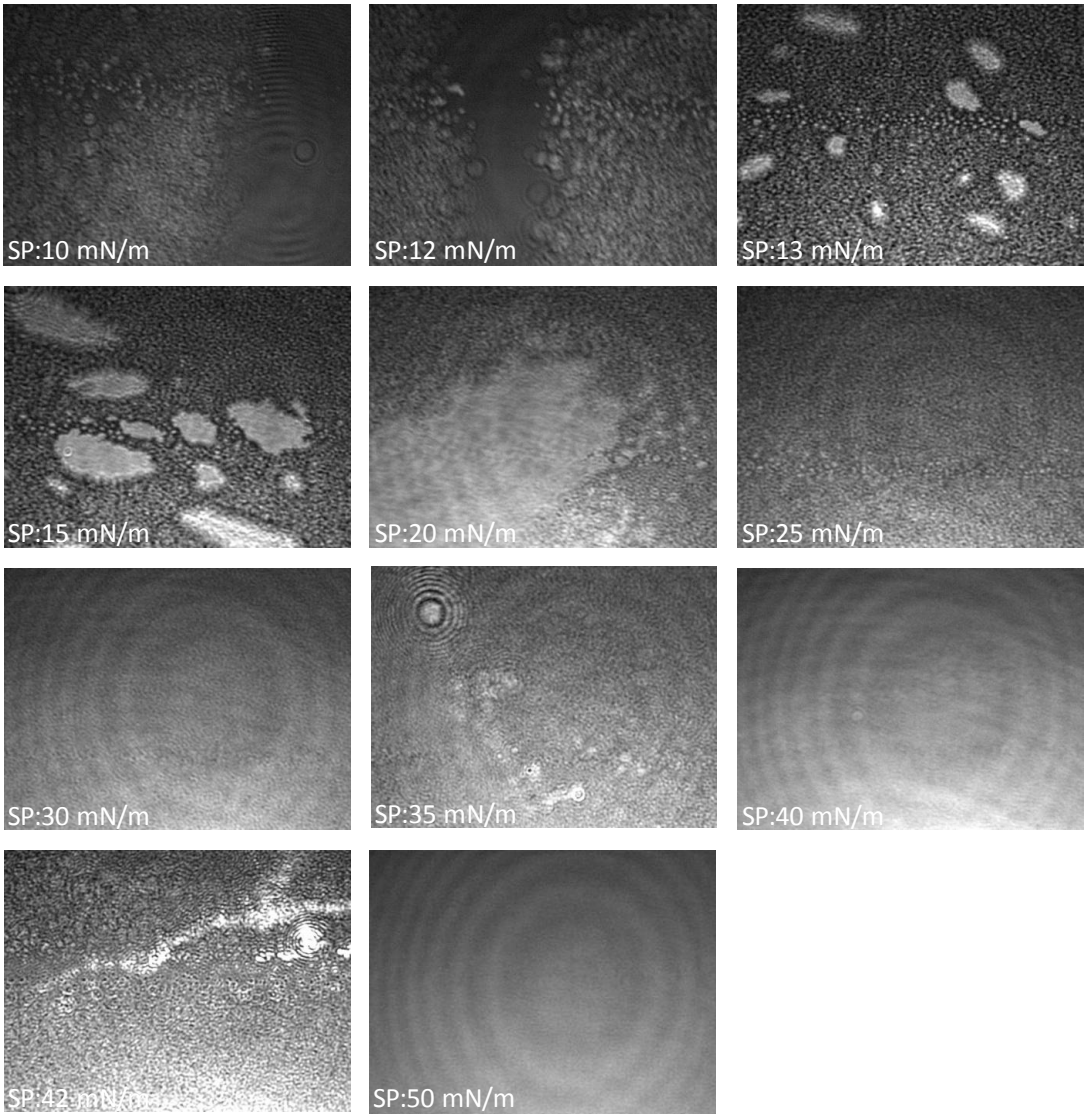

Figure 4.16. BAM images of 6:4 DSPC/PEG40 St mixed monolayer at the air-water interface

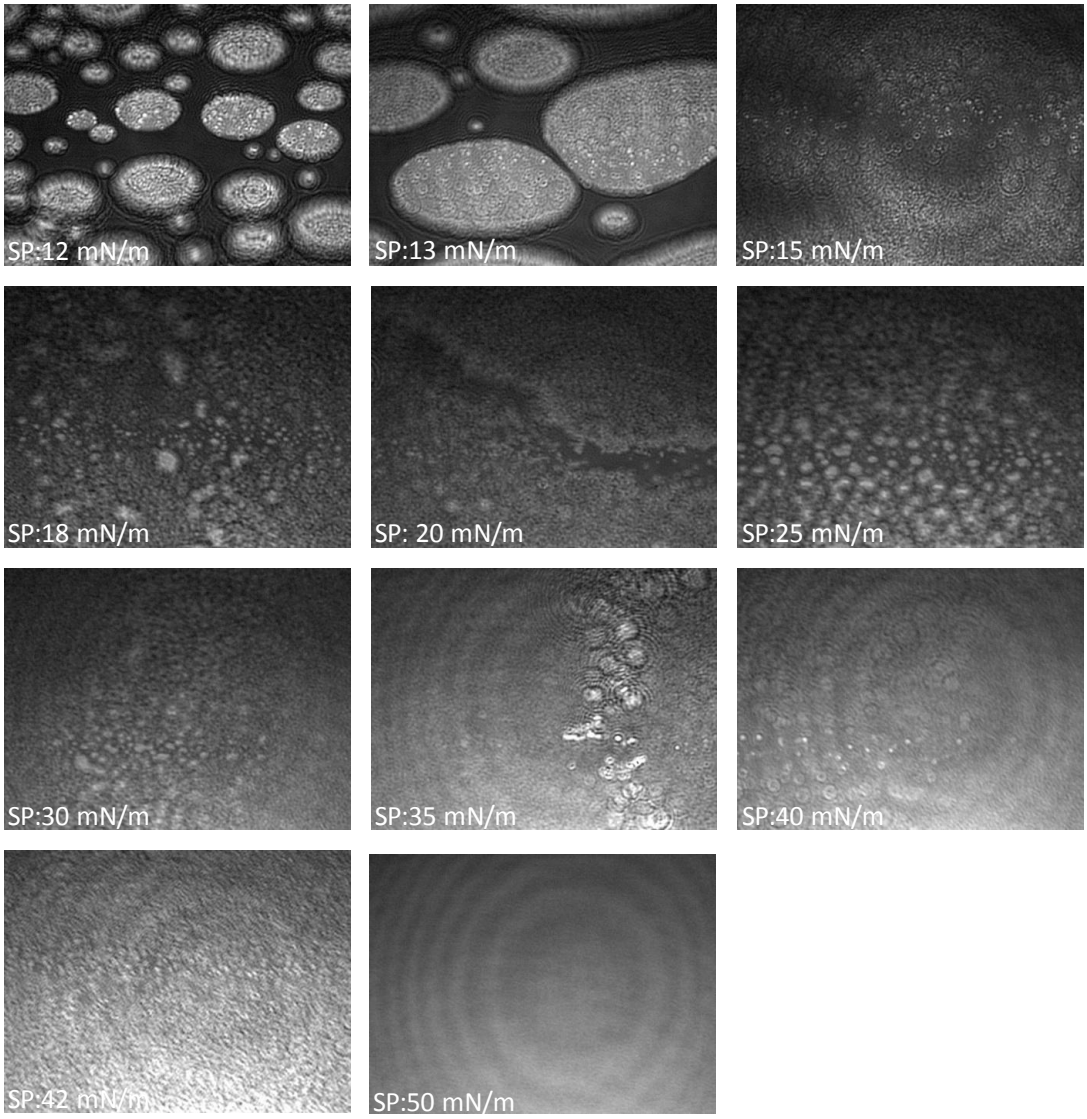

Figure 4.17. BAM images of 5:5 DSPC/PEG40 St mixed monolayer at the air-water interface

Atomic force microscopy was employed to examine the films transferred onto mica. The mixed films were transferred at 30 mN/m below the collapse pressure of PEG40 St and 40 mN/m above the collapse pressure of PEG40 St. Figure 4.18 shows AFM images of DSPC/PEG40 St mixed films at 30 mN/m. The AFM images of DSPC/PEG40 St mixed monolayer at 9:1 molar ratio demonstrated dark domains including small domains.The brighter small circular domains illustrated the morphology of PEG chains which did not cover the DSPC surface completely. Similarly, bright circular domain was also observed by *Kwangmeyung et al* for DPPC/ PEG lipid mixed monolayer (Kim, Kim et al. 2000). Further addition of PEG40 St to DSPC induced phase separation like detected for DSPC/DLPC mixed monolayer (Oguchi, Sakai et al.

2010). The phase separation of mixed monolayers increased with increasing mol fraction of PEG40 St up to DSPC/PEG40 St mixed monolayer at 5:5 molar ratio as illustrated in Figure 4.18. The separated phases and globular structures that DSPC and PEG40 St indeed form mostly individual domains with spaces in between and some small fraction were dissolved in each other. The distance of molecules in DSPC/PEG40 St mixed monolayer at 5:5 molar ratio was very large due to amount of PEG40 St and different phases were far away from each other which was good agreement with BAM images of this mixed monolayer. Therefore flower like shape of DSPC/PEG40 St mixed monolayer at 6:4 molar ratio demolished .Also, the morphology of DSPC/PEG40 St mixed monolayers at 40 mN/m were shown in Figure 4.19 and Figure 4.20. The images of DSPC/PEG40 St mixed monolayers demonstrated that the surfaces were not homogenous. PEG40 St molecules formed small circular domains whereas DSPC molecules existed in the matrix. For DSPC/PEG40 St mixed monolayer at 9:1 molar ratio it was noticed that PEG molecules could not cover the DSPC surface completely, so brighter DSPC rich regions were detected. When the concentration of PEG40 St was 30 mol % in the monolayer, PEG40 St molecules covered the phospholipid monolayer evenly. However, as seen clearly from AFM images of 5:5 DSPC/PEG40 St mixed monolayer phase separation increased with increasing PEG40 St content. In addition to the regions composed of DSPC and PEG40 St molecules exhibited big circular domains, dark PEG40 St rich regions appeared. The AFM images of DSPC/PEG40 St mixed monolayers assigned that DSPC and PEG40 St were not completely miscible in the conditions investigated here and phase separation was directly visualized. Additionally, AFM images of the mixtures at 40 mN/m provided sufficient experimental evidence for the presence of PEG40 St above the plateau region. Mixing of PEG40 St and DSPC promotes the staying of PEG40 St molecules in the monolayer.

BAM images of mixed monolayers at 9:1 and 5:5 molar ratios taken during compression-expansion cycles support this result. Although BAM images of mixed monolayer except 5:5 molar ratio at 40 mN/m displayed a homogeneous monolayer, AFM images at this surface pressure reveals that the monolayers in fact were not uniform. The reason for BAM images seems homogenous that nanometer scale lateral resolution of AFM provides a much more detailed image of the molecular presence of reorganization in the monolayer.

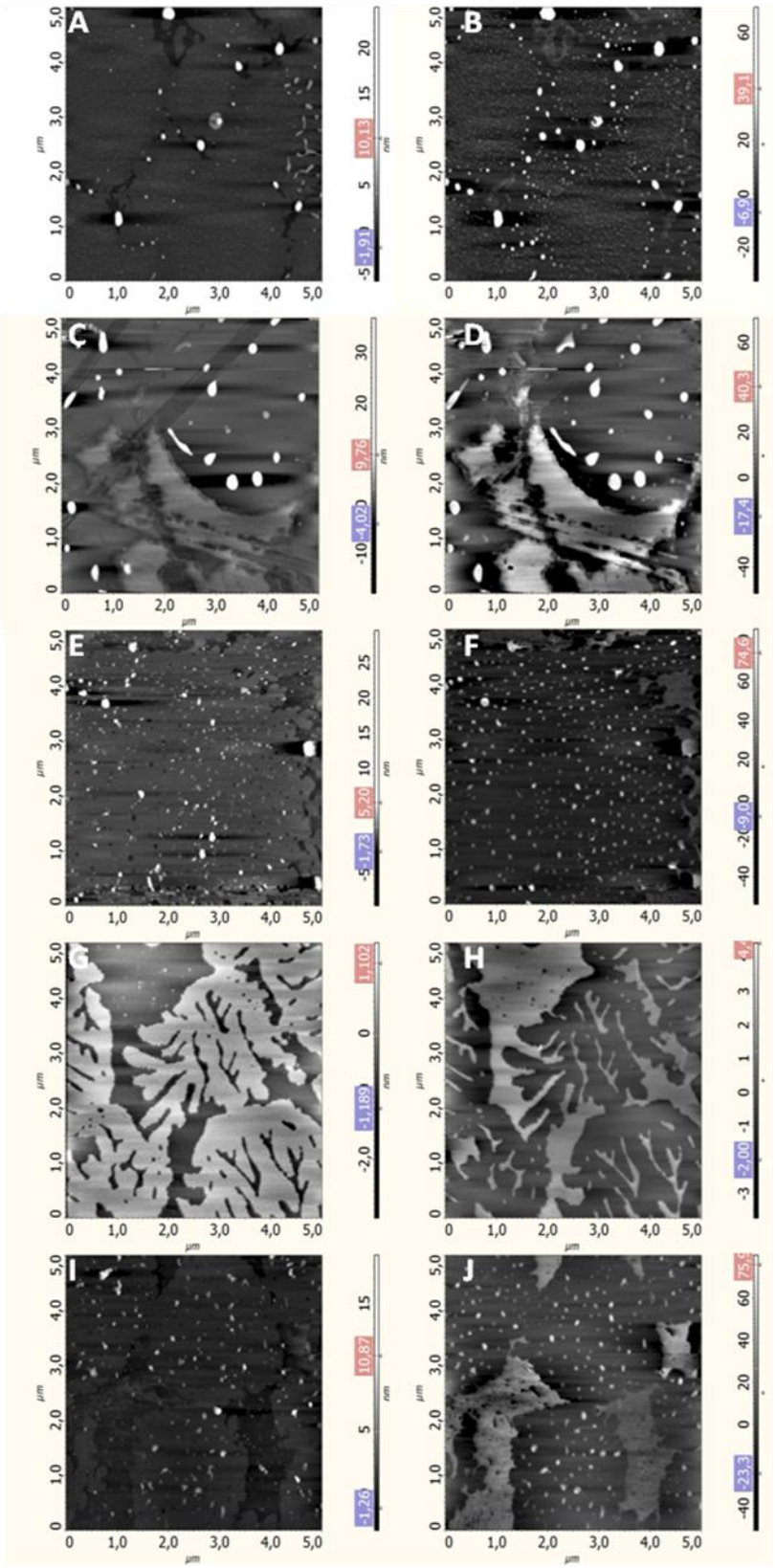

Figure 4.18. AFM topography (A,C,E,G,I) and phase (B,D,F,H,J) images (5x5 µm) of mixed DSPC/PEG40 St monolayers for 0.1 (A,B), 0.2 (C,D), 0.3 (E,F), 0.4 (G,H) and 0.5 (I,J) PEG40 St molar ratios at 30 mN/m

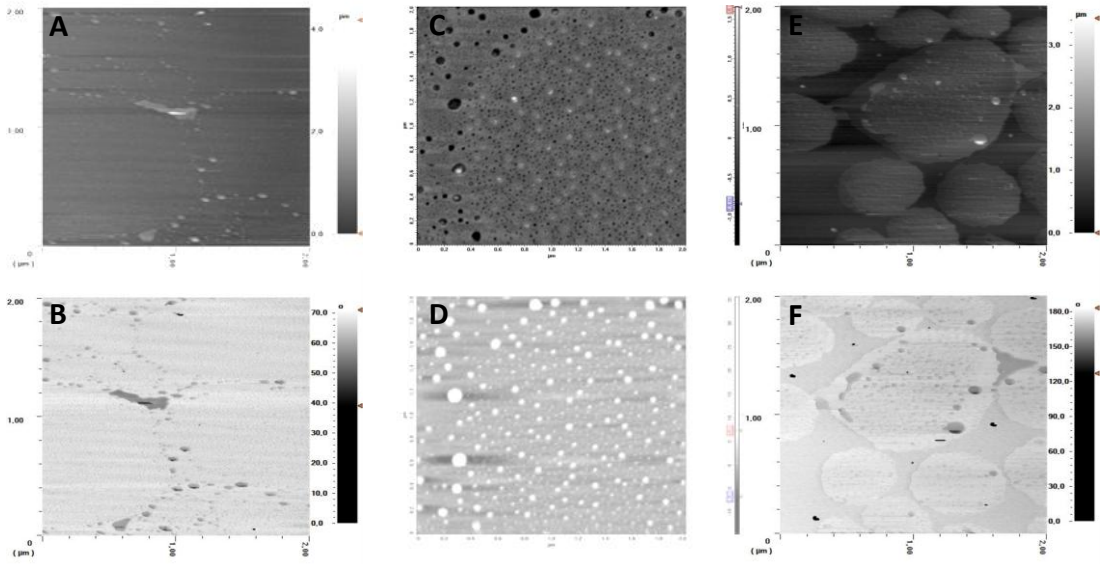

Figure 4.19. AFM topography (A,C,E) and phase (B,D,F) images (2x2 μm) of mixed DSPC/PEG40 St monolayers for 0.1 (A,B), 0.3 (C,D), 0.5 (E,F) PEG40 St molar ratios at 40 mN/m

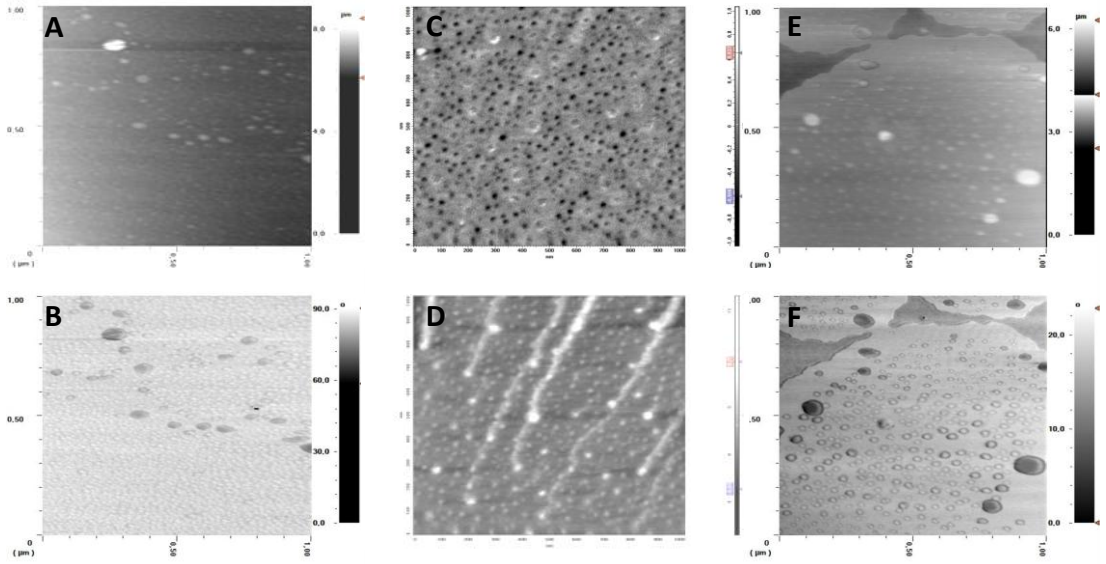

Figure 4.20. AFM topography (A,C,E) and phase (B,D,F) images (1x1 μm) of mixed DSPC/PEG40 St monolayers for 0.1 (A,B), 0.3 (C,D), 0.5 (E,F) PEG40 St molar ratios at 40 mN/m.

These LB, BAM and AFM results provide insight into phase behavior and molecular interactions of MBs shell components. Thermodynamically analysis of DSPC and PEG40 St molecules signified that these components were miscible and attractive forces between molecules dominant. However, when the BAM images and AFM

images of the mixed films were investigated, separated phases were detected. Possibility, at some regions of mixed monolayers PEG40 St molecules inserted into DSPC molecules and some regions composed of the condensed lipid-rich phase and less condensed emulsifier-rich phase. Additionally, BAM images of the mixed films taken during the cycles experiments and AFM images of the films coated at 40 mN/m demonstrated that PEG molecules showed conformational change and the surface was covered not only DSPC molecules but also PEG40 St molecules. PEG40 St molecules remained at the surface in regions composed of DSPC and PEG40 St due to conformational change of PEG chain and attractive forces between DSPC and PEG40 St.

4.1.2. The Effects of PEG-grafted Phospholipids on Shell Structure of Microbubbles

Although there are number of studies on phase behavior of DSPE-PEG2000, it's mixture with phospholipid such as DMPC, DSPC, DPPC and their effect on microbubble shell structure (Chou and Chu 2003, Borden, Martinez et al. 2006, Lozano and Longo 2009, Lozano and Longo 2009, Luna, Falcão et al. 2011), to our knowledge the effect of DSPE-PEG1000 and DSPE-PEG350 both as a monolayer at the air/water interface and as a microbubble shell material has not received any attention of the researchers. Therefore, the purpose of this section was that the investigation of DSPE-PEGn monolayers and their mixtures with DSPC to understand the effect of PEG chain length on monolayer phase behavior. In previous part of this study, it was shown that increasing content of emulsifier having single aliphatic chain, namely PEG40 St, had a positive effect on microbubble stability, so another purpose of this section was to assess the effect of having double aliphatic chain in the hydrocarbon part of the emulsifier on monolayer phase behavior and its potential effect on microbubble stability. For these purposes, DSPC/DSPE-PEGn mixtures at 9:1 and 5:5 molar ratios were prepared and investigated by Langmuir–Blodgett (LB) method and Brewster Angle Microscopy (BAM) similar to DSPC/PEG40 St mixtures.

4.1.2.1. Phase Behavior and Morphology of DSPC/DSPE-PEG2000 Binary Monolayers

DSPE-PEG2000 and DSPC/ DSPE-PEG2000 solutions readily spread at the air/water interface like poly (ethylene oxide) and most PEG-lipid conjugates which can form monolayer (Tsukanova and Salesse 2004). Monolayer characteristics at the air/water interface can be directly investigated via surface pressure versus mean area per molecule isotherms (π-A).Figure 4.21 demonstrates π-A isotherms of pure DSPE-PEG2000 and DSPC/DSPE-PEG2000 mixed monolayers. As seen in Figure 4.21, the surface pressure was detectable for DSPE-PEG2000 monolayer and DSPC/ DSPE-PEG2000 mixed monolayers at fairly large molecular areas due to the grafted polymeric chain. Pure DSPC monolayer formed more condensed film than pure DSPE-PEG2000 monolayer. The head group of DSPE-PEG2000 consists of a hydrophilic PEG chain that causes different phase behavior than DSPC at the air/water interface (Chou and Chu 2002).The isotherms of pure DSPE-PEG2000 monolayer showed more expanded behavior than pure DSPE and two transition regions which was good agreement with current literature (Baekmark, Elender et al. 1995, Majewski, Kuhl et al. 1997, Baekmark, Wiesenthal et al. 1999, Naumann, Brooks et al. 1999, Xu, Holland et al. 2001, Chou and Chu 2002, Chou and Chu 2003, Jebrail, Schmidt et al. 2008, Lozano and Longo 2009, Luna, Falcão et al. 2011). The low pressure transition region was observed nearly at 8 mN/m while the high pressure transition region was at nearly 19 mN/m. Same results for surface pressures of the transition regions were detected by *Naumann et al* (Naumann, Brooks et al. 1999). Generally, the low pressure transition is interpreted as a pancake-to-mushroom conformational change in the PEG chain, whereas the transition observed at high pressure is still as a matter of discussion (Naumann, Brooks et al. 1999, Xu, Holland et al. 2001, Tsukanova and Salesse 2003, Jebrail, Schmidt et al. 2008). Based on theoretical predictions by *de Gennes and Alexander, Baekmark et al* proposed that the high pressure transition is assigned as conformational transition of polymer chain a mushroom-to-brush (Baekmark, Elender et al. 1995). However, in a subsequent study *Baekmark et al* showed that this high pressure transition cannot be attributed to a mushroom-to-brush transition but it is correlated with strong local ordering of the lipopolymer CH_2 groups (Baekmark, Wiesenthal et al. 1999). Indeed, recent studies performed with PEG2000-grafted phospholipid monolayers at the air/water interface have demonstrated that the high

pressure transition in their isotherms is associated with the ordering of aliphatic chains in the phospholipid part of lipopolymer (Naumann, Brooks et al. 1999, Xu, Holland et al. 2001, Tanwir and Tsoukanova 2008, Lozano and Longo 2009).Our results for pure DSPE-PEG2000 was similar to these observations. At low surface pressures the distance between the molecules was large since PEG chains were adsorbed to the water surface and formed a flat so-called pancake structure.

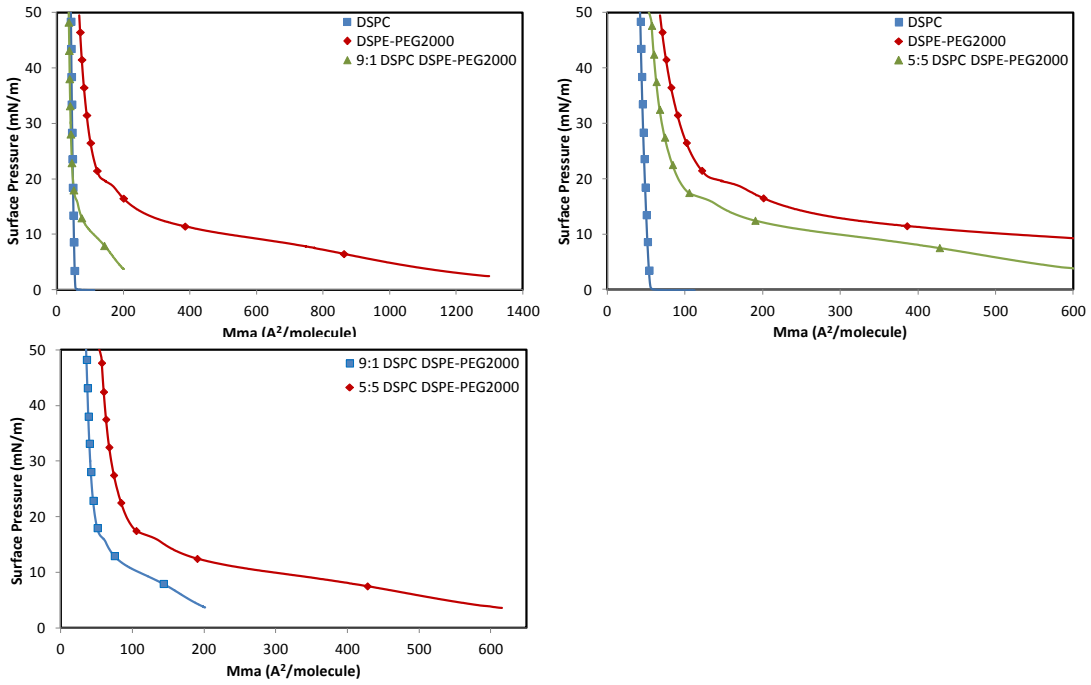

Figure 4.21. The surface pressure –mean molecular area (π-A) isotherms for pure and DSPC/DSPE-PEG2000 mixed monolayers at the air/water interface

The conformation of the polymer chains exerts a repulsive force dependent on polymer chain size and below the high pressure transition region lateral interactions between alkyl chain do not play significant role (Baekmark, Wiesenthal et al. 1999). On increasing the surface pressure the polymer chains desorbed from the water surface and this low pressure transition region indicated that a change in conformation in the polymer head group of DSPE-PEG2000 known as a pancake-to-mushroom transition. Above the region, PEG chains submerged in subphase and buried underneath the monolayer. Furthermore, the pressure reaching the high pressure transition plateau corresponded to orientation of the aliphatic chains and aliphatic chain condensation which may be possible after the PEG chains undergo a conformational transition to

pseudobrushes and they were more stretched towards the water. Therefore, the spatial barrier holding the aliphatic chains at separated distance is eliminated and the aliphatic chains can be brought close to each other. Also, in this region the cohesive forces between aliphatic chains is balanced by the PEG molecules in the water (Xu, Holland et al. 2001, Tanwir and Tsoukanova 2008).

As shown in Figure 4.21, isotherms of the mixed monolayers of DSPC/ DSPE-PEG2000 at two different molar ratios (9:1, 5:5 DSPC/ DSPE-PEG2000) showed more expanded behavior than pure DSPC and fell between the two pure components' isotherms. Similar to pure DSPE-PEG2000 isotherm the mixed monolayers isotherms of DSPC/ DSPE-PEG2000 at 9:1 and at 5:5 molar ratios illustrated two transition regions nearly at 8 mN/m and 16 mN/m respectively. The low pressure transition region of mixed monolayers was attributed to structural change in grafted PEG2000 chains. Moreover, in the high pressure transition region aliphatic chains of DSPE-PEG2000 became more ordered and cohesive interactions between aliphatic chains (C_{18} chains) of DSPC and DSPE-PEG2000 increased (Tanwir and Tsoukanova 2008, Lozano and Longo 2009, Stepniewski, Pasenkiewicz-Gierula et al. 2011).Another observation was that the high pressure transition region of mixed monolayers became more broaden and the mean molecular occupied area shifted towards larger area with increasing amount of DSPE-PEG2000.These results indicated that the presence of DSPE-PEG2000 made the mixed monolayers more expanded than pure DSPC due to random PEG side chains (Chou and Chu 2002, Chou and Chu 2003, Tanwir and Tsoukanova 2008).

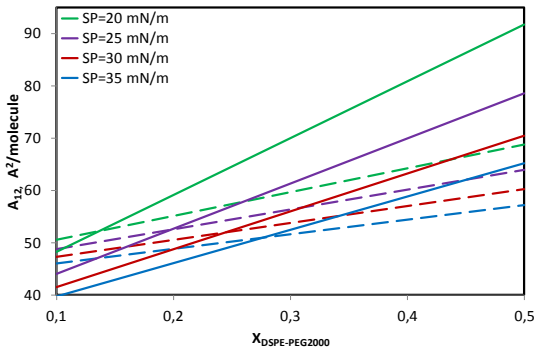

Figure 4.22. The mean molecular area (A_{12}) vs. $x_{DSPE\text{-}PEG2000}$ plots for DSPC/DSPE-PEG2000 mixed monolayers

A_{ideal} and A_{exc} values for DSPE-PEG2000 mixed monolayers were calculated based on Equation 3.1 and Equation 3.2 respectively. Figure 4.22 demonstrates that the

deviation of real mean molecular area (A_{12}) of the mixed monolayer from ideality at different surface pressures. A_{12} values are given in as a function of mol fraction of DSPE-PEG2000 and dashed lines represent the calculated A_{ideal}. As seen from Figure 4.22, the real mean molecular areas (A_{12}) at various surface pressures were different from the calculated A_{ideal} .These results were similar to earlier observations showing that DSPC and DSPE-PEG2000 exhibited nonideal mixed behavior and miscible at the air/water interface (Chou and Chu 2002, Chou and Chu 2003, Tanwir and Tsoukanova 2008).

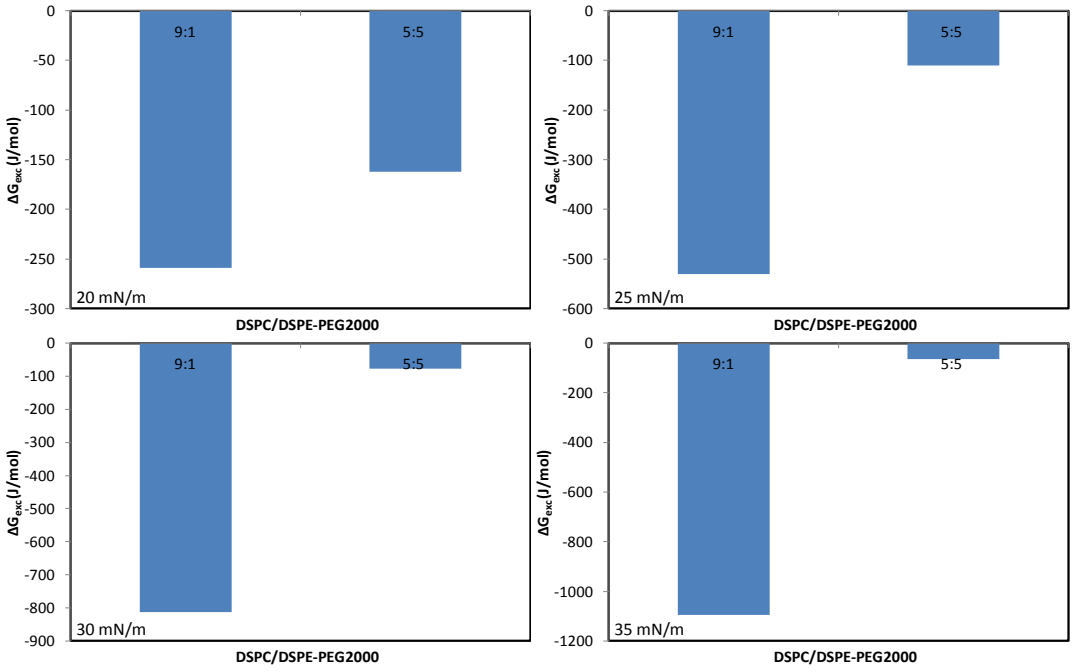

Figure 4.23. The excess free energy of mixing (ΔG_{exc}) values of DSPC/DSPE-PEG2000 mixed monolayers at different surface pressure

In Figure 4.23, the excess free energies of mixed monolayers (ΔG_{exc}) were plotted at different surface pressures. Obviously, the excess free energies of these binary mixed systems were negative which indicated the presence of attractive interaction between molecules. These characteristics of the mixed monolayers were in good agreement with those observed previously in various PC/PE-PEG2000 systems (Chou and Chu 2002, Chou and Chu 2003). The molecules in DSPC/DSPE-PEG2000 mixed monolayer couldn't get close to each other with increasing DSPE-PEG2000 amount due to expansion and repulsive effect of PEG chain. Therefore ΔG_{exc} value of DSPC/DSPE-

PEG2000 mixed monolayer at 5:5 molar ratio was less negative than the value of mixed monolayer at 9:1 molar ratio and the interaction between molecules were weaker.

The compression modulus (C_s^{-1}) values of pure components' monolayers and DSPC/ DSPE-PEG2000 mixed monolayers at the air/water interface were given in Figure 4.24. The compressibility of a monolayer at two-dimensional plane is an indicative of the film elasticity(Chou and Chu 2002).It was observed that pure DSPE-PEG2000 monolayer exhibited more compressible behavior than pure DSPC monolayer owing to extensive PEG chain. The C_s^{-1} plots of mixed monolayers were situated between the C_s^{-1} plots for pure components. Also as expected, the compressibility of mixed monolayers increased with increasing DSPE-PEG2000 amount. These results demonstrated that the incorporation of DSPE-PEG2000 to DSPC monolayer made the monolayers more compressible as observed previously by other researchers (Chou and Chu 2002, Chou and Chu 2003, Lozano and Longo 2009). Another observation was that pure DSPE-PEG2000 and DSPC/ DSPE-PEG2000 mixed monolayers showed two minimum peaks corresponding to transition regions of the isotherms given in Figure 4.21. The first peak seen at low surface pressure supported that the change in conformation in the polymer headgroup of DSPE-PEG2000 similarly observed by *Lozano and Longo* (Lozano and Longo 2009) and the second peaks at high surface pressure indicated that alkyl chain orientation.

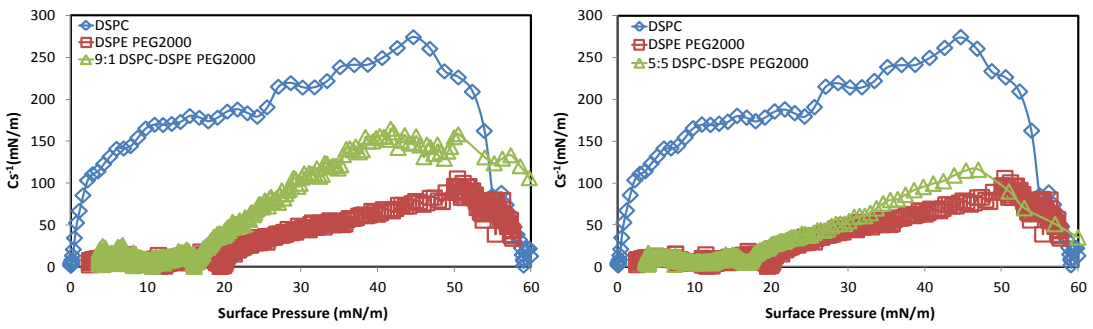

Figure 4.24. The compression modulus (C_s^{-1}) values of pure components and DSPC/DSPE-PEG2000 mixed monolayers at different surface pressure

BAM images of pure and mixed monolayers were taken at different surface pressures. During monitoring the BAM images the focus was set in the middle of the image. The corresponding BAM images of pure DSPE-PEG2000 is seen in Figure 4.25.

At low surface pressures the images were very dark for pure DSPE-PEG2000 film. The darkness of the images signifies that the film was either very thin or the density of the molecules very low (Stepniewski, Pasenkiewicz-Gierula et al. 2011). The monolayer became more visible with raising surface pressures and bright grains appeared. Structures at nearly 9 mN/m denoted that the PEG chains passed from pancake to mushroom region and these chains extend towards the water subphase. Then the morphology remained the same in the entire region up to the maximum pressure. Similar morphological changes were detected for DPPE-PEG2000 and DSPE-PEG2000 monolayers by *Jebrail et al* (Jebrail, Schmidt et al. 2008). The results of BAM experiments of the mixed monolayer of DSPC/ DSPE-PEG2000 at 9:1 molar ratio can be seen in Figure 4.26. Homogeneous surface morphology was detected at low surface pressures. Upon compression, small bright domains which might occur due to PEG chains and alkyl chain orientation appeared at nearly 9 mN/m and at nearly 16 mN/m. Then the monolayer became more homogenous with increasing surface pressure. Figure 4.27 demonstrates BAM images of the mixed monolayer of DSPC/ DSPE-PEG2000 at 5:5 molar ratio. In this mixture the amount of DSPE-PEG2000 was higher, so the molecules get together late due to expansion effect of PEG chain and at lower surface pressures the dark regions were seen clearly. Similar to the BAM results of the mixed monolayer of DSPC/ DSPE-PEG2000 at 9:1 molar ratio bright small domains were observed at nearly 9 mN/m and at nearly 16 mN/m for the mixed monolayer of DSPC/ DSPE-PEG2000 at 5:5 molar ratio and the monolayer became more homogeneous with compression as shown Figure 4.27. As seen in BAM images of mixed monolayers the bright circular domains might indicate that individual domains or dissolved molecules in each other. Additionally, Atomic force microscopy was employed to examine the mixed films at 9:1 and 5:5 molar ratios detailed. Even though BAM images at 30 mN/m showed homogeneous surfaces, as seen in Figure 4.28 that phase separation was directly visualized by AFM for mixed DSPC/ DSPE-PEG2000 for 0.1 and 0.5 DSPE-PEG2000 molar ratios.

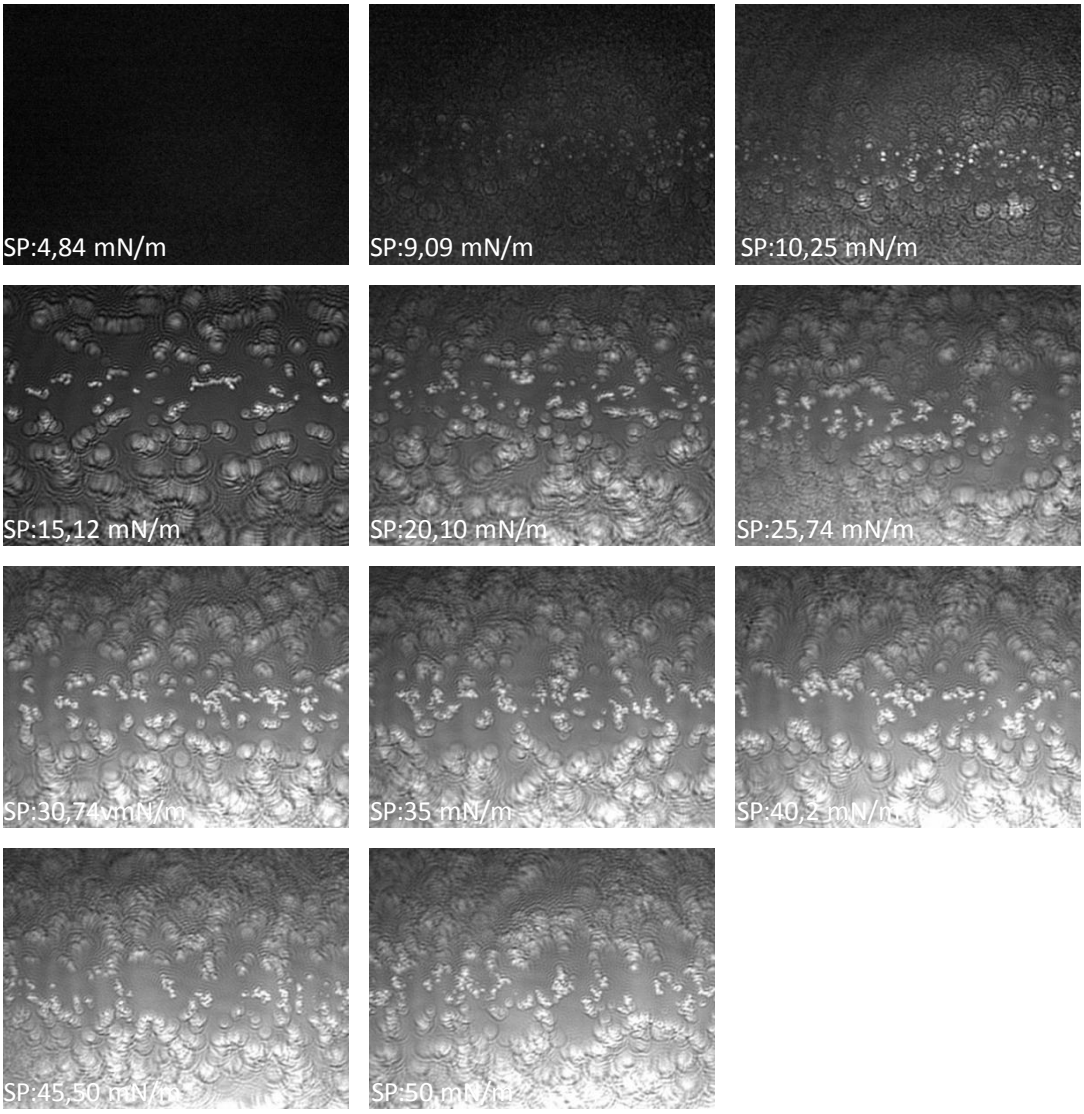

Figure 4.25. BAM images of pure DSPE-PEG2000 monolayer at the air-water interface

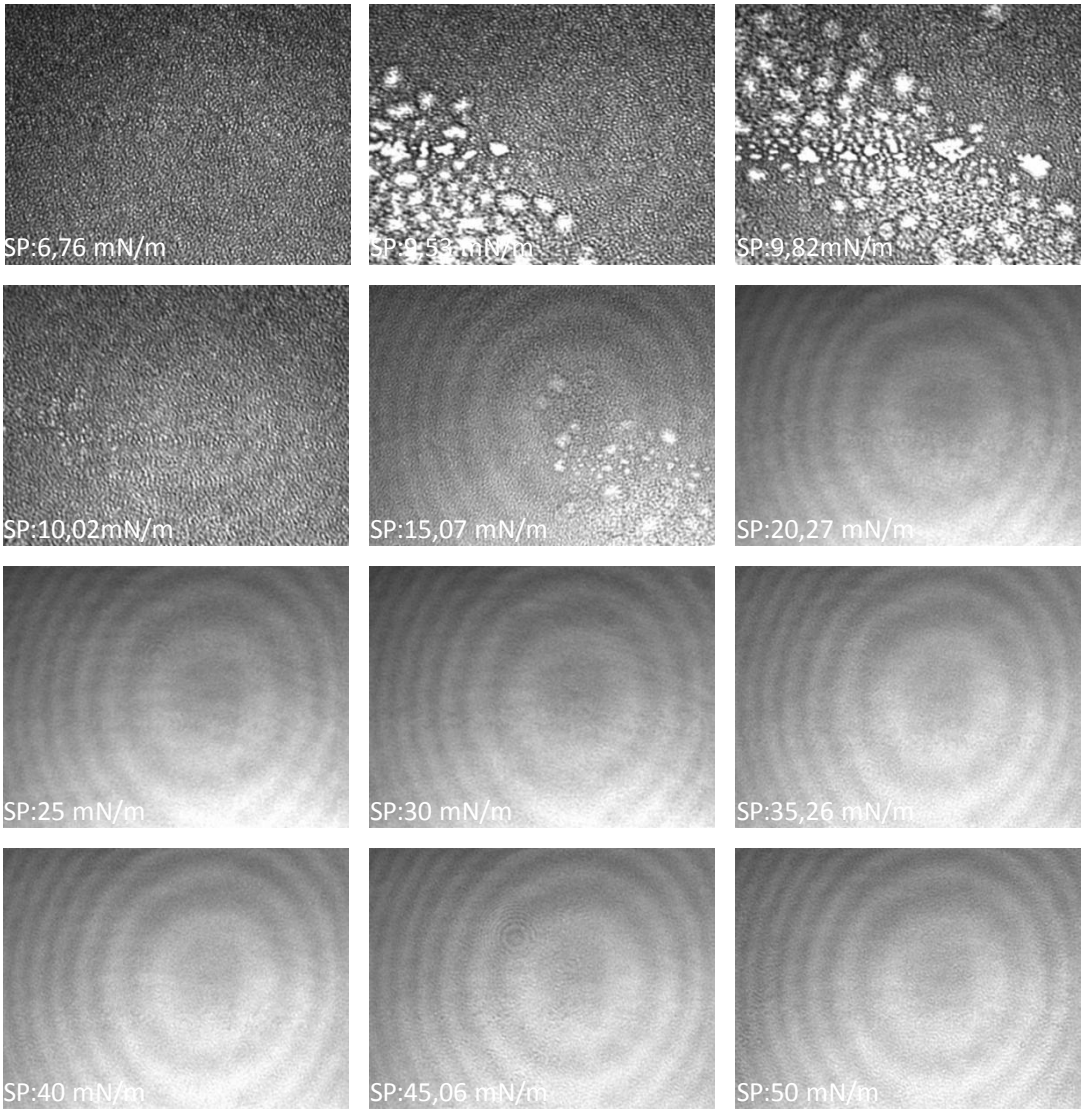

Figure 4.26. BAM images of 9:1 DSPC/DSPE-PEG2000 mixed monolayer at the air-water interface

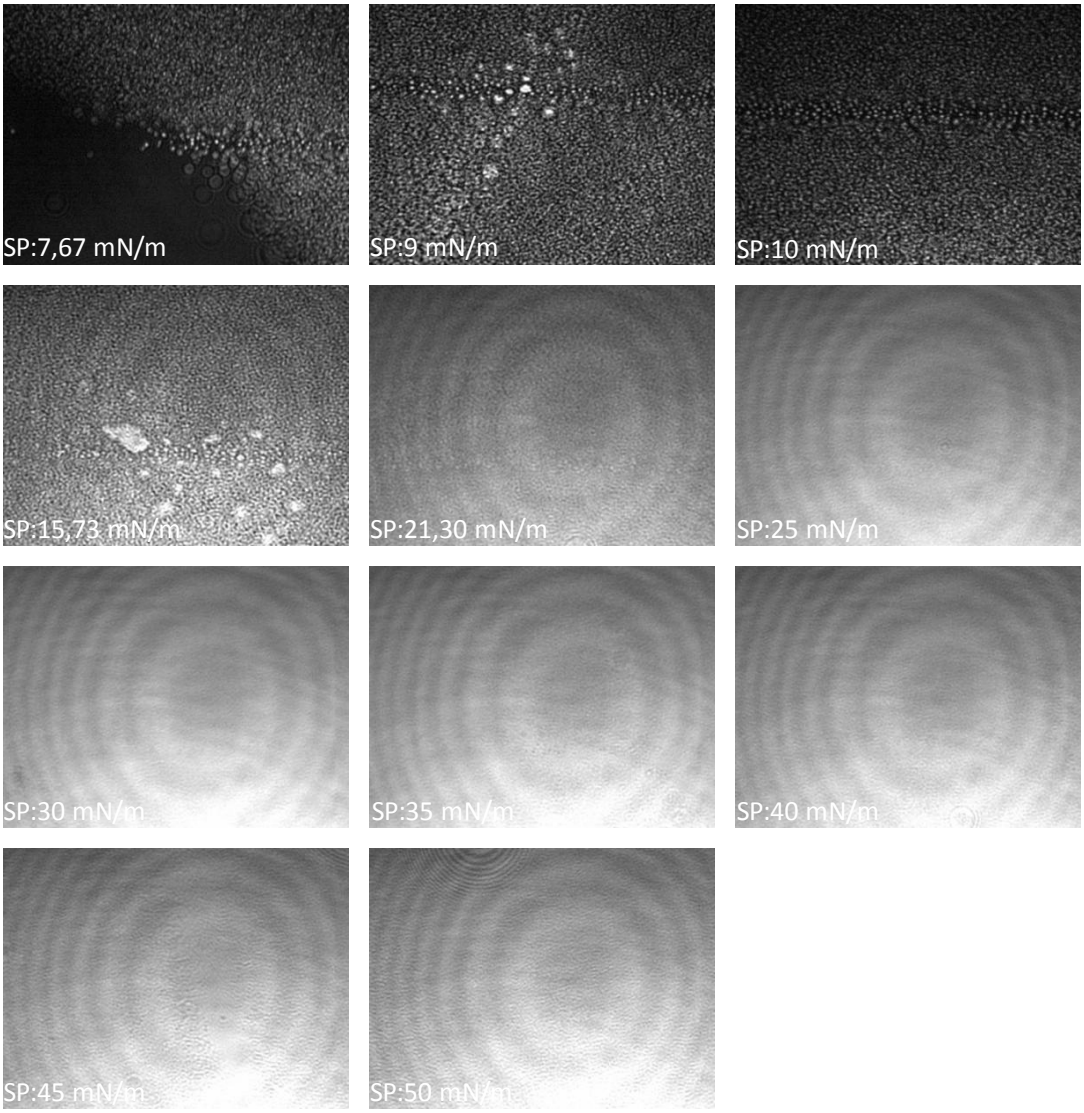

Figure 4.27. BAM images of 5:5 DSPC/DSPE-PEG2000 mixed monolayer at the air-water interface

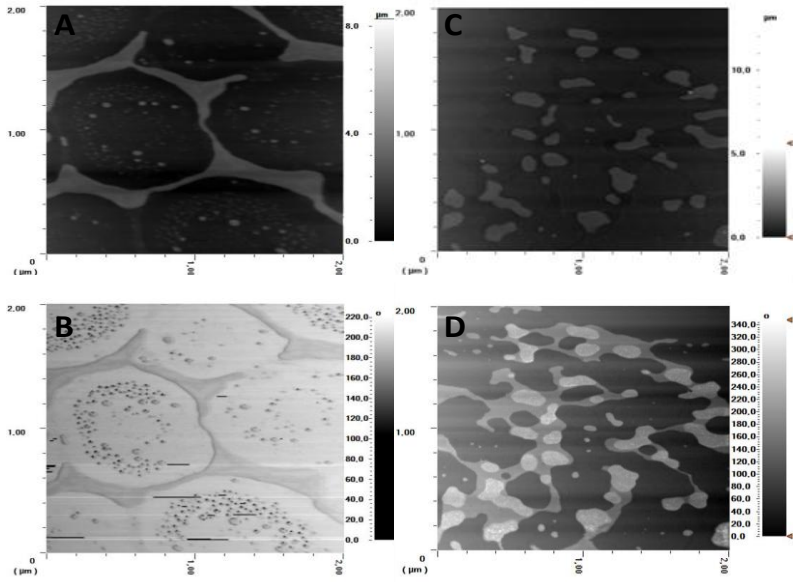

Figure 4.28. AFM topography (A,C) and phase (B,D) images (2x2 μm) of mixed DSPC/DSPE-PEG2000 monolayers for 0.1 (A,B), 0.5 (C,D) DSPE-PEG2000 molar ratios at 40 mN/m.

4.1.2.2. Phase Behavior and Morphology of DSPC/DSPE-PEG1000 Binary Monolayers

For pure DSPE-PEG1000 and DSPC/DSPE-PEG1000 binary systems the surface surface pressure (π) versus mean area per molecule (A) isotherms were produced using LB technique. Figure 4.29 illustrates π-A isotherms of pure DSPC, pure DSPE-PEG1000 and their mixed monolayer at two different molar ratios**.** The pure DSPE-PEG1000 monolayer showed less expanded behavior than the pure DSPE-PEG2000 monolayer. As seen in Figure 4.29, mean molecular areas of pure DSPE-PEG1000 monolayer were smaller compared to pure DSPE-PEG2000 monolayer at same surface pressures due to the short PEG chain in the head group of DSPE-PEG1000. The incorporation of DSPE-PEG1000 into DSPC made the mixed monolayer more expanded than pure DSPC monolayer as with DSPE-PEG2000.The low transition region interpreted as a pancake-to-mushroom conformational change in the PEG chain were observed in the isotherms of the mixed DSPC/DSPE-PEG1000 monolayers and the pure DSPE-PEG1000 monolayer nearly at 8 mN/m. In addition to the high transition regions which indicate that the ordering of aliphatic chains in the phospholipid part of DSPE-PEG1000 nearly at 18 mN/m were detected for pure DSPE-PEG1000 monolayer

while nearly at 16 mN/m the monolayers. The transition regions of the mixed monolayers became distinctive and isotherms located at large mean molecular areas with increasing amount of DSPE-PEG1000 because of repulsive interactions between hydrophilic PEG chains.

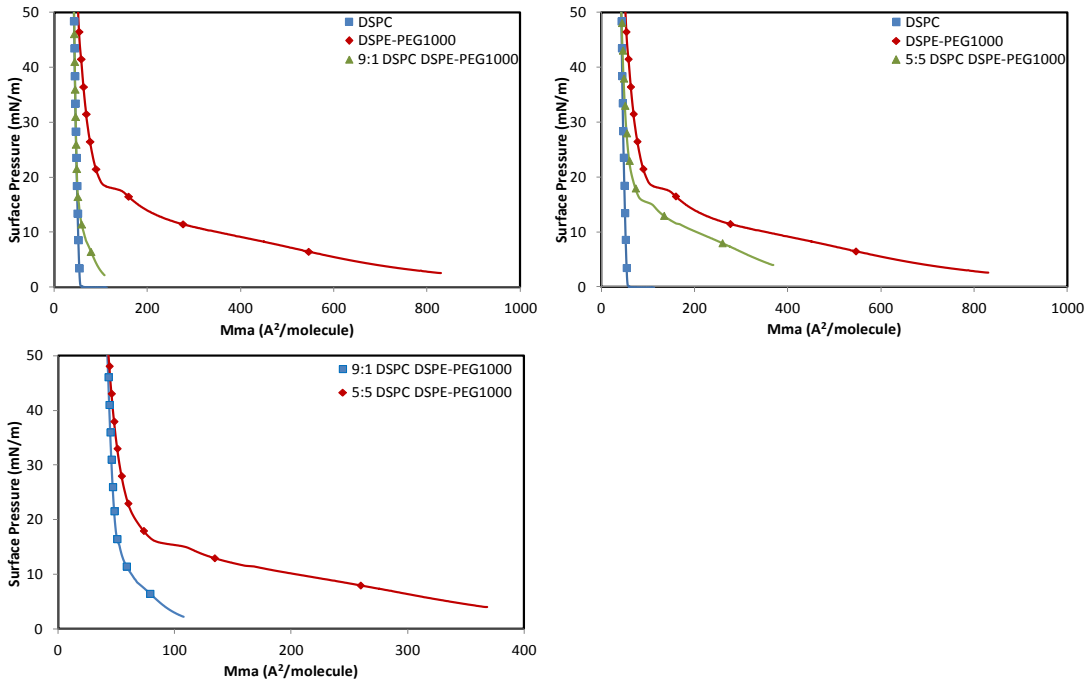

Figure 4.29. The surface pressure –mean molecular area (π-A) isotherms for pure and DSPC/DSPE-PEG1000 mixed monolayers at the air/water interface

The calculated A_{ideal} and A_{exc} values for DSPE-PEG1000 mixed monolayers were given in Figure 4.30.The dashed lines signifies the the calculated A_{ideal} and A_{12} values are given in as a function of mol fraction of DSPE-PEG1000. As seen in Figure 4.30, the deviations of real mean molecular area (A_{12}) of mixed monolayer from ideality were noticed at different surface pressures. In this case DSPC and DSPE-PEG1000 molecules showed nonideal mixture behavior and they were miscible at the air/water interface likewise the results obtained for DSPC/ DSPE-PEG2000 mixed monolayers (Chou and Chu 2002, Chou and Chu 2003, Tanwir and Tsoukanova 2008).

The excess free energies of mixed monolayers (ΔG_{exc}) calculated to obtain information about the type of molecular interaction between DSPC and DSPE-PEG1000 molecules are demonstrated in Figure 4.31. The ΔG_{exc} values of DSPC/DSPE-PEG1000 mixed monolayers were negative, so attractive interactions

between these molecules were dominant. As contrast to DSPC/DSPE-PEG2000 mixed monolayers, the greatest negative ΔG_{exc} values of DSPC/DSPE-PEG1000 mixed monolayer were observed at 5:5 molar ratio and at this ratio molecular interaction could be stronger. The reason of this situation might be that the short PEG chains of DSPE-PEG1000 molecules did not prevent the interactions of DSPC and DSPE-PEG1000 molecules and these molecules could get together and interact each other.

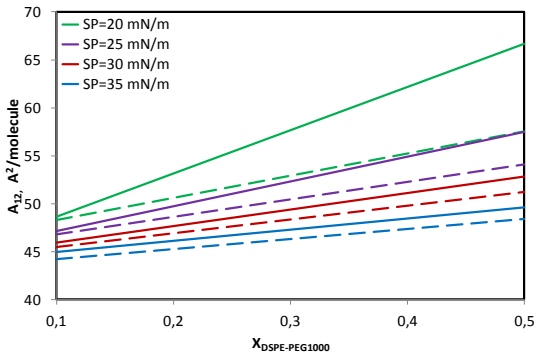

Figure 4.30. The mean molecular area (A_{12}) vs. $x_{DSPE\text{-}PEG1000}$ plots for DSPC/DSPE-PEG1000 mixed monolayers

To investigate the compressibility of pure DSPE-PEG1000 and DSPC/DSPE-PEG1000 mixed monolayers at the air/water interface the compression modulus (C_s^{-1}) values of the monolayers were evaluated (Figure 4.32). The pure DSPE-PEG1000 monolayer exhibited lower compression modulus value than pure DSPC and made the mixed monolayers compressible due to widespread PEG chain. Also, two minimum peaks which represent the transition regions observed in pure DSPE-PEG1000 and DSPC/DSPE-PEG1000 mixed monolayers' isotherms were noticed as in the monolayers containing DSPE-PEG2000.

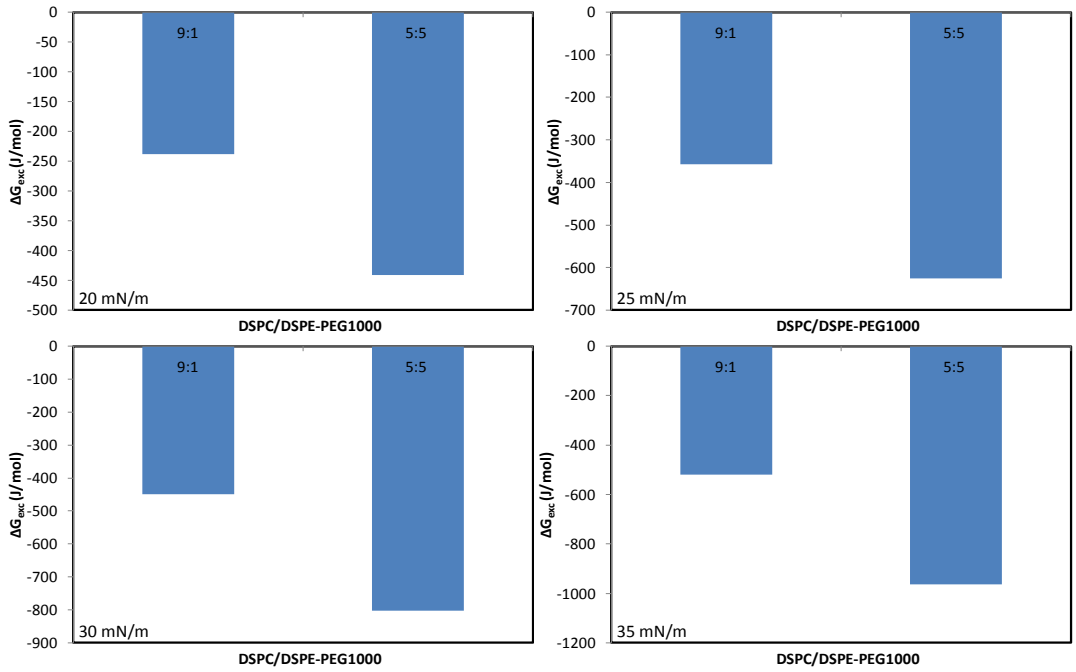

Figure 4.31. The excess free energy of mixing (ΔG_{exc}) values of DSPC/DSPE-PEG1000 mixed monolayers at different surface pressure

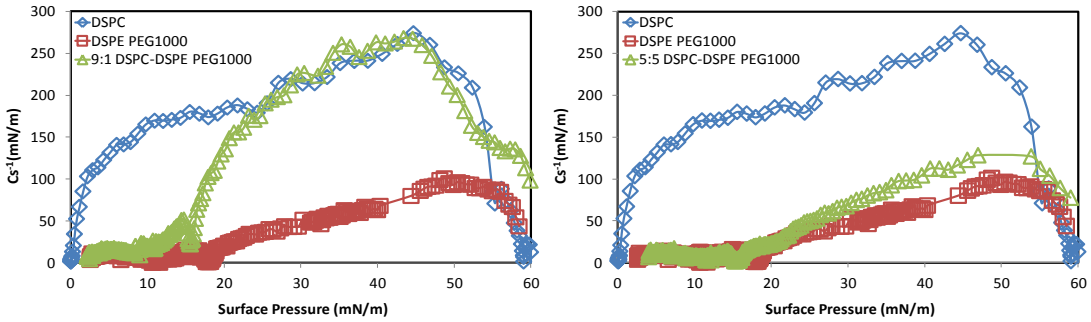

Figure 4.32. The compression modulus (C_s^{-1}) values of pure components and DSPC/DSPE-PEG1000 mixed monolayers at different surface pressure

BAM images of pure DSPE-PEG1000 monolayer taken at various surface pressures during compression are shown in Figure 4.33. At large mean molecular areas the images were dark and small bright spots appeared. Presumably, PEG chains arranged and the hydrocarbon chains were positioned more vertical to the surface with compression, so these spots gradually get together and were noticed clearly. Then the monolayer became more homogeneous than pure DSPE-PEG2000 monolayer but the small bright spots were seen up to high surface pressures. BAM images observed on the

DSPC/DSPE-PEG1000 mixed monolayer at 9:1 molar ratio are given in Figure 4.34. These images resemble BAM images of DSPC/DSPE-PEG2000 mixed monolayer at 9:1 molar ratio .At low pressure region circular domains that were brighter than the surrounding area were seen and then homogeneous surface was detected as a result of the compression. The uniformly bright images can indicate that a more well defined molecular arrangement (Brandal, Viitala et al. 2007). The morphology of DSPC/DSPE-PEG1000 mixed monolayer at 5:5 molar ratio shown in Figure 4.35 is similar to BAM images of DSPC/DSPE-PEG2000 mixed monolayer with 50% of DSPE-PEG2000 on air/water interface. The distances between molecules were larger due to a lot of PEG chains and dark regions were detected at low surface pressures. Also, the bright domains emerged at nearly low and high pressure transition regions. Addition to these results, to obtain more information about phase behaviors at the surface AFM images of DSPC/DSPE-PEG1000 mixed monolayers at 9:1 and 5:5 molar ratios were taken. As seen in Figure 4.36, unlike observations of BAM images at 30mN/m, AFM images at this surface pressure showed non-homogenous surface which might indicate that DSPC and DSPE-PEG1000 molecules were partially miscible.

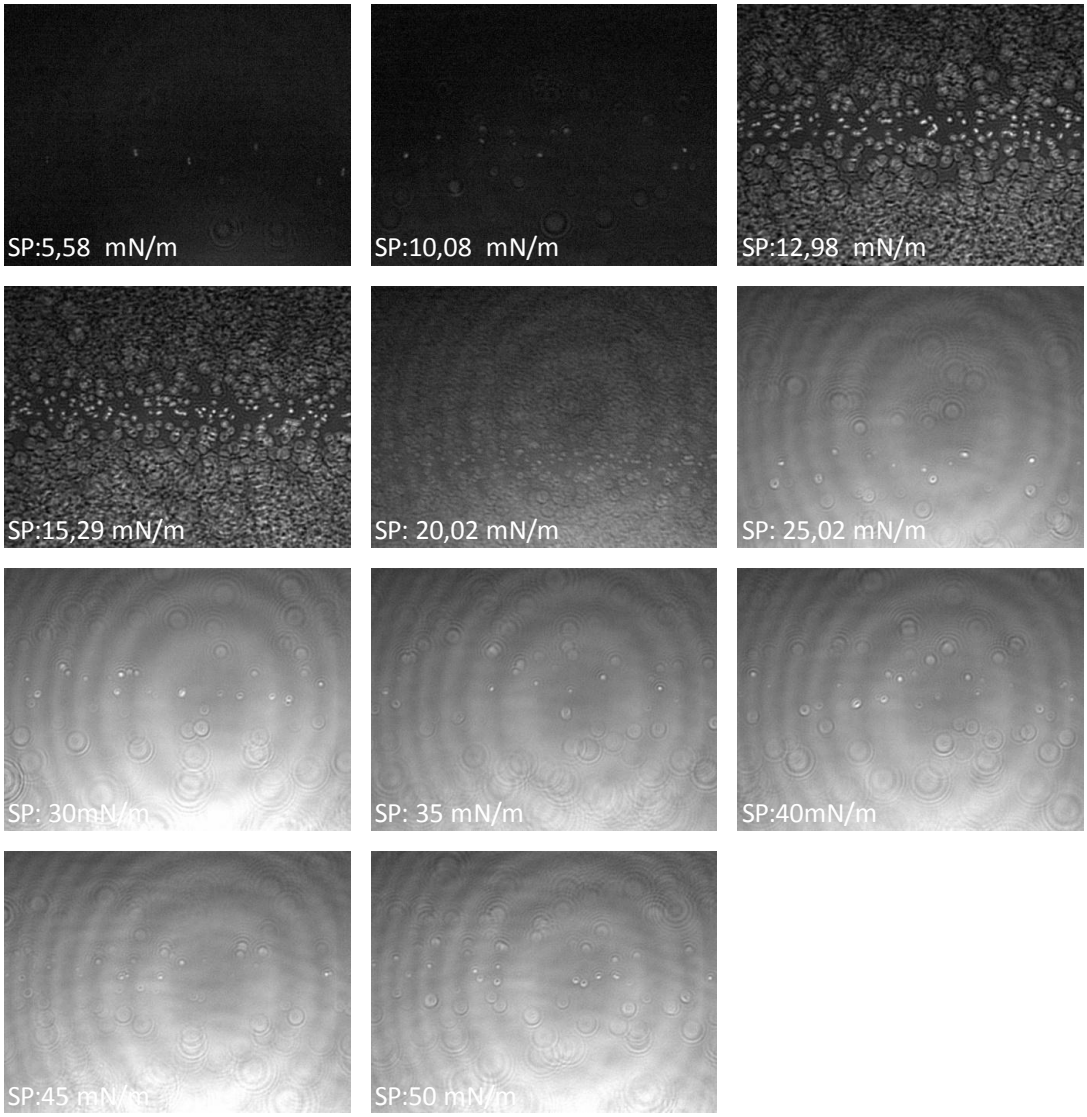

Figure 4.33. BAM images of pure DSPE-PEG1000 monolayer at the air-water interface

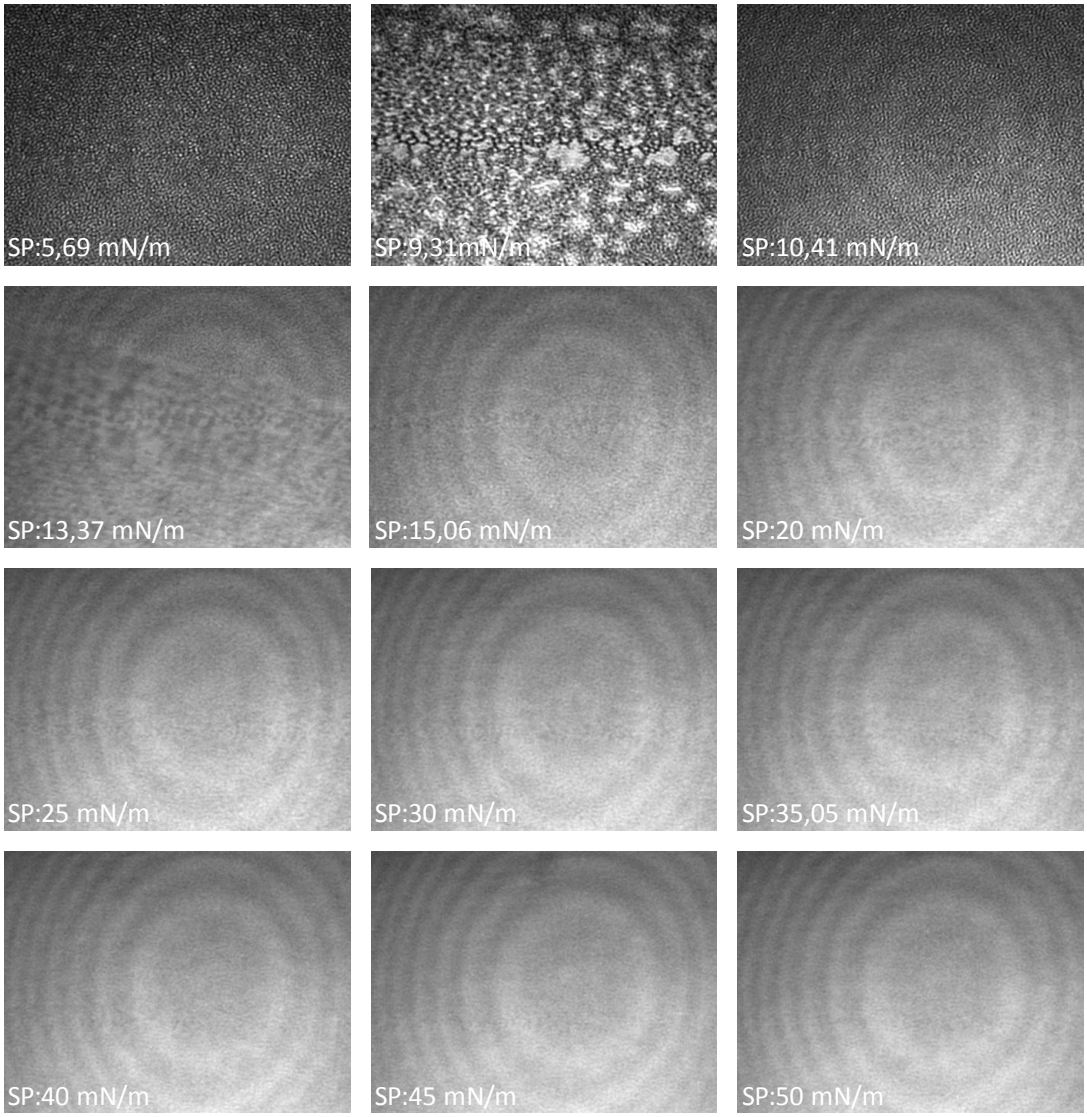

Figure 4.34. BAM images of 9:1 DSPC/DSPE-PEG1000 mixed monolayer at the air-water interface

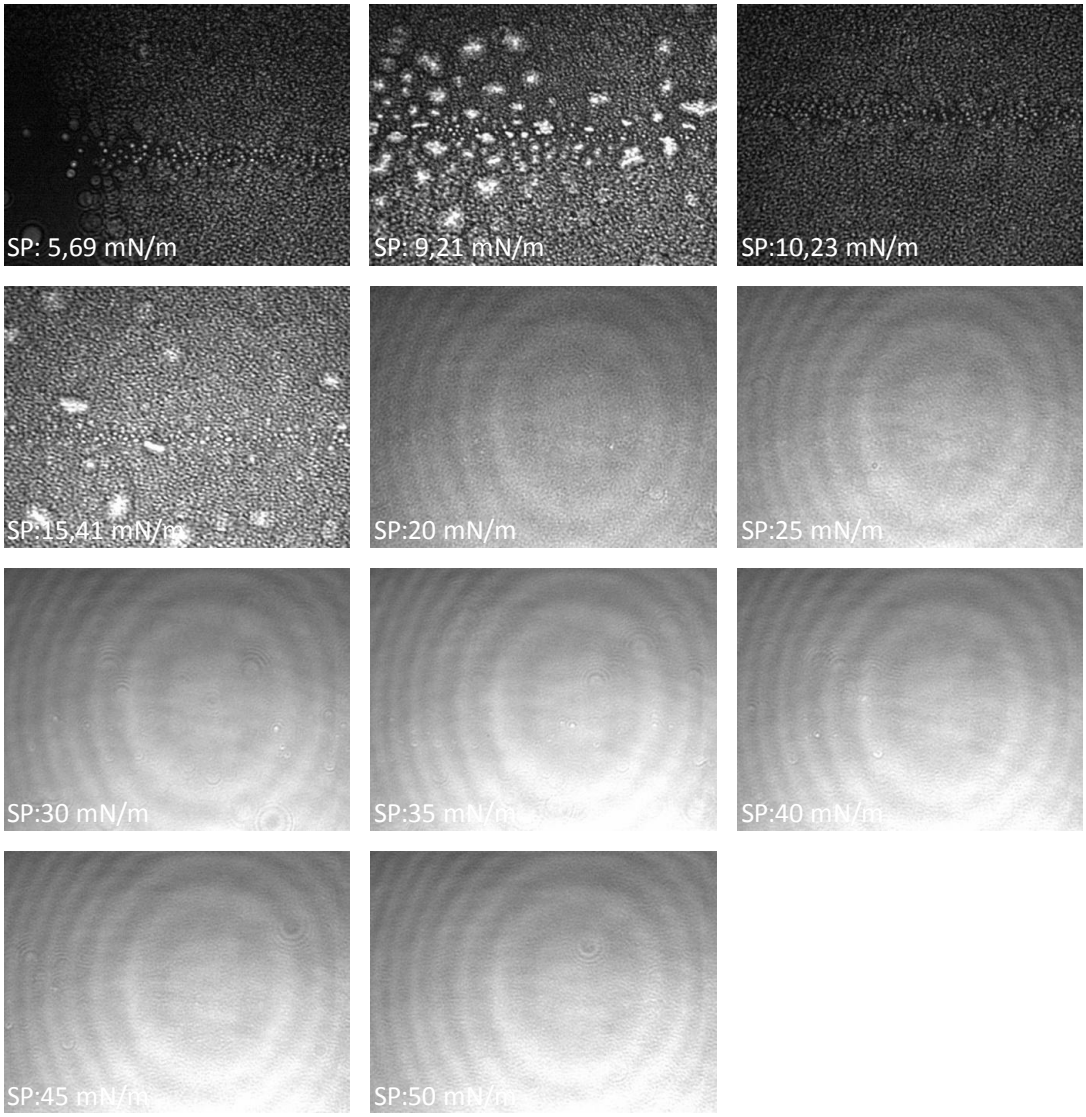

Figure 4.35. BAM images of 5:5 DSPC/DSPE-PEG1000 mixed monolayer at the air-water interface

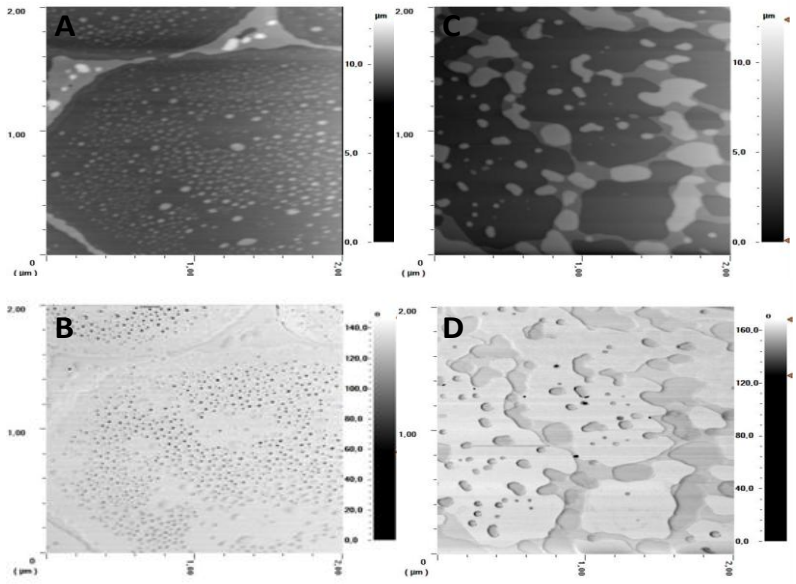

Figure 4.36. AFM topography (A,C) and phase (B,D) images (2x2 µm) of mixed DSPC/DSPE-PEG1000 monolayers for 0.1 (A,B), 0.5 (C,D) DSPE-PEG1000 molar ratios at 40 mN/m.

4.1.2.3. Phase Behavior and Morphology of DSPC/DSPE-PEG350 Binary Monolayers

The changes of surface pressures with area per molecule for pure DSPE-PEG350 and DSPC/DSPE-PEG350 mixed monolayer were shown in Figure 4.37. Pure DSPE-PEG350 monolayer demonstrated more expanded behavior than pure DSPC but only high pressure transition region was observed in its isotherm at nearly 16 mN/m unlike isotherms of pure DSPE-PEG2000 and pure DSPE-PEG1000. Mixing of DSPE-PEG350 and DSPC molecules created monolayers showed expanded behavior up to high pressure transition region. Similar to pure DSPE-PEG350, the isotherms of DSPC/DSPE-PEG350 mixed monolayers did not exhibit low pressure transition region and they displayed the high pressure transition region at nearly 16 mN/m. Although low pressure transition region is usually attributed that the orientation of PEG chain part of the lipopolymers, this region disappeared with decreasing length of PEG chain in lipopolymers. Therefore, the conformational change of PEG chain which occurred at this region could not seen clearly due to short PEG chain. Similar result was discussed by Mathe et al that monolayers of lipopolymers consisting of short PEG chain showed phase transition determined by the alkyl chain, while monolayers of lipopolymers

including long PEG chain exhibited typical lipopolymer behavior and two transition regions (Mathe, Gege et al. 2000).Moreover the area per molecules increased as observed for DSPC/DSPE-PEG2000 and DSPC/DSPE-PEG1000 mixed monolayers, when the ratio of DSPE-PEG350 in DSPC/DSPE-PEG350 mixture increased.

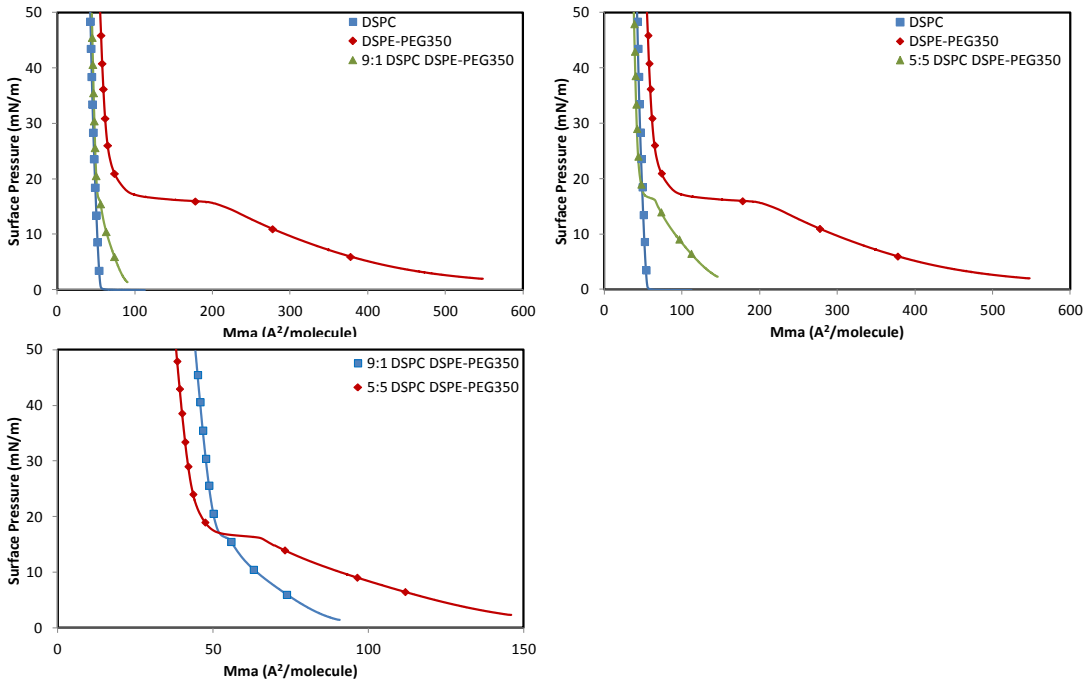

Figure 4.37. The surface pressure –mean molecular area (π-A) isotherms for pure and DSPC/DSPE-PEG350 mixed monolayers at the air/water interface

To detect deviation from ideal behavior, A_{ideal} values of DSPC/DSPE-PEG350 mixed monolayers were calculated and compared to A_{12} values of these monolayers. The A_{ideal} and A_{12} values were plotted as a function of mol fraction of DSPE-PEG350 and their differences were discerned in Figure 4.38.According to Figure 4.38, molecules in DSPC/DSPE-PEG350 mixed monolayers behaved non-ideal and they were miscible. When excess free energies of the mixed monolayers (ΔG_{exc}) given in Figure 4.39 were examined, attractive interaction between DSPC and DSPE-PEG350 molecules were noticed. The greatest negative ΔG_{exc} values of DSPC/DSPE-PEG350 mixed monolayers were observed at 5:5 molar ratio as found for DSPC/DSPE-PEG1000 mixed monolayers.

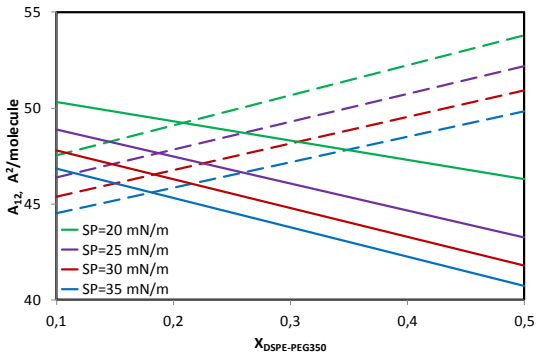

Figure 4.38. The mean molecular area (A_{12}) vs. $x_{DSPE\text{-}PEG350}$ plots for DSPC/DSPE-PEG350 mixed monolayers

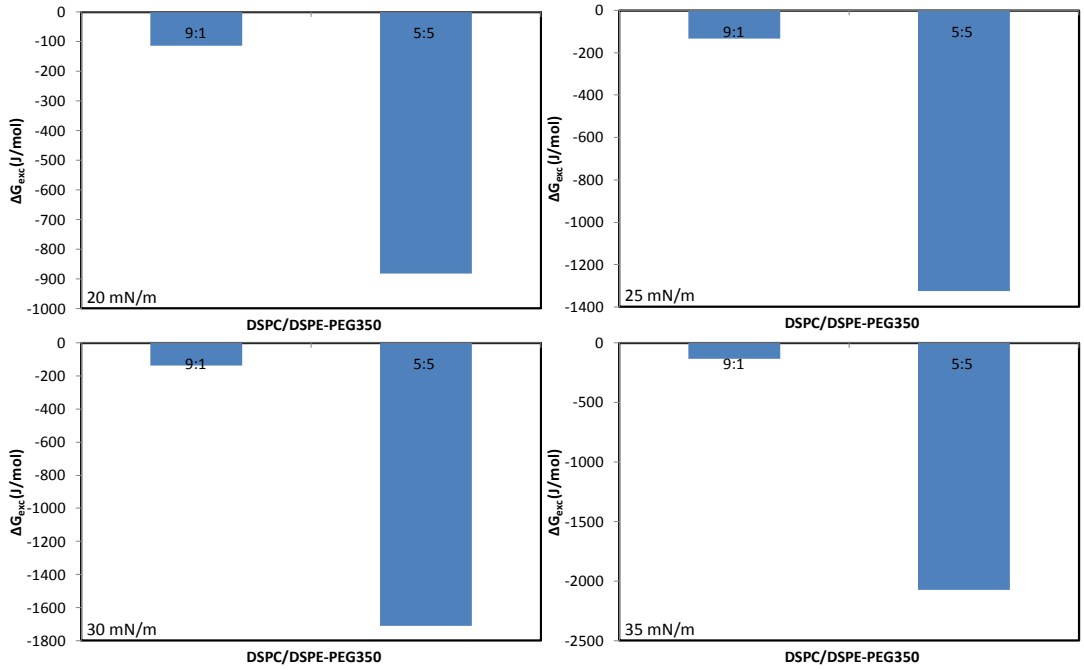

Figure 4.39. The excess free energy of mixing (ΔG_{exc}) values of DSPC/ DSPE-PEG350 mixed monolayers at different surface pressure

Another observation was that the compression modulus (C_s^{-1}) values of pure DSPE-PEG350 and DSPC/DSPE-PEG350 mixed monolayers given in Figure 4.40 exhibited one minimum peak at nearly 16 mN/m which denoted the high pressure transition region. This results supported outcomes obtained from surface pressure versus mean area per molecule isotherms of the monolayers. Similarly found for the DSPC/DSPE-PEG2000 and DSPC/DSPE-PEG1000 monolayers, mixed monolayers

which were more compressible than DSPC were observed with insertion of DSPE-PEG350 molecules into the monolayers.

As seen in Figure 4.41, BAM images of pure DSPE-PEG350 were dark at low surface pressures and any differentiation were not noticed up to 15 mN/m. *Mathe et al* discussed that lipopolymers composed of short PEG chain behaved like lipids which include fully saturated alkyl chains (Mathe, Gege et al. 2000). Possibly, low pressure transition region was not detected for pure DSPE-PEG350 monolayer because of this reason. Then, small bright spots emerged at nearly 15 mN/m and they fused together with increasing surface pressure. Unlike pure DSPE-PEG1000 and pure DSPE-PEG2000 monolayer, the BAM images became uniform upon compression because the molecules could approach to each other closely owing to short PEG chains. Compared to DSPC/DSPE-PEG2000 and DSPC/DSPE-PEG1000 mixed monolayers at 9:1 molar ratio, BAM images of DSPC/DSPE-PEG350 mixed monolayer seen in Figure 4.42 indicated that more homogeneous surface and any phase separations were not detected.BAM images of DSPC/DSPE-PEG350 mixed monolayer of 50% DSPE-PEG350 were demonstrated in Figure 4.43. Similarly observed for DSPC/DSPE-PEG2000 and DSPC/DSPE-PEG1000 mixed monolayers at 5:5 molar ratio, molecular distance was large and bright domains were seen and nearly at 16 mN/m.

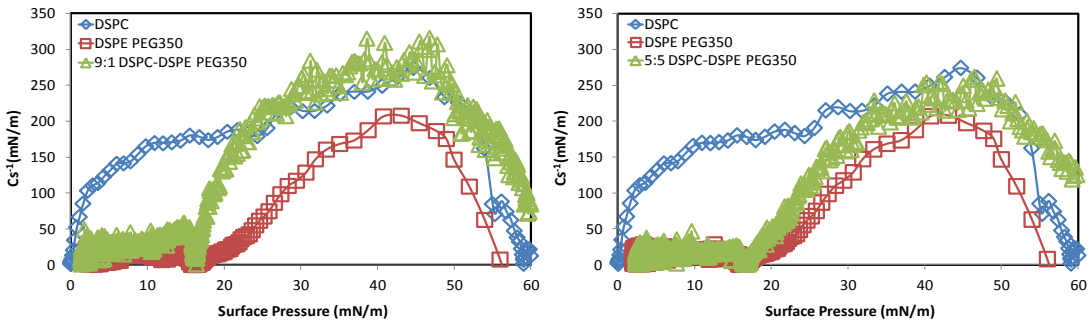

Figure 4.40. The compression modulus (C_s^{-1}) values of pure components and DSPC/ DSPE-PEG350 mixed monolayers at different surface pressure

According to these results, the incorporation of DSPE-PEG350, DSPE-PEG1000, DSPE-PEG2000 into DSPC monolayer gives expansion effect to the mixed monolayers at the air/water interface. Also, as can be seen in surface pressure-molecular area isotherms, for pure monolayers the surface pressures of the high pressure transition regions are different from each other. This region is observed for DSPE-PEG2000 monolayer nearly at 20 mN/m, for DSPE-PEG1000 monolayer nearly at 18 mN/m and for DSPE-PEG350 monolayer nearly at 16 mN/m. Therefore, this result supports that the transition region is associated with both aliphatic chain order and conformational change in PEG chains.DSPE-PEG350, DSPE-PEG1000, DSPE-PEG2000 and DSPC are found to be nonideally miscible and attractive forces between the molecules are dominant as evidenced from the results of compression isotherms and thermodynamically analysis of the mixed systems composed of these components. The comparison of the mixed monolayers showed that mean molecular areas increase with increasing length of PEG chain as observed by *Dori et al* (Dori, Bianco-Peled et al. 2000), because the mean molecular area of the isotherms are determined by the size of polymer (Baekmark, Wiesenthal et al. 1999). Also, it was observed that attractive forces between molecules become stronger with increasing PEG content for DSPC/DSPE-PEG1000 and DSPC/DSPE-PEG350 mixed monolayers unlike DSPC/DSPE-PEG2000 mixed monolayers. The PEG2000 chain length is longer than the lengths of PEG1000 and PEG350 chains, so repulsive forces between PEG2000 molecules higher and they prevent strong interaction between molecules in the monolayer mixture. The performed BAM studies indicate that phase separations for the mixed monolayers which include 50% lipopolymer at low and high surface pressure regions. The two phase can be interpreted in the mixed monolayers as a single-component DSPC phase and a mixed DSPC/lipopolymer phase like identified by *Tanwir et al* (Tanwir and Tsoukanova 2008). For DSPC/DSPE-PEG2000 mixed monolayers consisting of 10% DSPE-PEG2000 the phase separations at these regions are detected whereas DSPC/DSPE-PEG1000 mixed monolayer at 9:1 molar ratio exhibits only difference on surface at low surface pressure region. However, in contradiction to homogeneous surface observed on the macroscopic level, AFM studies performed for DSPC/DSPE-PEG2000 and DSPC/DSPE-PEG1000 mixed monolayers at 30 mN/m exhibited that separated phases at the surfaces. DSPC/DSPE-PEG350 mixed monolayer at 9:1 molar ratio do not reveal any difference because the length of PEG chain of DSPE-PEG350 molecule is shorter than DSPE-PEG2000 and DSPE-PEG1000 molecules' and molecules in this mixture

can get close to each other and create homogenous surface. As a conclusion, the repulsive and attractive interaction between binary molecules is influenced by the composition of mixed monolayer and the distribution of lipopolymers in DSPC varies depending not only on the surface pressure but also on the lipopolymer content.

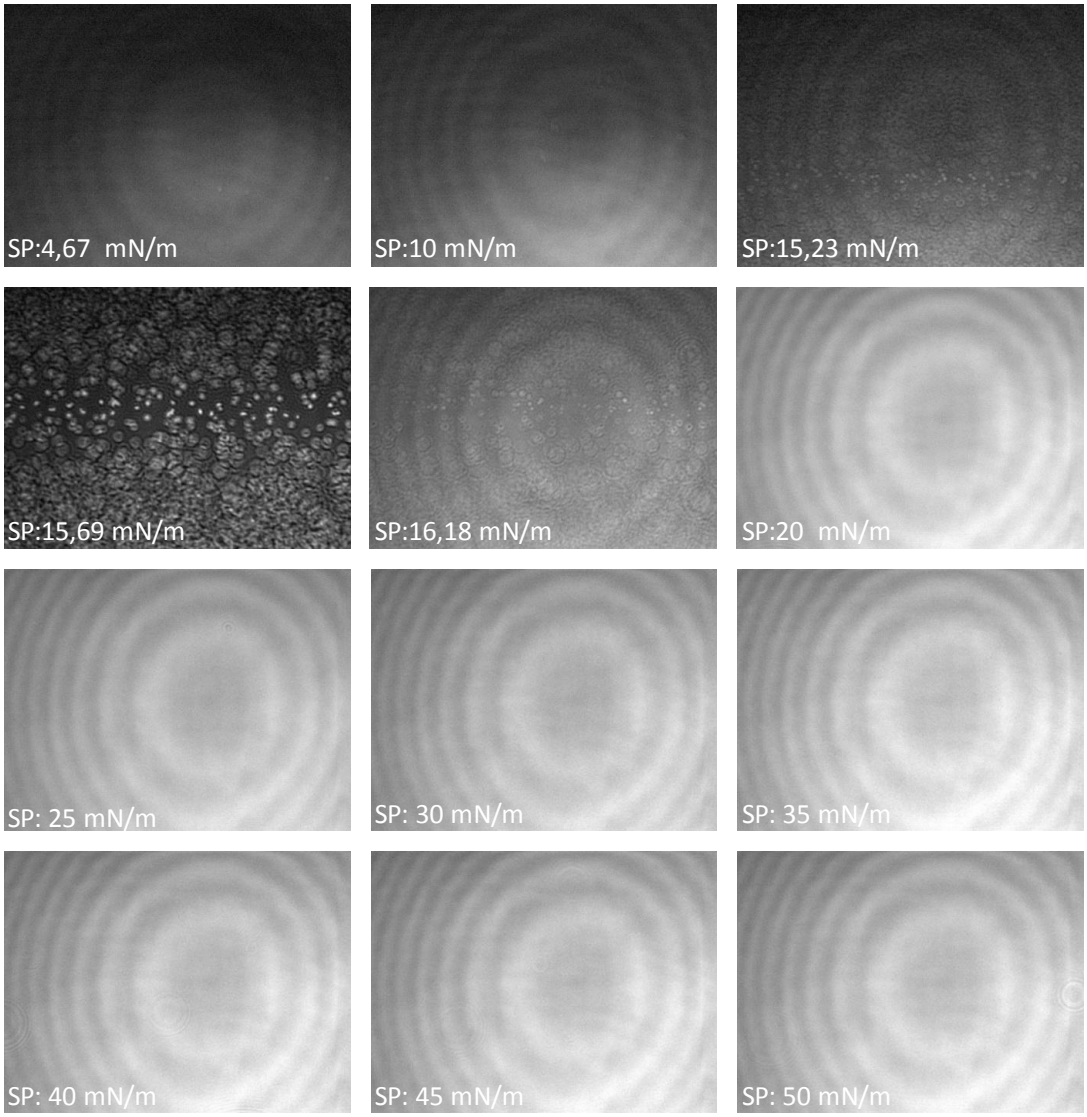

Figure 4.41. BAM images of pure DSPE-PEG350 monolayer at the air-water interface

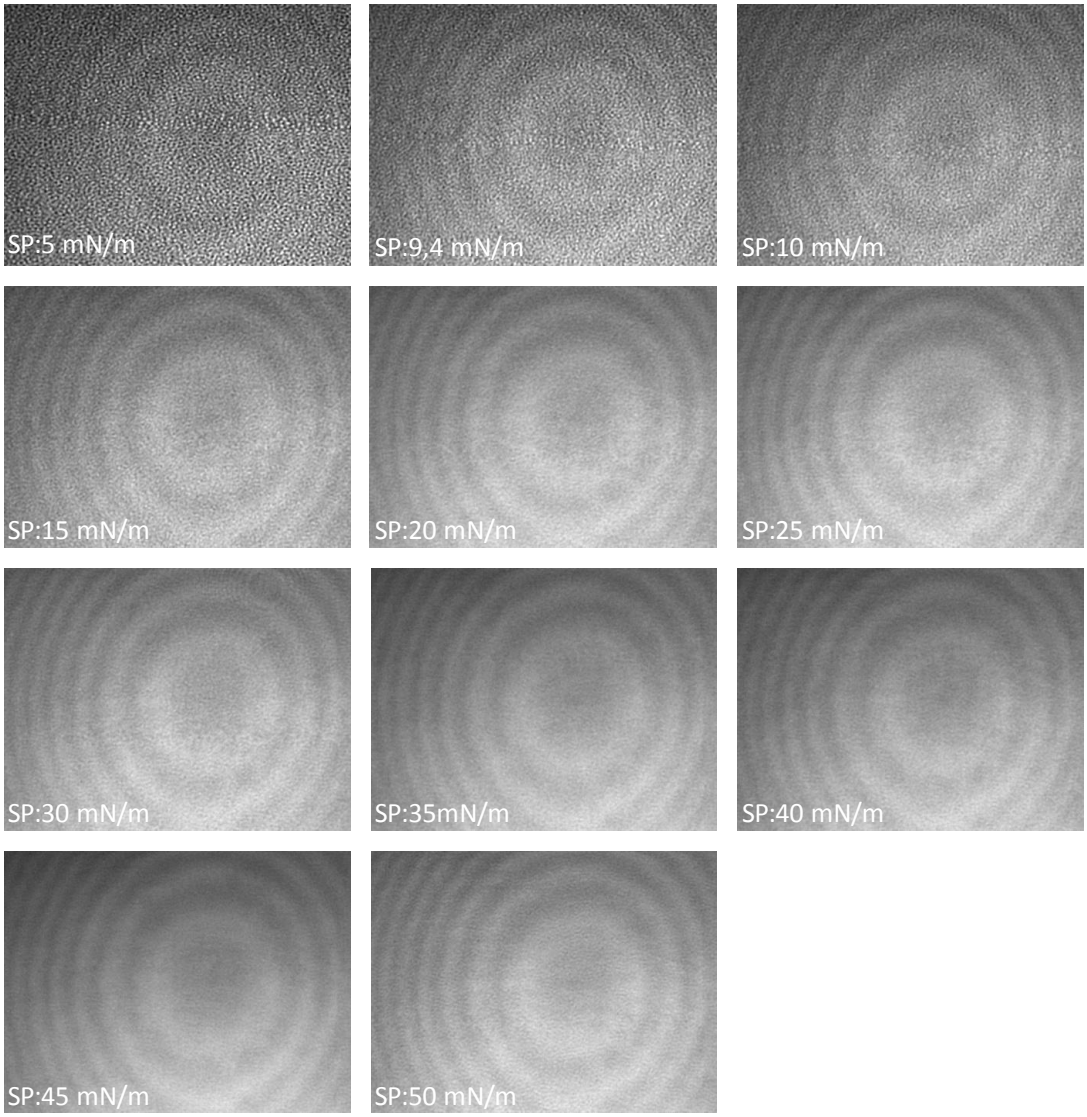

Figure 4.42. BAM images of 9:1 DSPC/DSPE-PEG350 mixed monolayer at the air-water interface

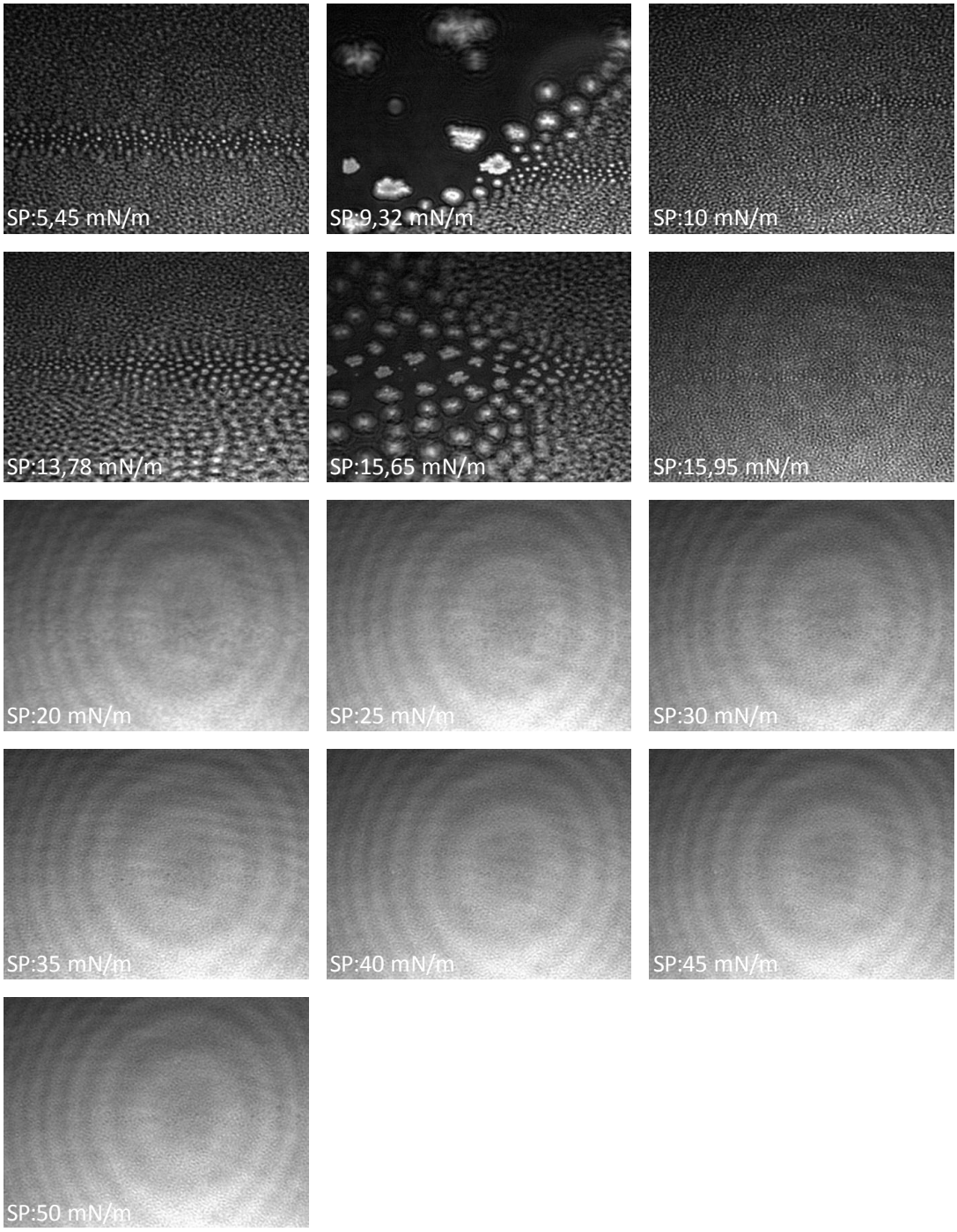

Figure 4.43. BAM images of 5:5 DSPC/DSPE-PEG350 mixed monolayer at the air-water interface

4.2. The Effect of Addition of Phospholipids Capable of H-bonding to MB Formulation on Shell Structure

Despite the presence of some commercial microbubbles composed of three or more different components (Tinkov, Bekeredjian et al. 2009), to our knowledge the interactions between the components and their effect on microbubbles stability have not been investigated as of yet. Herein, in this section an additional component was added into DSPC/PEG40 St mixture in order to observe the effect of this component on molecular interactions and shell stability. PG, PE and PA phospholipids exist in the cell membranes, so DSPG, DSPE and DSPA phospholipids having the same hydrocarbon chain length were added as additional components. The interactions of these phospholipids with DSPC and PEG40 St molecules can be different due to their different hydrogen bonding capability. Therefore, the ternary mixtures composed of one of these phospholipids, DSPC and PEG40 St were prepared in which molar fraction of DSPC was kept constant at 0.7 in one case (7:2:2; 7:1.5:1.5; 7:1:2) while keeping the molar fraction of PEG40 St constant at 0.5 in the other case (2:5:3; 4:5:1; 0:5:5) and their effects on shell stability were investigated by Langmuir –Blodgett (LB) method and Brewster Angle Microscopy (BAM) similar to our other mixtures.

4.2.1. Phase Behavior and Morphology of DSPC/PEG40 St/DSPG Mixed Monolayers

In this part the effect of DSPG (1,2-dioctadecanoyl-sn-glycero-3-phospho-(1'-rac-glycerol) (sodium salt)) used as additional lipid in MBs' shell formulation on phase behavior and morphology of monolayers were investigated. As demonstrated in DSPC/PEG40 St and DSPC/PEG-lipid mixed monolayers, compositional changes of the monolayers affected the interactions between components and phase behavior. Therefore, two different sets of mixtures were prepared in which molar fraction of DSPC was kept constant at 0.7 in one case while keeping molar fraction of PEG40 St at 0.5 in the other case. These mixtures were examined similarly to our binary mixtures. The surface pressure (π) versus mean area per molecule (A) isotherms recorded during compression of monolayers formed by the DSPC/PEG40 St/DSPG mixtures prepared at 7:2:1, 7:1.5:1.5, 7:1:2 molar ratios were shown in Figure 4.44. As seen from Figure

4.44, pure DSPG monolayer showed liquid-condensed (LC) phase behavior at the air-water interface similar to pure DSPC monolayer which is in a good agreement with the literature (Bos and Nylander 1996, Greenough and Blanchard 2009). Although DSPC and DSPG have same hydrocarbon chain length, they differ significantly in the structure of the polar headgroup. PG molecules are negatively charged whereas PCs possess zwitterionic character and the size of headgroup of PC is bigger than that of PG's (Bos and Nylander 1996, Wydro and Witkowska 2009).

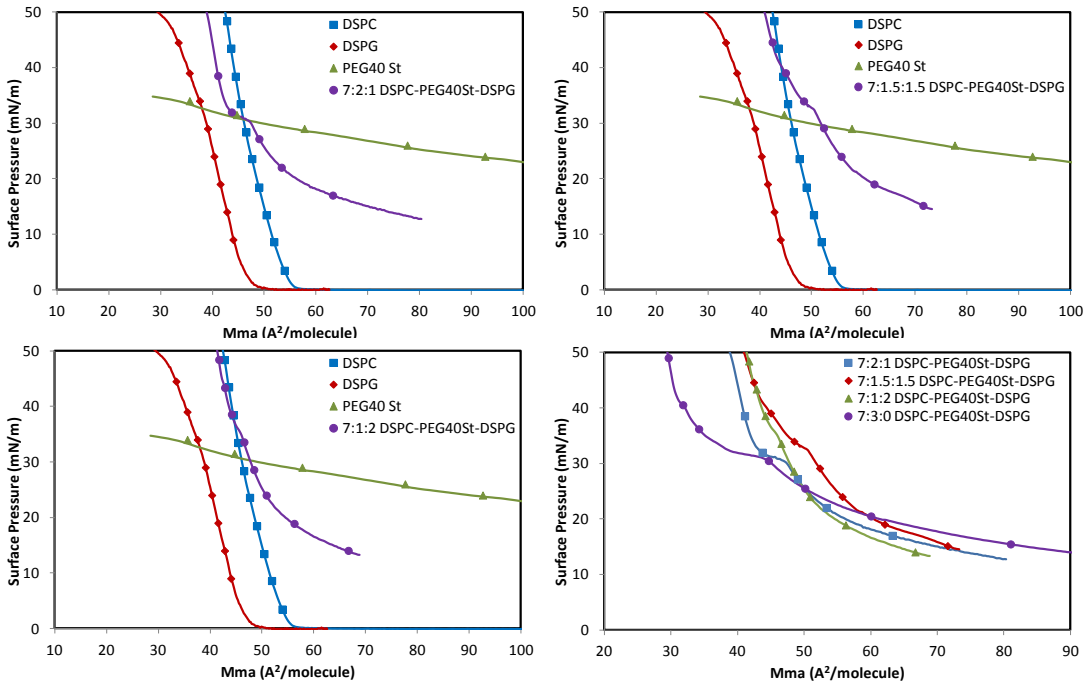

Figure 4.44. The surface pressure –mean molecular area (π-A) isotherms for pure and DSPC/PEG40 St/DSPG mixed monolayers at molar ratios of 7:2:1, 7:1.5:1.5, 7:1:2 at the air/water interface

Comparing the π-A isotherms recorded for DSPC and DSPG monolayers it was noticed that isotherm of DSPG was located at smaller areas than the isotherm obtained for DSPC due to the effect of headgroup of the phospholipids. It was revealed that the distance between DSPG molecules was smaller than between DSPC molecules and small glycerol group of DSPG caused formation of a monolayer in which molecules were slightly more densely packed than in DSPC film (Bos and Nylander 1996). The isotherms of the mixed monolayer given in Figure 4.44 indicated that the monolayers at low surface pressures were initially in liquid-expanded (LE) phase, but a plateau at

nearly 35 mN/m shifted to liquid-condensed phase with increasing surface pressure as observed for binary DSPC/PEG40 St mixed monolayers. When the ratio of DSPG in the mixture was increased, the isotherms shifted to larger area per molecule. Even though PG molecules were able to form hydrogen bonds thanks to the presence of hydroxyl groups, PG-PG hydrogen bonds may be weakened due to electrostatic repulsions existing between negatively charged phosphatidylglycerol molecules (Inoue and Nibu 1999, Watry, Tarbuck et al. 2003, Dickey and Faller 2008, Maniti, Cheniour et al. 2009, Wydro and Witkowska 2009, Wydro, Flasiński et al. 2012).

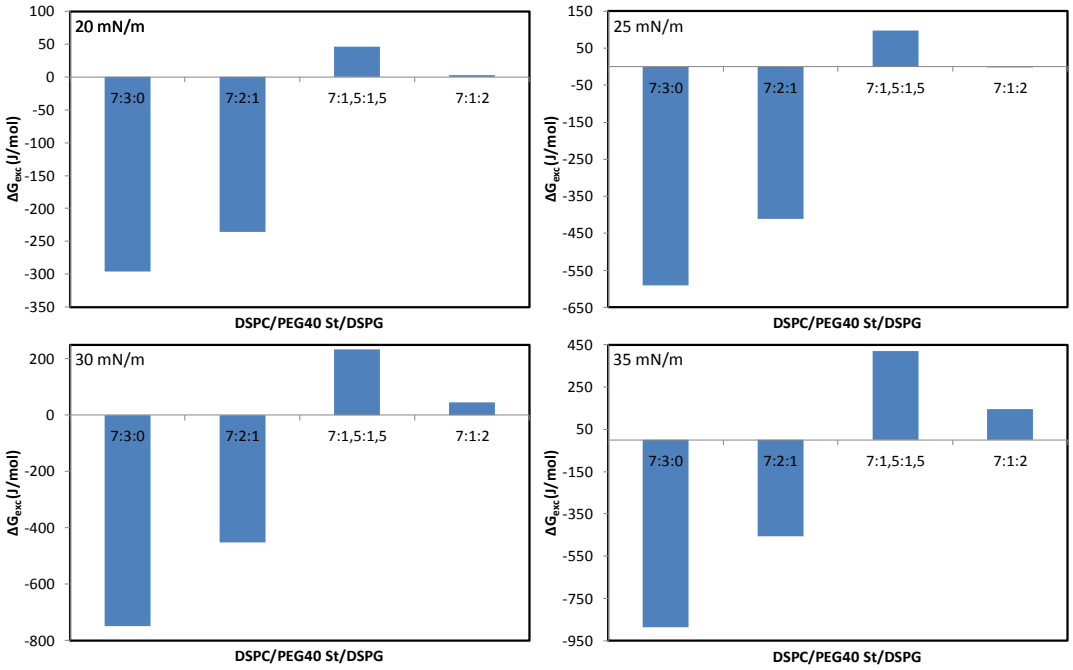

Figure 4.45. The excess free energy of mixing (ΔG_{exc}) values of DSPC/PEG40 St/DSPG mixed monolayers at molar ratios of 7:2:1, 7:1.5:1.5, 7:1:2 at different surface pressure

To compare the interactions between the investigated mixed systems the excess Gibbs energies of the mixtures were calculated and plotted at different surface pressures (Figure 4.45). The ΔG_{exc} values of DSPC/PEG40 St/DSPG mixed monolayer at 7:2:1 molar ratio were negative at all surface pressures whereas ΔG_{exc} values of other mixtures were positive. This suggested that attractive forces between molecules in the mixture were dominant for 7:2:1 molar ratio and repulsive forces were strong for the other molar ratios. The electrostatic repulsions existing between negatively charged phosphatidylglycerol molecules might cause reduction of attractive forces between the

molecules. Moreover, mixed monolayer at molar ratio of 7:1.5:1.5 displayed more positive values than the others at different surface pressures due to probably repulsive interactions between the bulky hydrophilic PEG chains and the electrostatic repulsion between PGs. The compression modulus (C_s^{-1}) values for mixed monolayer at 7:2:1, 7:1.5:1.5, 7:1:2 molar ratio are shown in Figure 4.46. C_s^{-1} values of the mixtures were similar and they showed a minimum at nearly 35 mN/m as noticed DSPC/PEG40 St binary films.

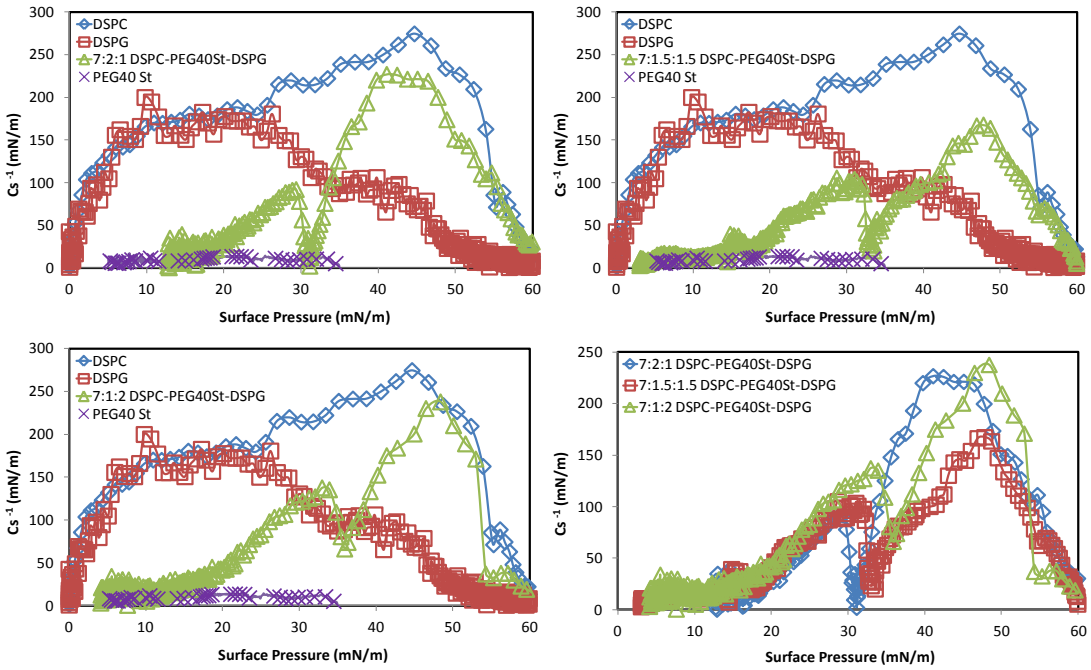

Figure 4.46. The compression modulus (C_s^{-1}) values of DSPC/PEG40 St/DSPG mixed monolayers at 7:2:1, 7:1.5:1.5, 7:1:2 molar ratios

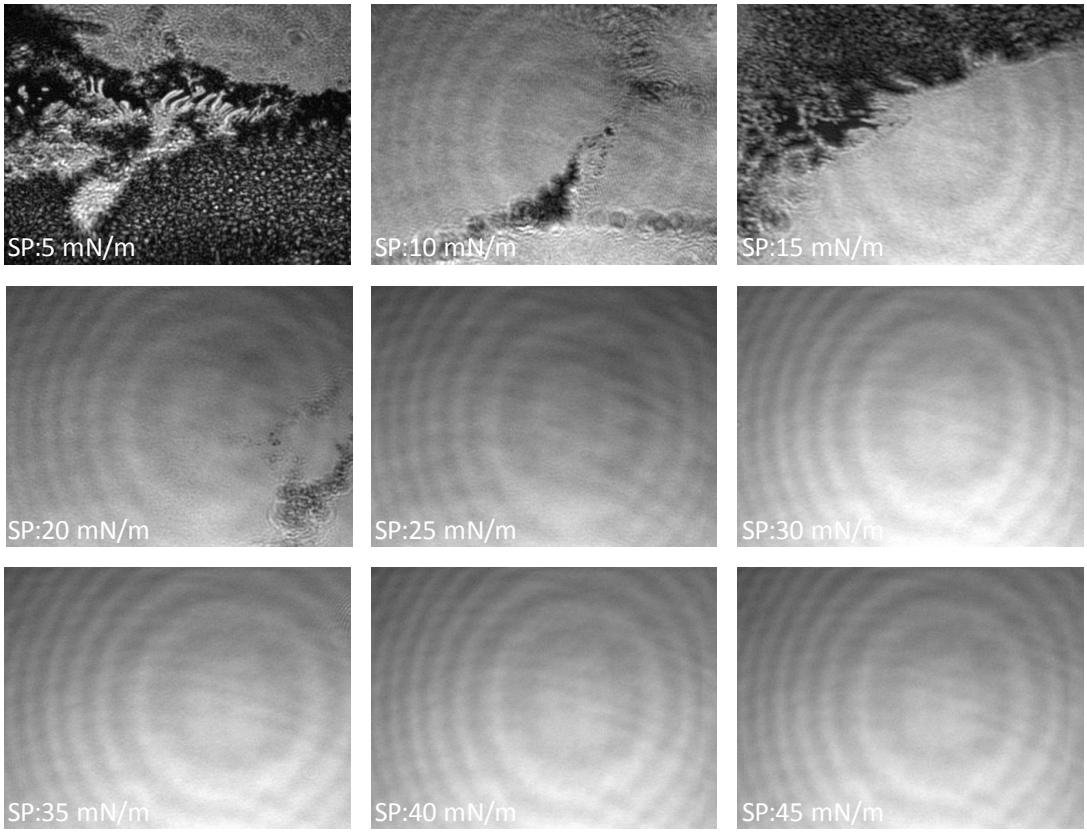

Figure 4.47. BAM images of pure DSPG monolayer at the air-water interface

BAM images at different surface pressures recorded for pure DSPG shown in Figure 4.47 were similar to BAM images of pure DSPC monolayer. At low surface pressures pure DSPG displayed the patches of the condensed phase and they fused together and covered the surface completely with compression. The covered surface was homogeneous due to condensed phase behavior of DSPG monolayer. Unlike DSPC/PEG40 St mixed monolayers, BAM images of DSPC/PEG40 St/DSPG mixed monolayers illustrated in Figure 4.48, Figure 4.49 and Figure 4.50 did not show large individual domains composed of rich condensed phase. As shown in Figure 4.48, Figure 4.49 and Figure 4.50, small circular domains were noticed which distributed in the expanded phase and the surface became completely uniform like pure DSPG with increasing surface pressures. Incorporation of DSPG molecule between DSPC and PEG40 St molecules may contribute to fusion of condensed and expanded phase. However, BAM images of DSPC/PEG40 St/DSPG mixed monolayer at 7:1.5:1.5 molar ratio showed large molecular distance, so darker regions were seen up to 30 mN/m. The repulsive forces between molecules in this mixed monolayer caused to remove the molecules and molecular distance increased. Also, DSPC/PEG40 St/DSPG mixed

monolayer at 7:2:1 molar ratio having negative ΔG_{exc} values demonstrated coalescence of the molecules at 20 mN/m due to attractive forces between components.

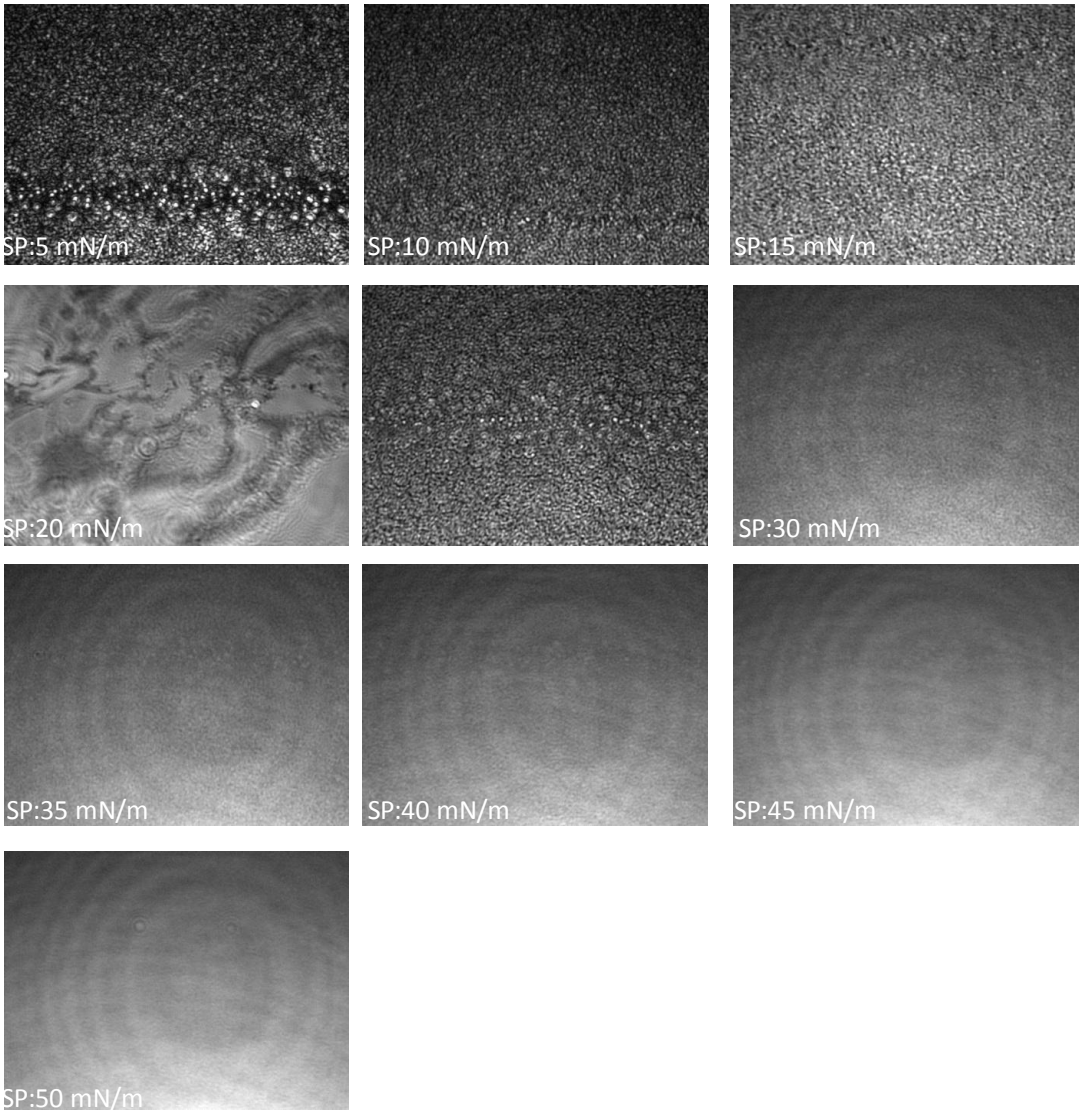

Figure 4.48. BAM images of 7:2:1 DSPC/PEG40 St/DSPG mixed monolayer at the air-water interface

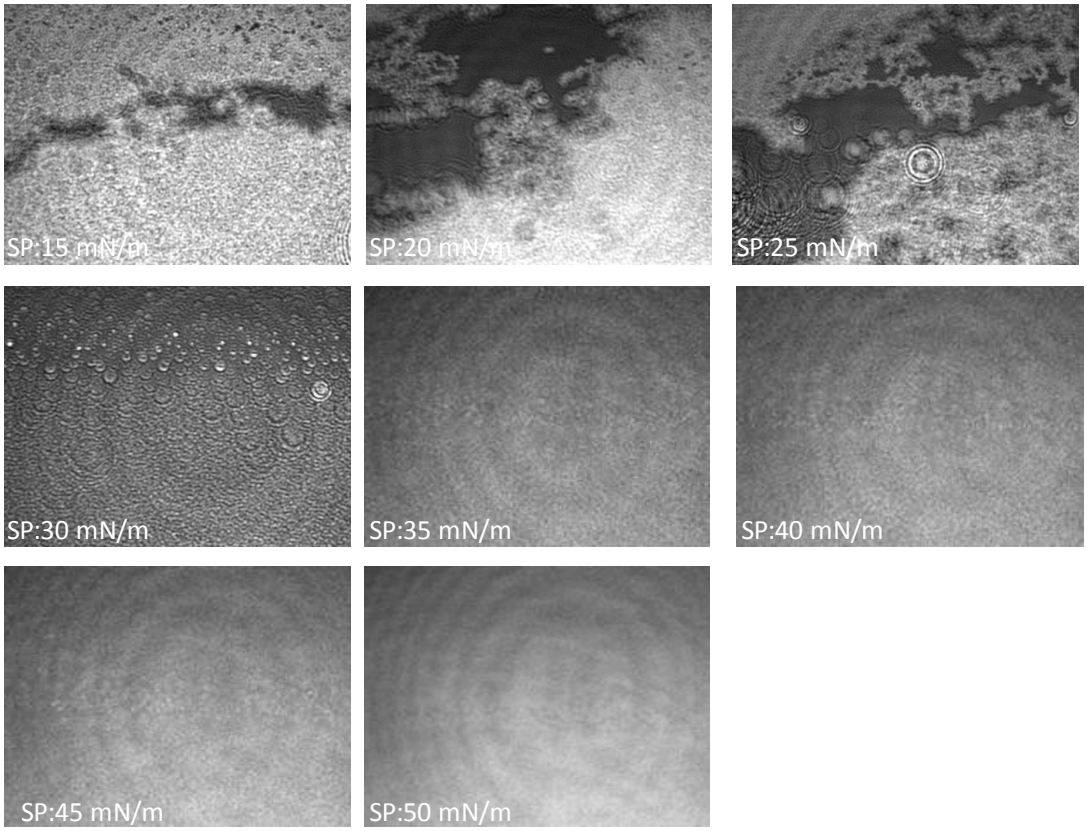

Figure 4.49. BAM images of 7:1.5:1.5 DSPC/PEG40 St/DSPG mixed monolayer at the air-water interface

The surface pressure (π) versus mean area per molecule (A) isotherms of DSPC/PEG40 St/DSPG mixtures prepared at 4:5:1, 2:5:3, 0:5:5 molar ratios with the content of PEG40 St kept constant can be seen in Figure 4.51. As observed for 7:2:1, 7:1.5:1.5, 7:1:2 molar ratios, the isotherms demonstrated a plateau at nearly 35 mN/m and shifted to larger area per molecule with increasing amount of DSPG. Also, the plateau regions of these mixed monolayers extended due to large content of PEG40 St. ΔG_{exc} values of the mixed monolayer of DSPC/PEG40 St/DSPG at 4:5:1 molar ratios were negative whereas ΔG_{exc} values became positive for the mixed monolayers composed of large amount of DSPG as shown in Figure 4.52.That means attractive forces between molecules in the DSPC/PEG40 St/DSPG mixed monolayer at molar ratios of 4:5:1 were dominant and repulsive forces increased when DSPC content was reduced. Additionally, similar to the mixed monolayers at 7:2:1, 7:1.5:1.5, 7:1:2 molar ratios Cs^{-1} plots of these mixed monolayers given in Figure 4.53 displayed a minimum peak corresponding to surface pressure of the plateau seen in the isotherms of the mixtures. The Cs^{-1} values were smaller than the calculated values for the mixed

monolayers prepared with the mol fraction of DSPC kept constant at 0.7 because of large amount of PEG40 St enhanced the compressibility of the mixtures.

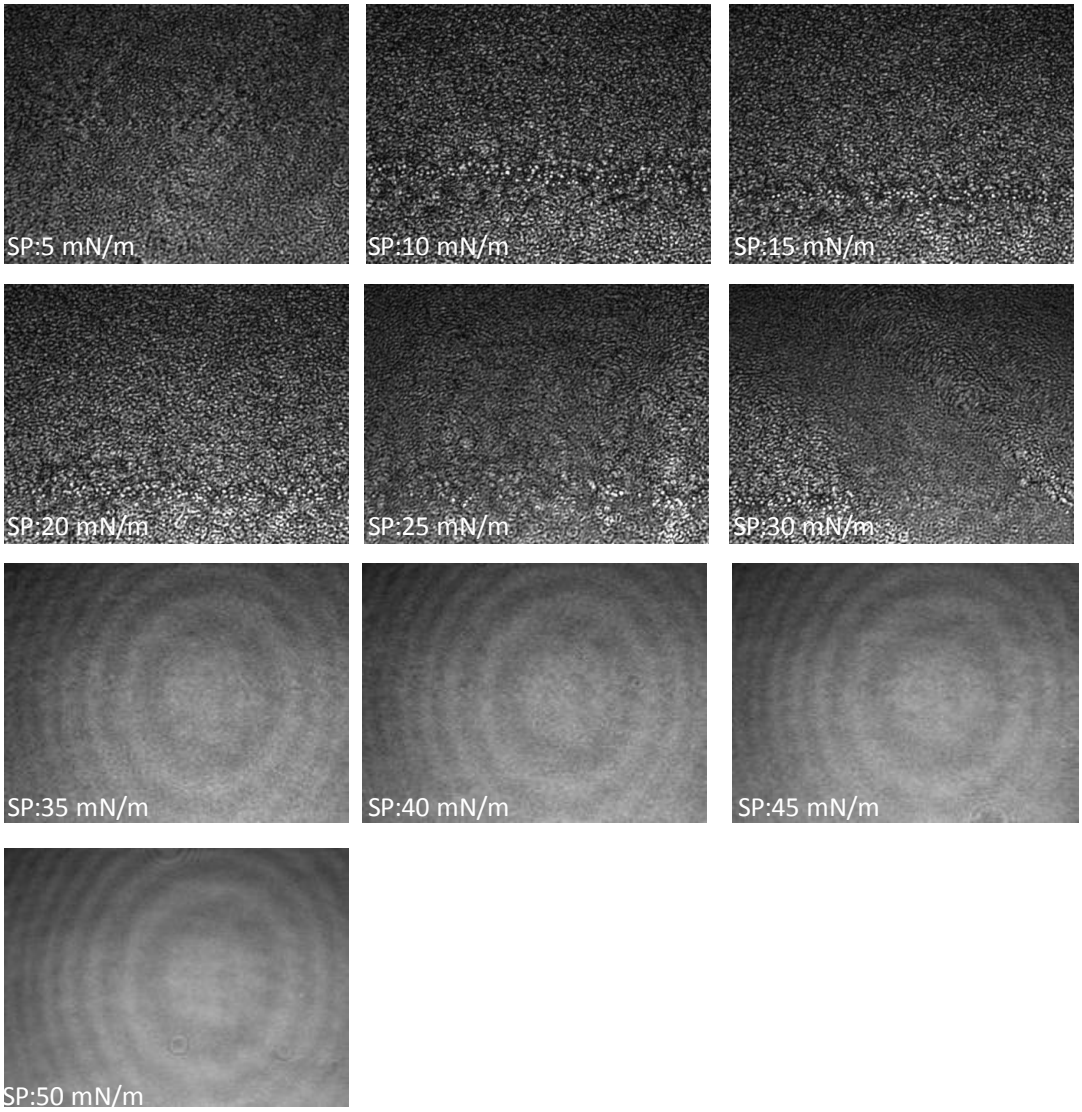

Figure 4.50. BAM images of 7:1:2 DSPC/PEG40 St/DSPG mixed monolayer at the air-water interface

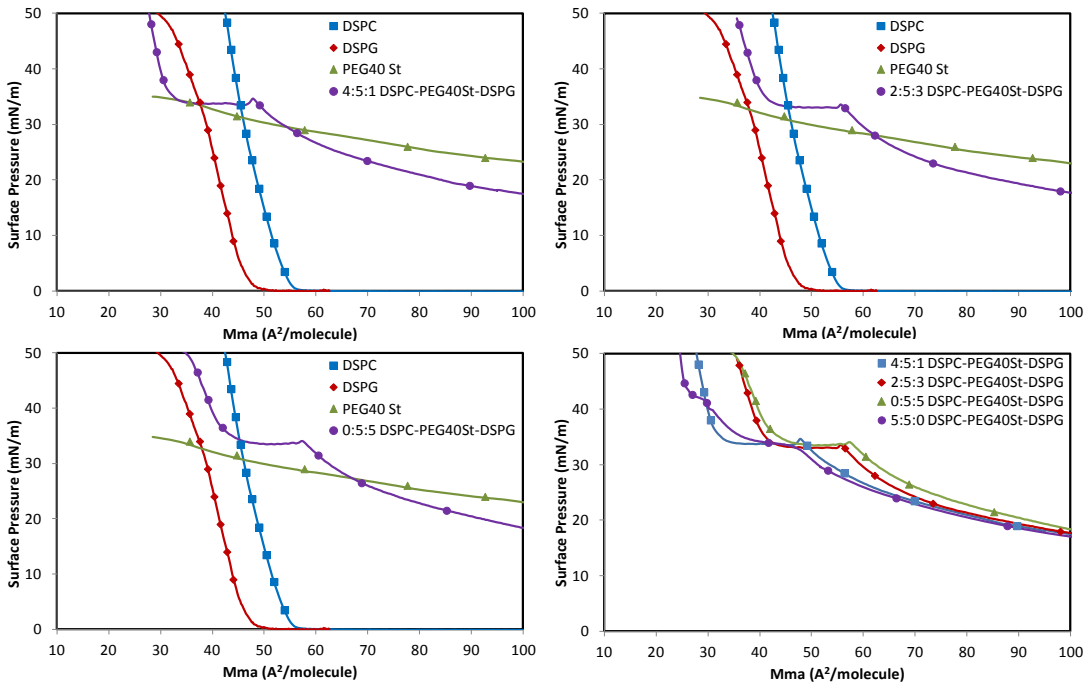

Figure 4.51. The surface pressure –mean molecular area (π-A) isotherms for pure and DSPC/ PEG40 St/DSPG mixed monolayers at molar ratios of 4:5:1, 2:5:3, 0:5:5 at the air/water interface

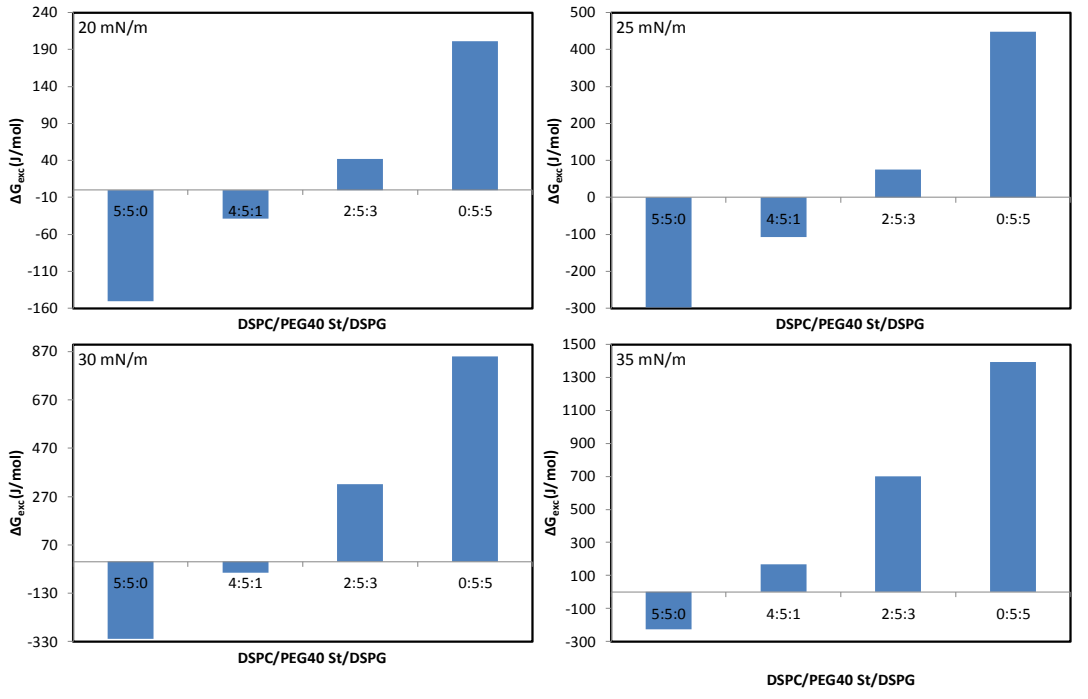

Figure 4.52. The excess free energy of mixing (ΔG_{exc}) values of DSPC/PEG40 St/DSPG mixed monolayers at molar ratios of 4:5:1, 2:5:3, 0:5:5 at different surface pressure

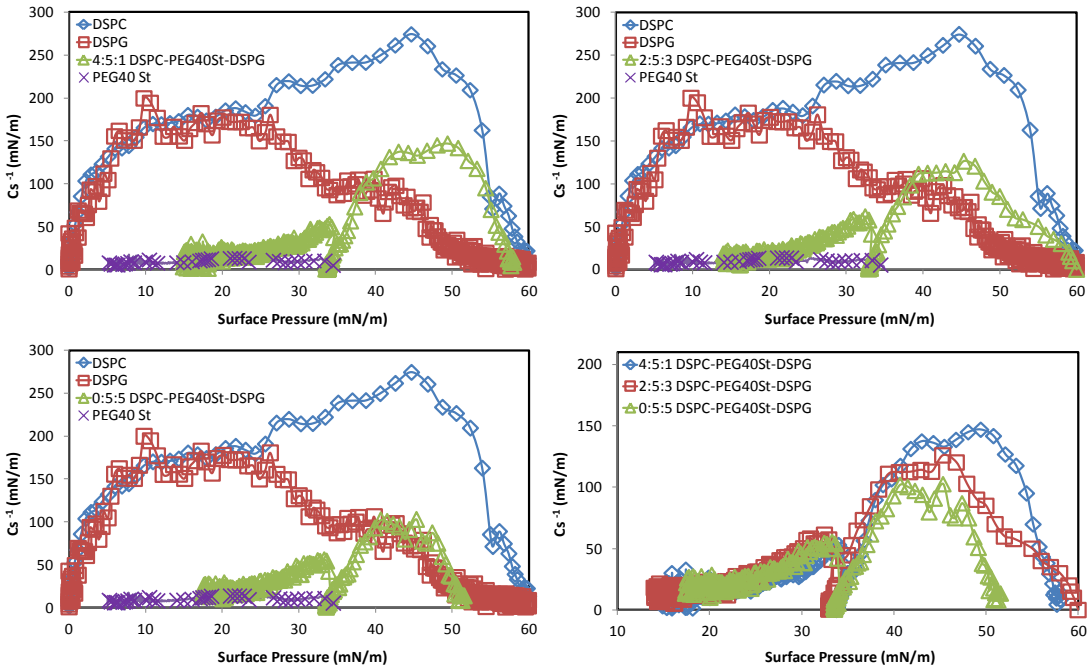

Figure 4.53. The compression modulus (C_s^{-1}) values of DSPC/PEG40 St/DSPG mixed monolayers at 4:5:1, 2:5:3, 0:5:5 molar ratios

BAM images of DSPC/PEG40 St/DSPG mixed monolayer at 4:5:1 molar ratio taken at different surface pressures are shown in Figure 4.54. Although very little phase separation was observed at 20 mN/m, generally homogenous surface was detected at low surface pressures. At nearly 33 mN/m large bright circular domains appeared and these domain fused together with increasing surface pressure. After that the surface became uniformly brighter. Figure 4.55 displays the BAM images of the mixed monolayer of DSPC/PEG40 St/DSPG at 2:5:3 molar ratio. The small separated phases were noticed up to 30 mN/m. Unlike observed for 4:5:1 molar ratio, large bright circular domains were not seen at nearly 33 mN/m but brightness appeared at surface and homogenous film was observed. The dark regions at the surface were seen clearly in BAM images of DSPC/PEG40 St/DSPG mixed film at molar ratios of 0:5:5 (Figure 4.56) due to probably large molecular distance between the molecules. Unlike DSPC/PEG40 St mixed monolayer at 5:5 molar ratio, separated phases were not detected during compression which might indicate that DSPG and PEG40 St molecules could be more fused to each other than DSPC and PEG40 St molecules. However, at nearly 33 mN/m brightness of the surface increased and covered the surface completely similar to 2:5:3 molar ratio. The brightness noticed at these mixed films' surfaces might

denote that PEG40 St molecules changed their orientation and passed to more ordered condensed state with other molecules in the mixed film.

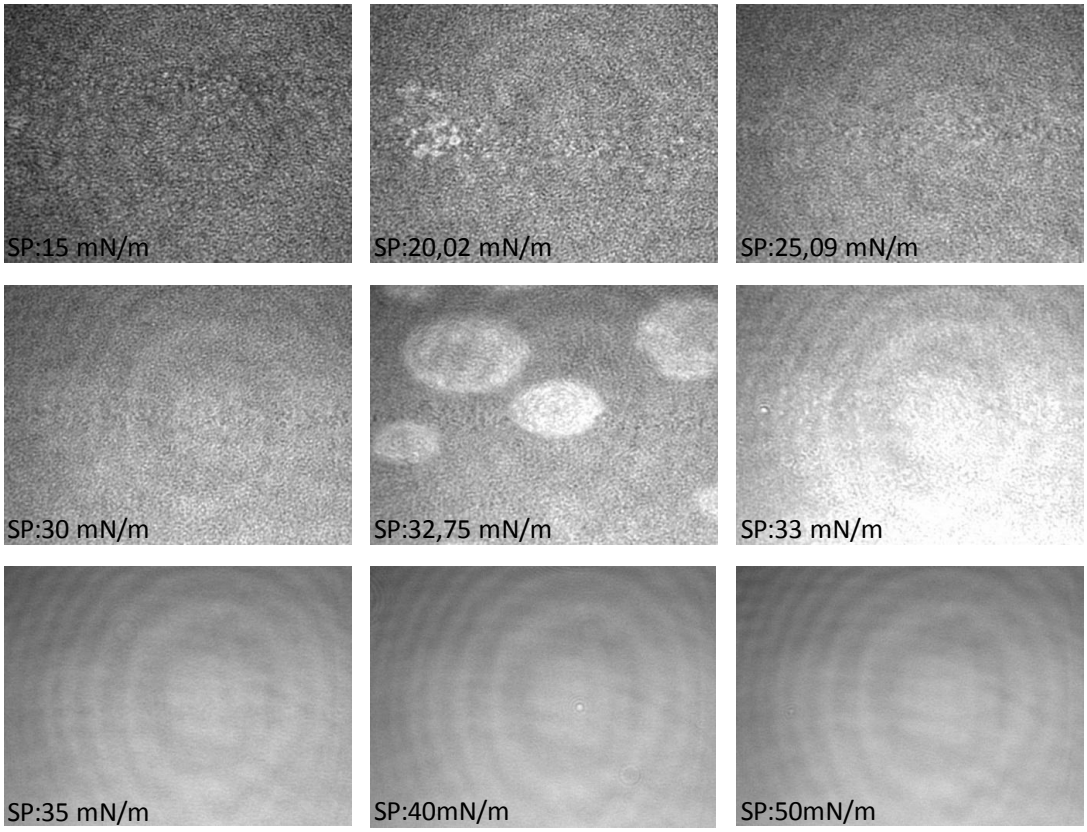

Figure 4.54. BAM images of 4:5:1 DSPC/PEG40 St/DSPG mixed monolayer at the air-water interface

DSPC/PEG40 St/DSPG mixed films at 2:5:3 and at 7:2:1 molar ratios were transferred onto mica at 30 mN/m and 40 mN/m of surface pressures. Figure 4.57 demonstrated AFM images of the mixed films coated at 30 mN/m. As seen from this figure, for DSPC/PEG40 St/DSPG mixed monolayer at 7:2:1 AFM image exhibited more uniform distribution than the mixed monolayer at 2:5:3 and further addition of PEG40 St to lipid monolayer induced phase separation. The topography image of 2:5:3 DSPC/PEG40 St/DSPG mixed monolayer at 30 mN/m revealed phase separation. The bright and dark zones in this topography were regarded as lipid and PEG40 St phases respectively. Additionally, the AFM images of these mixed films at 40 mN/m were given in Figure 4.58. Although these films did not provide homogeneous surfaces, more ordered films appeared at 40 mN/m than those at 30 mN/m due to condensation of the molecules with compression. BAM images of the mixed monolayers at the end of the

isotherm plateau region displayed a continuous featureless monolayer. However, the AFM images revealed the monolayers in fact were not homogenous. AFM provided a much more detailed picture of the mixed monolayers due to high resolution.

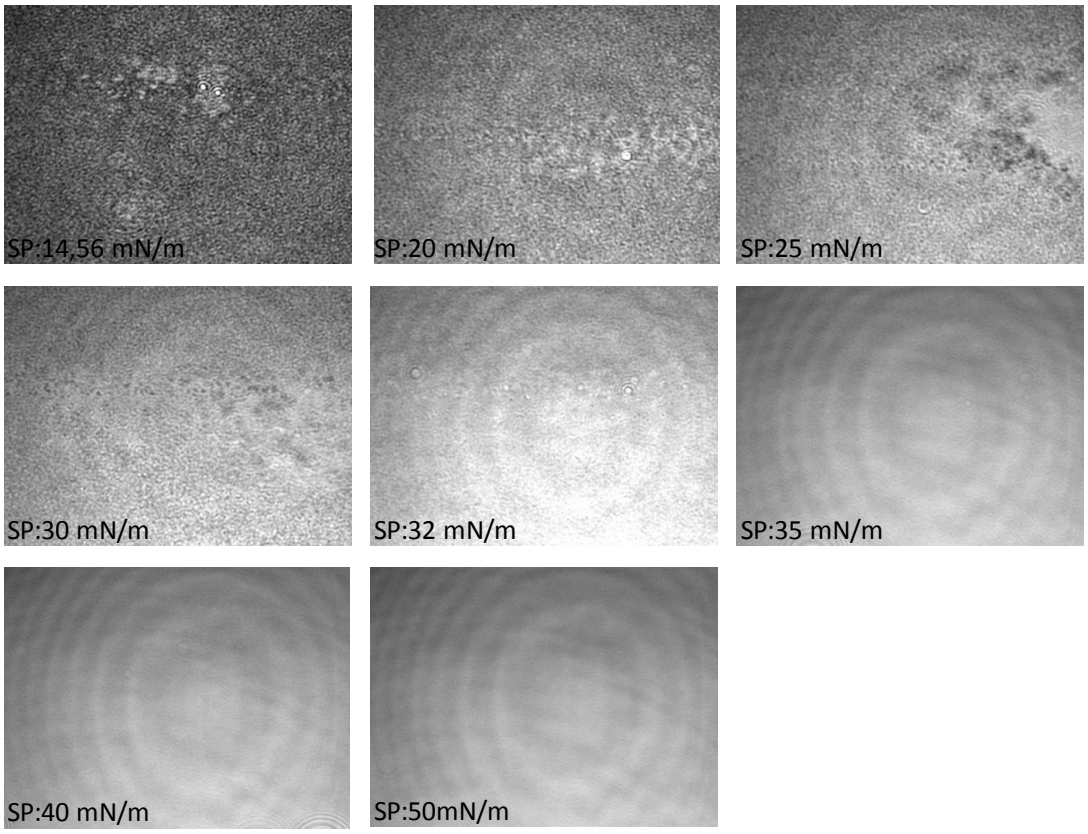

Figure 4.55. BAM images of 2:5:3 DSPC/PEG40 St/DSPG mixed monolayer at the air-water interface

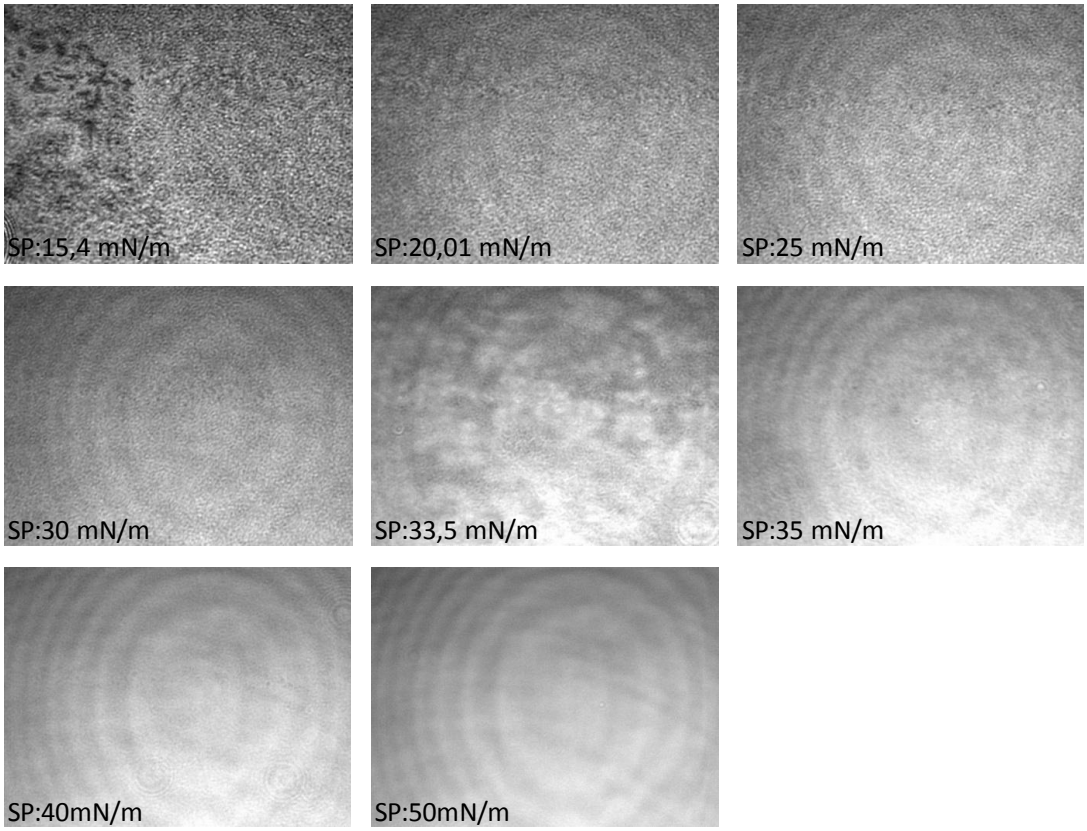

Figure 4.56. BAM images of 0:5:5 DSPC/PEG40 St/DSPG mixed monolayer at the air-water interface

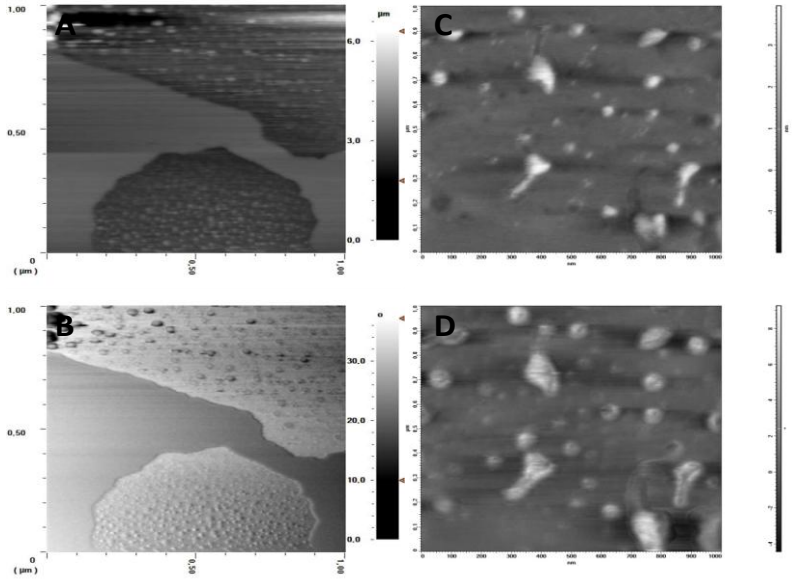

Figure 4.57. AFM topography (A,C,) and phase (B,D,) images (1x1 µm) of mixed DSPC/PEG40 St/DSPG monolayers for 2:5:3 (A,B) and 7:2:1 (C,D) molar ratios at 30 mN/m

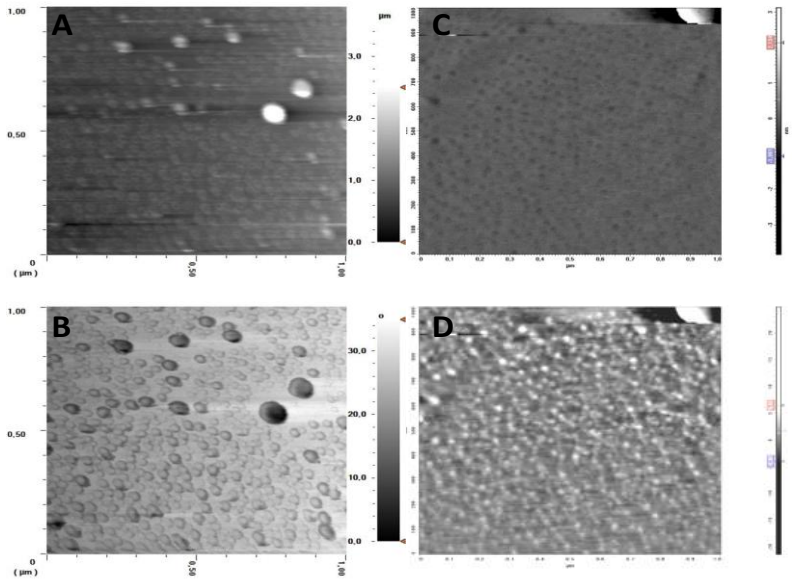

Figure 4.58. AFM topography (A,C,) and phase (B,D,) images (1x1 μm) of mixed DSPC/PEG40 St/DSPG monolayers for 2:5:3 (A,B) and 7:2:1 (C,D) molar ratios at 40 mN/m

4.2.2. The Phase Behavior and Morphology of DSPC/PEG40 St/DSPE Mixed Monolayers

In this section DSPE (1,2-distearoyl-*sn*-glycero-3-phosphoethanolamine) was used as additional lipid which differ significantly in the structure of the polar head group than DSPG. PG molecules are negatively charged whereas PE molecules have zwitterionic character similar to PC molecules. Both of DSPG and DSPE lipids are able to form intermolecular hydrogen bonds due to the presence of ammonium and hydroxyl groups in PE and PG molecules respectively (Watry, Tarbuck et al. 2003, Mansour and Zografi 2007, Dickey and Faller 2008, Wydro and Witkowska 2009).The differences in the structures of DSPG and DSPE may reflect different behavior in the mixed monolayer consisting of DSPC and PEG40 St. Therefore, the effect of addition of DSPE on the phase behavior and morphology of monolayers composed of DSPC, PEG40 St was investigated. In the first step of this investigation, the mixtures composed of these components were prepared keeping the molar fraction of DSPC at 0.7 in one set and PEG40 St at 0.5 in the other set of the experiments. The surface pressures (π) - mean area per molecule (A) isotherms for pure DSPE and for the mixed monolayers were recorded. The isotherms of pure components and DSPC/PEG40 St/DSPE mixtures

prepared at 7:2:1, 7:1.5:1.5, 7:1:2 molar ratios were shown in Figure 4.59. The shapes of the isotherm of DSPE monolayer denoted that this monolayer is characterized by liquid-condensed (LC) like organization which agrees well with previously published data (Bos and Nylander 1996, Dufrêne, Barger et al. 1997, Sánchez-González, Cabrerizo-Vilchez et al. 1998, Schneider, Dufrêne et al. 2000, Cannan, Zhang et al. 2004, Wydro and Witkowska 2009, Hąc-Wydro, Flasiński et al. 2012). Moreover, the isotherms indicated that DSPE was similar to DSPG and more tightly packed than DSPC due to different size of the headgroups: DSPC> DSPE≈DSPG (Bos and Nylander 1996, Mansour and Zografi 2007, Hąc-Wydro, Flasiński et al. 2012). The hydration of the ethanolamine groups and its smaller size permitted a close approach of the molecules, so the attractive van der Waals forces were strong for DSPE films (Garidel and Blume 1998, Sánchez-González, Cabrerizo-Vilchez et al. 1998, Doménech, Torrent-Burgues et al. 2005, Hac-Wydro, Kapusta et al. 2007).

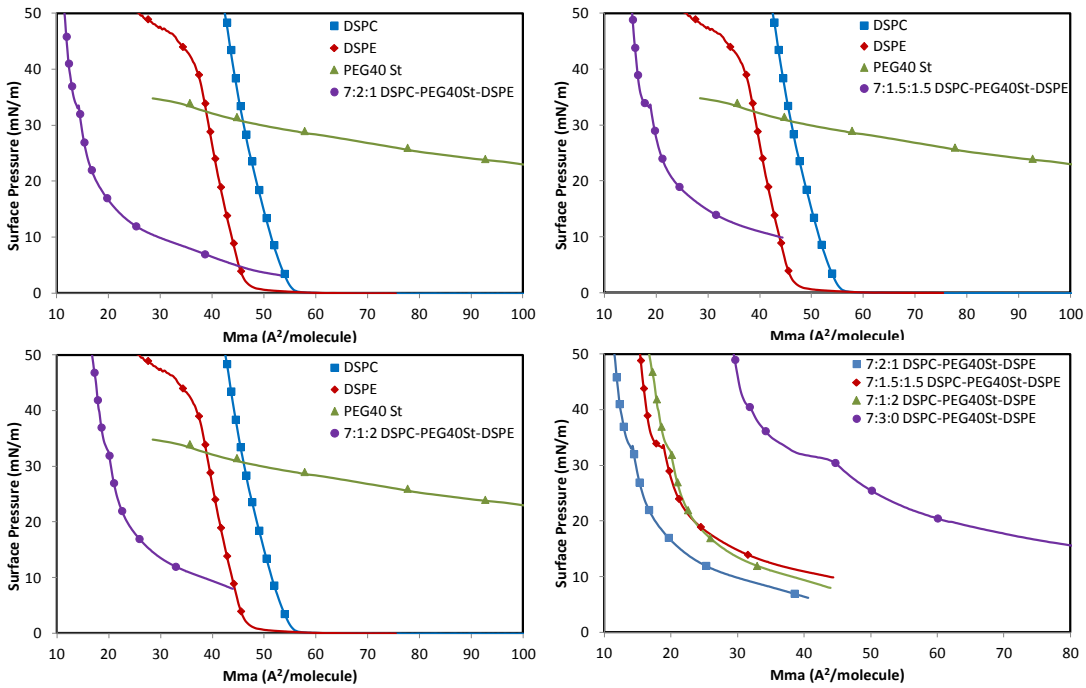

Figure 4.59. The surface pressure –mean molecular area (π-A) isotherms for pure and DSPC/PEG40 St/DSPE mixed monolayers at molar ratios of 7:2:1, 7:1.5:1.5, 7:1:2 at the air/water interface

As it can be noticed for the surface pressure-area isotherms recorded for all the investigated mixtures, the isotherms demonstrated significantly smaller area per molecule compared to that for pure components. DSPE can act as both hydrogen bond

donor via amine group and a hydrogen bond acceptor via the phosphate group while DSPC is not capable of acting as a hydrogen bond donor and has only the phosphate group as hydrogen bond acceptor. DSPE formed a more tightly packed structure due to the smaller headgroup size and greater number of attractive interactions resulting from hydrogen bonding between adjacent lipid molecules (Thurmond, Dodd et al. 1991, Garidel and Blume 1998, Watry, Tarbuck et al. 2003, Anglin and Conboy 2009, Wydro and Witkowska 2009).Therefore, the efficient hydrogen bonding capacity and small head group of DSPE created smaller mean molecular area for the mixed film at the air/water interface. Although the first addition of DSPE molecule into the mixtures decreased the area per molecule, further increase of DSPE content in the mixtures increased molecular areas as seen from Figure 4.59. We anticipate that with increasing DSPE amount the hydration of the ethanolamine group in the DSPE molecules hindered the approach of molecules in the mixtures and their interaction (Sánchez-González, Cabrerizo-Vilchez et al. 1998). In addition to this, at nearly 35 mN/m a plateau region which was ascribed to a change in orientation of the molecules upon compression was observed on the isotherms of the mixed monolayers.

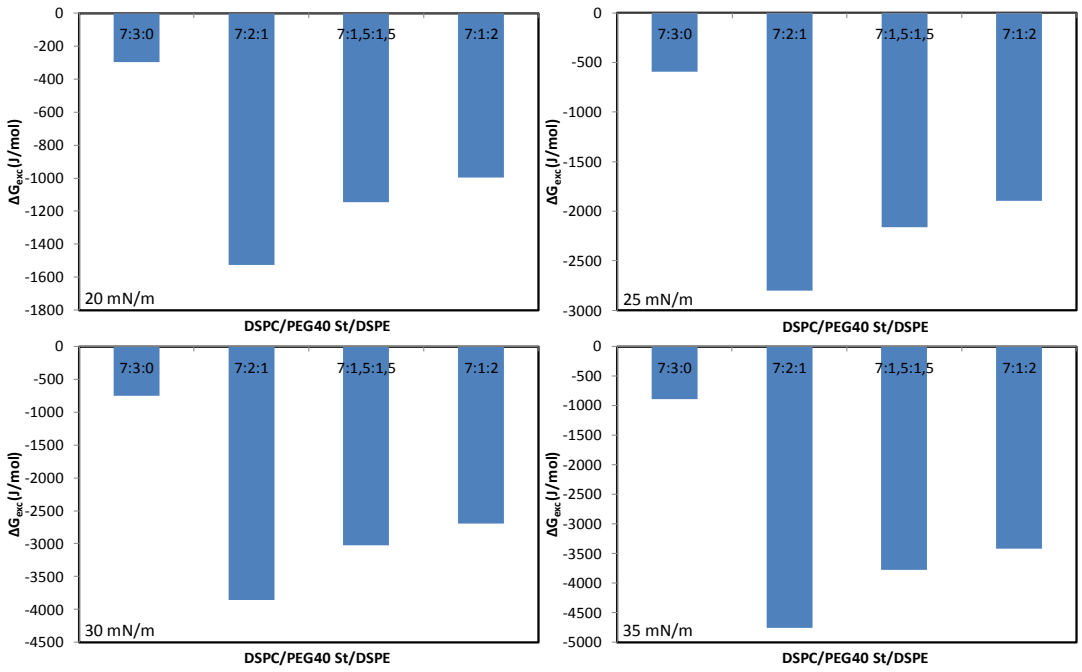

Figure 4.60. The excess free energy of mixing (ΔG_{exc}) values of DSPC/PEG40 St/DSPE mixed monolayers at molar ratios of 7:2:1, 7:1.5:1.5, 7:1:2 at different surface pressure

From the thermodynamic point of view, the interactions between the phospholipids and PEG40 St were analyzed basing on the excess free energy of mixing (ΔG_{exc}) values. The values of the ΔG_{exc} are presented at different surface pressures in Figure 4.60. The negative values were observed for DSPC/PEG40 St/DSPE mixed monolayers at molar ratios of 7:2:1, 7:1.5:1.5, 7:1:2 proved the existence of strong attractions between molecules in the films. Moreover, the minimum ΔG_{exc} values detected for DSPC/PEG40 St/DSPE mixed monolayer at 7:2:1 molar ratio corresponded to the mixture of the highest thermodynamic stability. The addition of low amount of DSPE molecules in the mixture increased the attractive forces between molecules due to their tightly packed structure and effective hydrogen bonding capacity between adjacent lipid molecules. Similar result found by *Gonzalez et al* denoted that attractive forces between molecules were dominant for the DSPC/DSPE mixed monolayer composed of low proportion of DSPE (Sánchez-González, Cabrerizo-Vilchez et al. 1998). Also, *Domenech et al* noticed that attractive interaction between PC and PE molecules and the mixtures composed of these molecules showed greatest stability (Doménech, Torrent-Burgues et al. 2005).

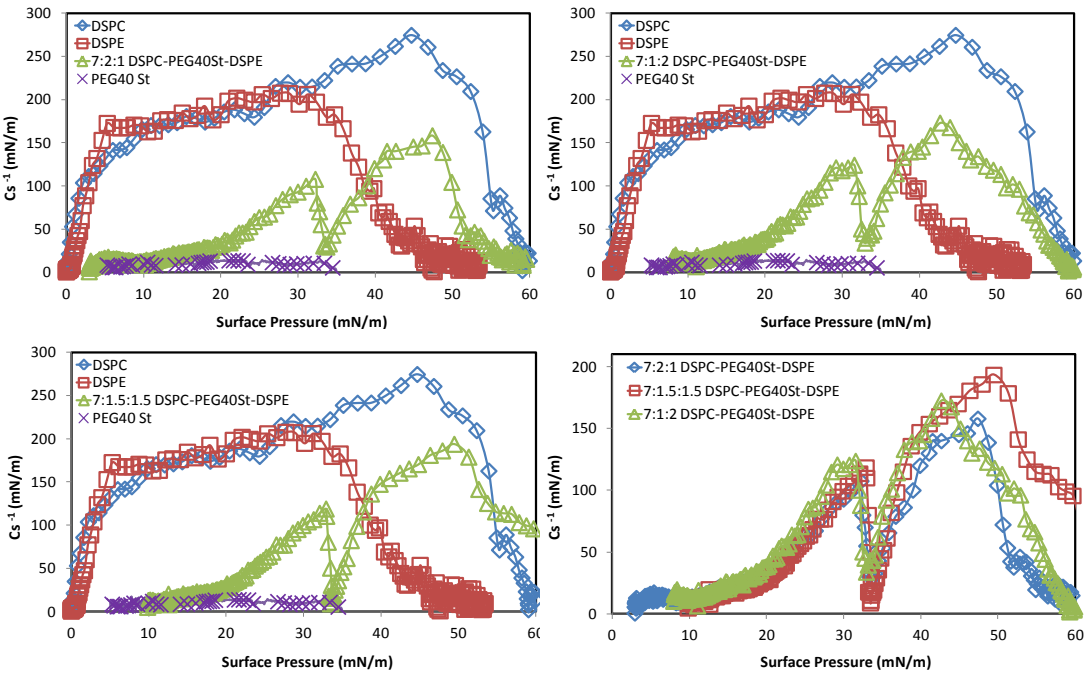

Figure 4.61. The compression modulus (C_s^{-1}) values of DSPC/PEG40 St/DSPE mixed monolayers at 7:2:1, 7:1.5:1.5, 7:1:2 molar ratios

To facilitate further analysis of the data obtained from π-A isotherms the compression modulus (C_s^{-1}) values of DSPC/PEG40 St/DSPE mixed monolayer at 7:2:1, 7:1.5:1.5, 7:1:2 molar ratios versus surface pressures (π) plots were shown in Figure 4.61. As can be seen, the compression modulus revealed that DSPE and DSPC formed more condensed monolayers than the mixed films due to the effect of PEG chain and these mixed films showed similar behavior. Also, the plateau regions visible in the isotherms were seen as minima similar to DSPC/PEG40 St/DSPG mixed monolayers. This suggested that a possibility of phase change in the investigated mixture system.

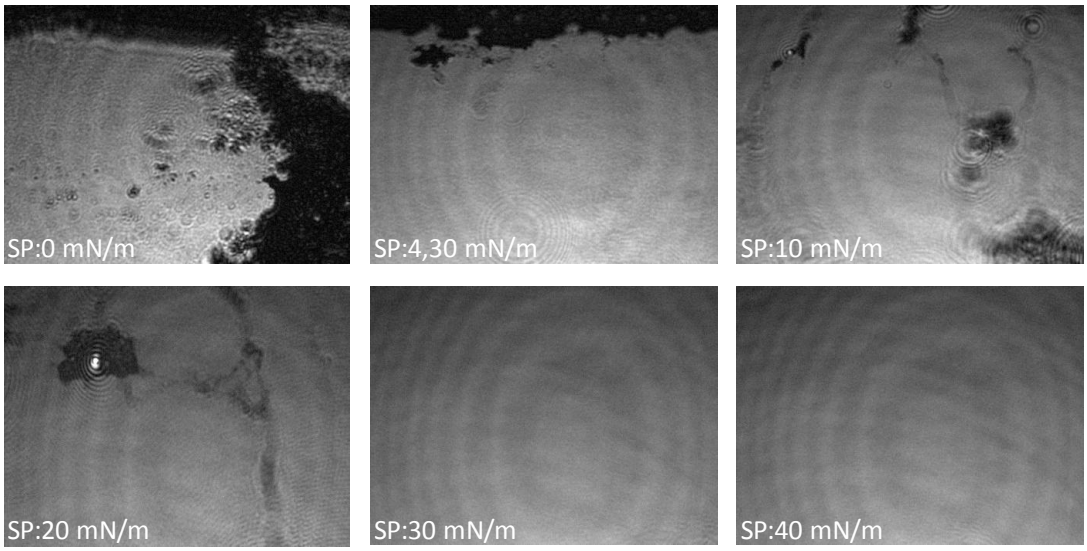

Figure 4.62. BAM images of pure DSPE monolayer at the air-water interface

To gain insight into phase behavior of the mixed films, Brewster Angle Microscopy enabling direct visualization of monolayers structures was employed. The BAM images of pure DSPE given in Figure 4.62 showed condensed domains at large areas. With further compression of the monolayer these domains joined together and formed finally a homogenous condensed phase up to collapse pressure. Previously, similar BAM images of pure DSPE were obtained by *Hac-Wydro et al* (Hąc-Wydro, Flasiński et al. 2012).

As shown in Figure 4.63, the recorded BAM images of DSPC/PEG40 St/DSPE mixed monolayer at 7:2:1 molar ratio demonstrated that straight condensed structures on the surface indicated that phase separation at low surface pressure, but the surface

became more homogeneous with increasing surface pressure. The BAM images for DSPC/PEG40 St/DSPE mixed monolayer at molar ratios of 7:1.5:1.5 were displayed in

Figure 4.64. Up to 15 mN/m different phases, more condensed bright and more expanded dark regions, were noticed, but with further compression uniform surface was obtained. Similar images (Figure 4.65) were detected for the monolayer of 7:1:2 molar ratio. For all the mixed systems, the recorded BAM images evidence a small amount of phase separation in the monolayer at low surface pressures. However, the surfaces became completely uniform with increasing surface pressures. It might indicate that at some regions the molecules in the mixtures were not fully miscible at low surface pressures as observed for DSPC/DSPE mixtures (Anglin and Conboy 2009).

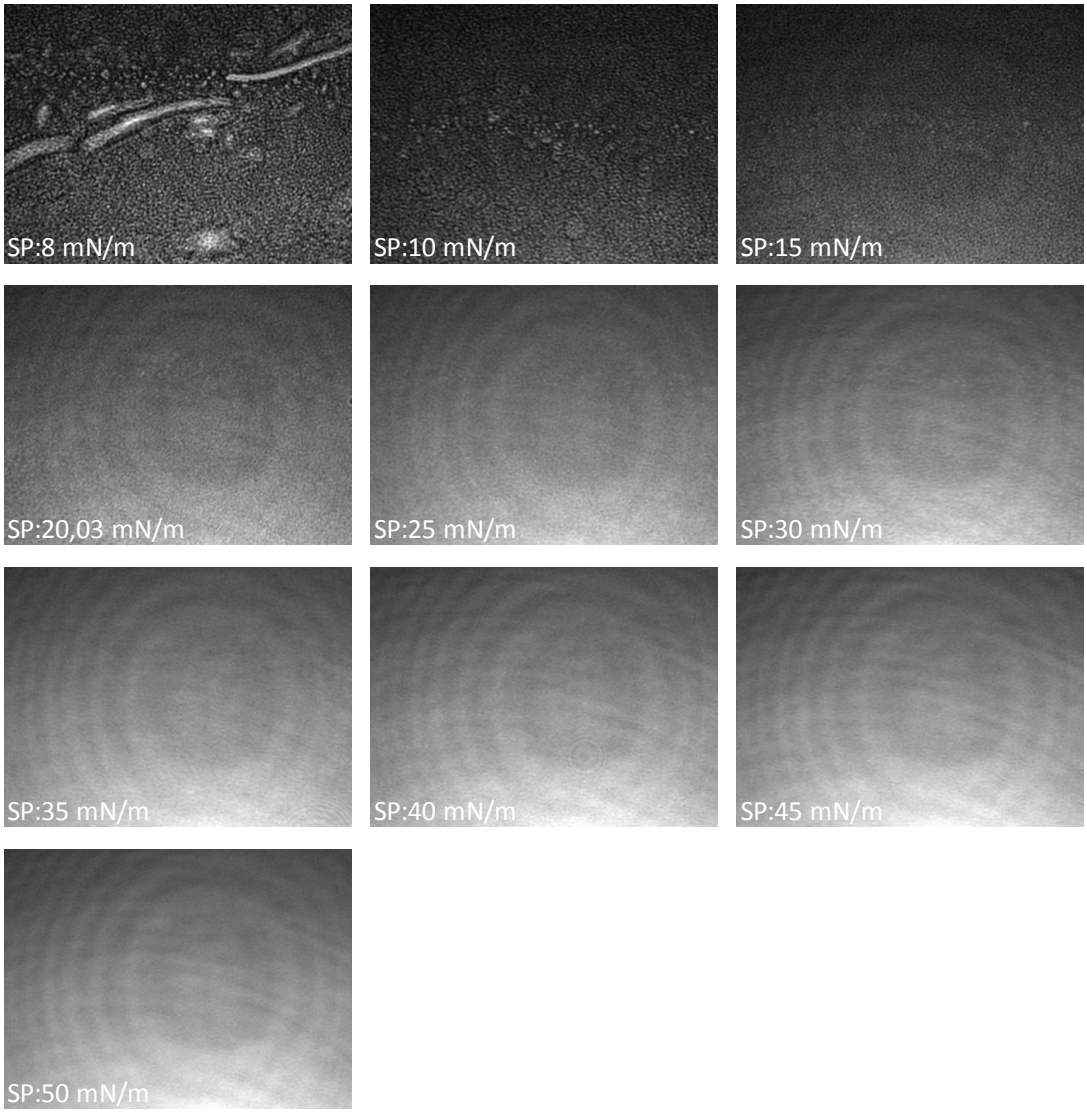

Figure 4.63. BAM images of 7:2:1 DSPC/PEG40 St/DSPE mixed monolayer at the air-water interface

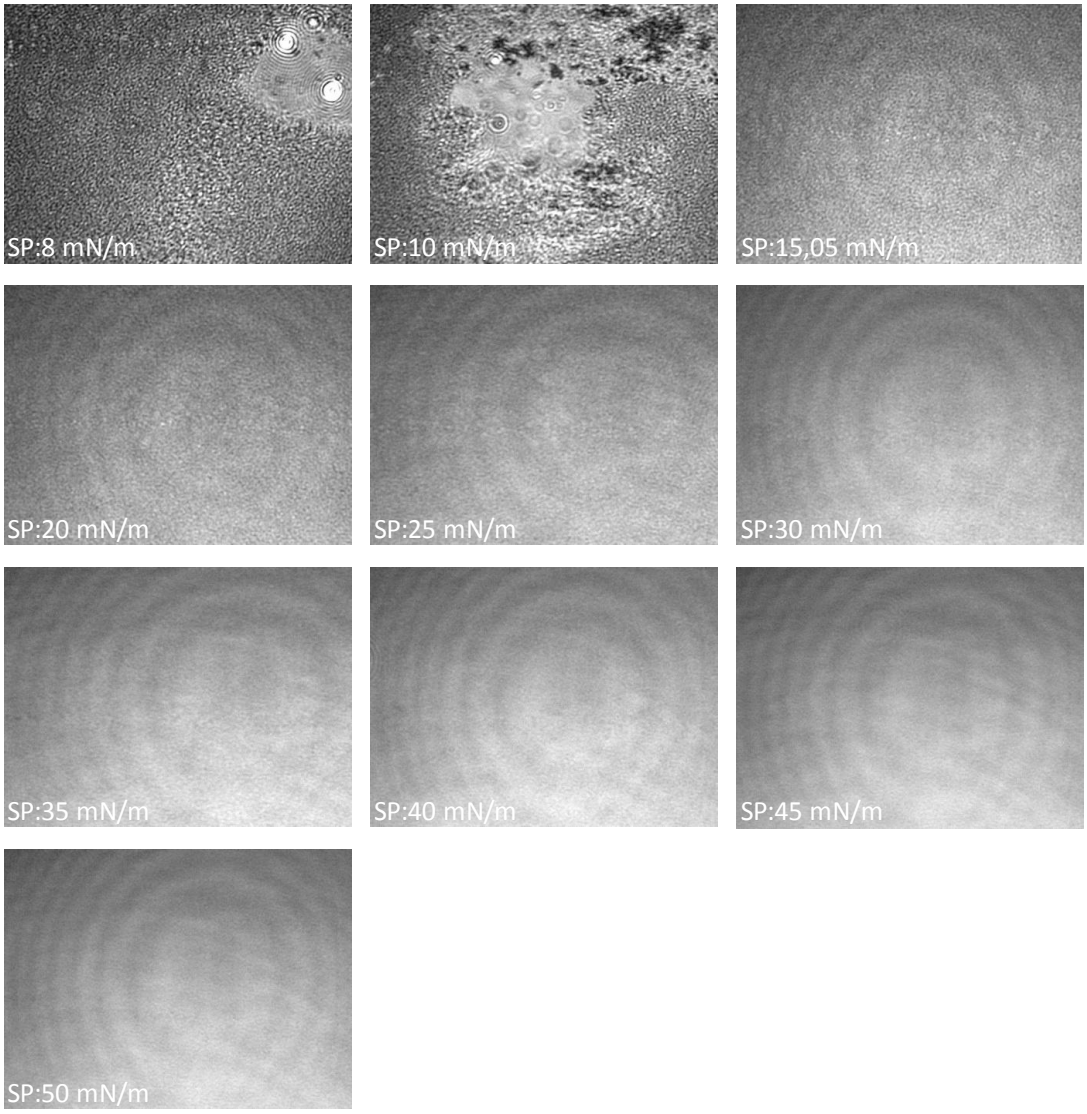

Figure 4.64. BAM images of 7:1.5:1.5 DSPC/PEG40 St/DSPE mixed monolayer at the air-water interface

The experimental surface pressure (π) versus mean area per molecule (A) isotherms corresponding to DSPC/PEG40 St/DSPE mixtures prepared at 4:5:1, 2:5:3, 0:5:5 molar ratios were shown in Figure 4.66. At low surface pressures the isotherms of these mixed monolayers exhibited more expanded behavior due to repulsive forces between large amount of PEG40 St molecules than isotherms for DSPC/PEG40 St/DSPE mixed monolayers of x_{DSPC}=0.7. Similar to the other investigated mixed monolayers, these isotherms showed a plateau at nearly 35 mN/m. After that more condensed films were observed at high surface pressures. Comparison of DSPC/PEG40 St/DSPE mixed monolayers at molar ratios of 4:5:1 and at molar ratios of 2:5:3 demonstrated that with increasing content of DSPE the isotherms shifted to smaller

molecular area owing to the efficient hydrogen bonding capacity and small head group of DSPE.

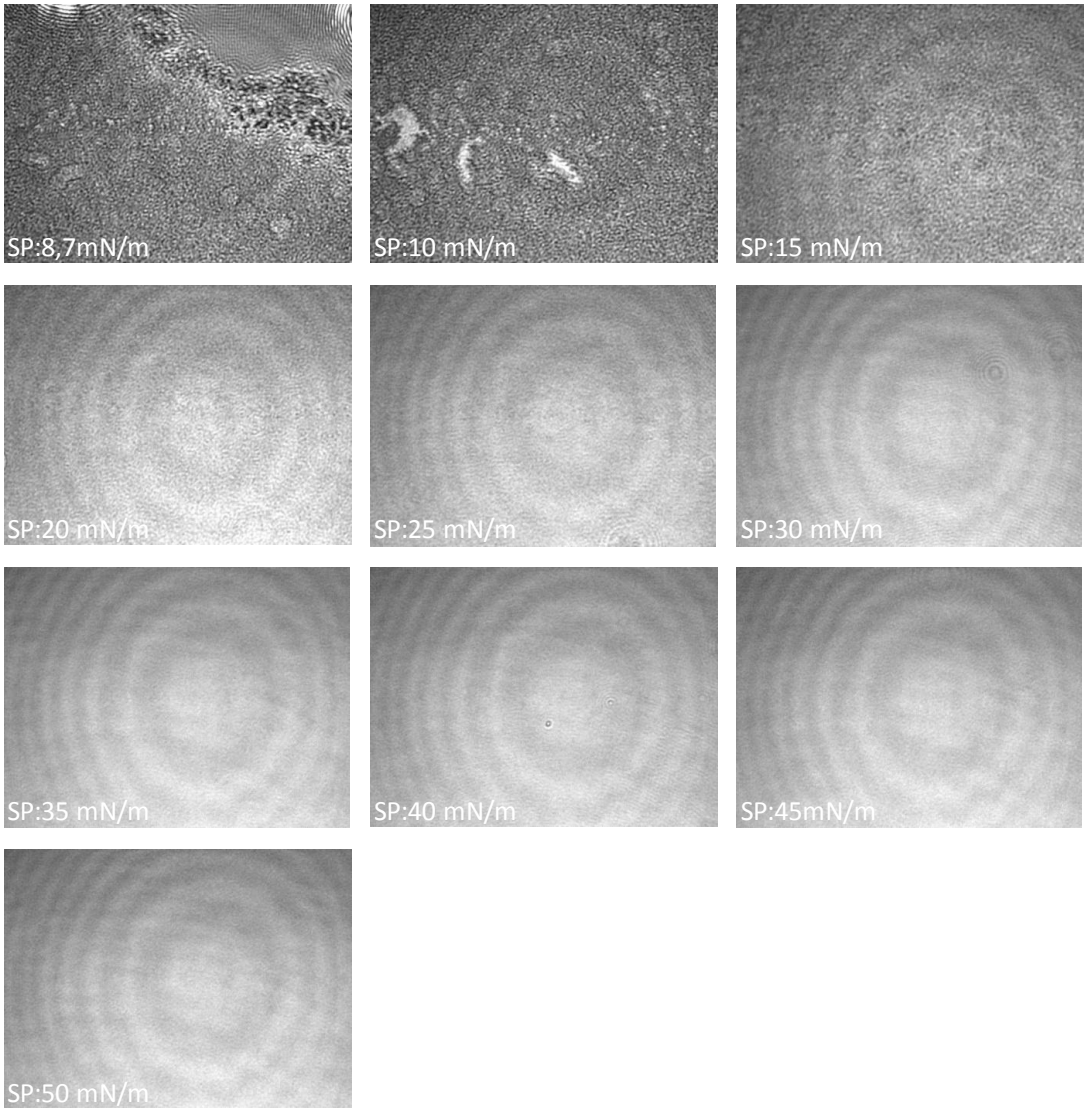

Figure 4.65. BAM images of 7:1:2 DSPC/PEG40 St/DSPE mixed monolayer at the air-water interface

On the contrary of the mixed films prepared with molar fraction of DSPC kept constant at 0.7, for these mixtures the monolayers located in much large mean molecular areas due to bulky PEG chains. Therefore, possibility of meet of DSPE molecules in these mixtures was low and they might form less hydrogen bond with themselves whereas they interact with the other molecules in the mixed films. In addition to isotherm analysis, calculated excess free energy of mixing (ΔG_{exc}) values plotted at different surface pressures were shown in Figure 4.67. The values of ΔG_{exc}

were negative in the whole range of the monolayer composition which denoted that attractive forces were dominant in the mixtures. The minimum ΔG_{exc} observed at the x_{DSPE}=0.3 for DSPC/PEG40 St/DSPE mixed monolayer indicated that at this molar composition mixed films are the most stable. In Figure 4.68 compressional modulus of pure and the mixed monolayers were presented as a function of surface pressure. The mixtures showed lower Cs^{-1} values than values of pure DSPC and pure DSPE. Moreover, a minimum point at nearly 35 mN/m and smaller Cs^{-1} values were noticed compared to DSPC/PEG40 St/DSPE mixed monolayers of x_{DSPC}=0.7 due to expansion effect of PEG chain.

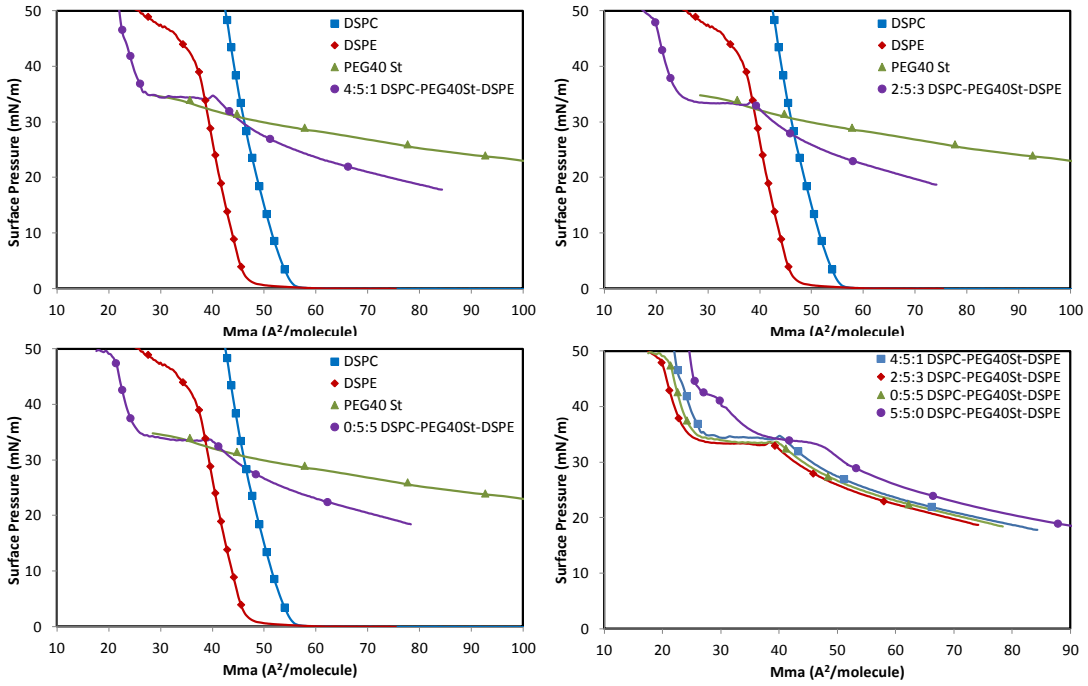

Figure 4.66. The surface pressure –mean molecular area (π-A) isotherms for pure and DSPC/PEG40 St/DSPE mixed monolayers at molar ratios of 4:5:1, 2:5:3, 0:5:5 at the air/water interface

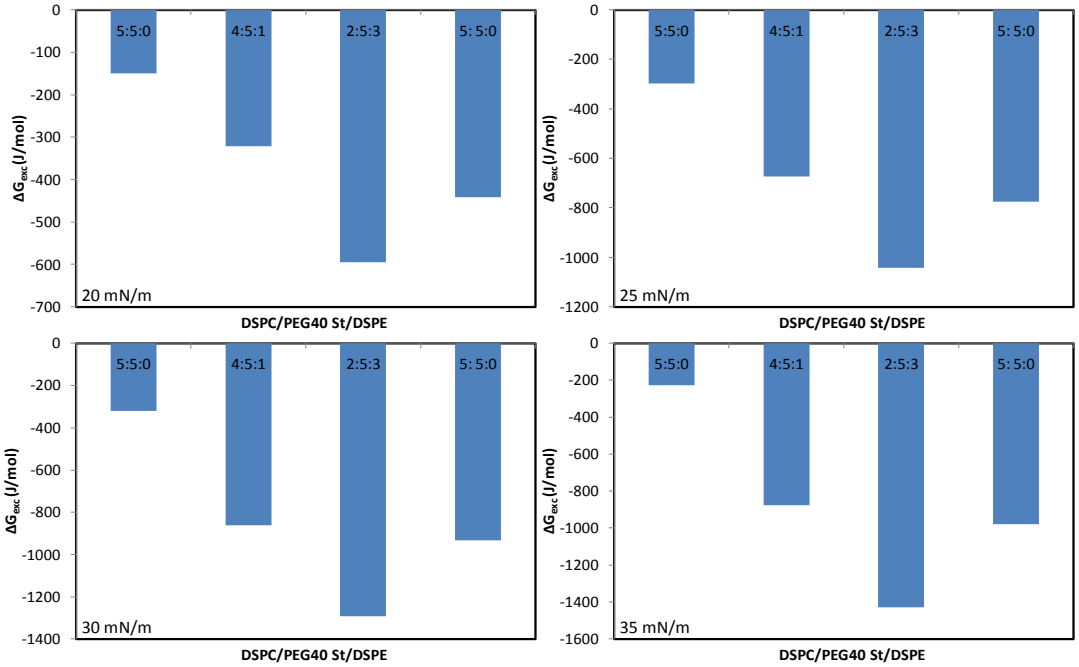

Figure 4.67. The excess free energy of mixing (ΔG_{exc}) values of DSPC/PEG40 St/DSPE mixed monolayers at molar ratios of 4:5:1, 2:5:3, 0:5:5 at different surface pressure

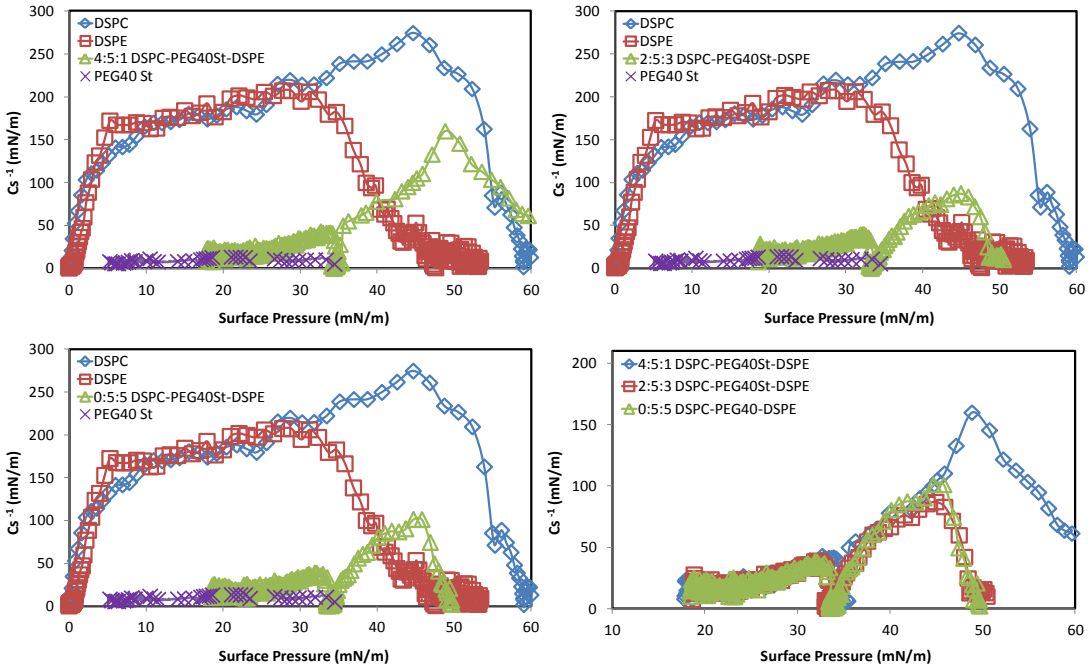

Figure 4.68. The compression modulus (C_s^{-1}) values of DSPC/PEG40 St/DSPE mixed monolayers at 4:5:1, 2:5:3, 0:5:5 molar ratios

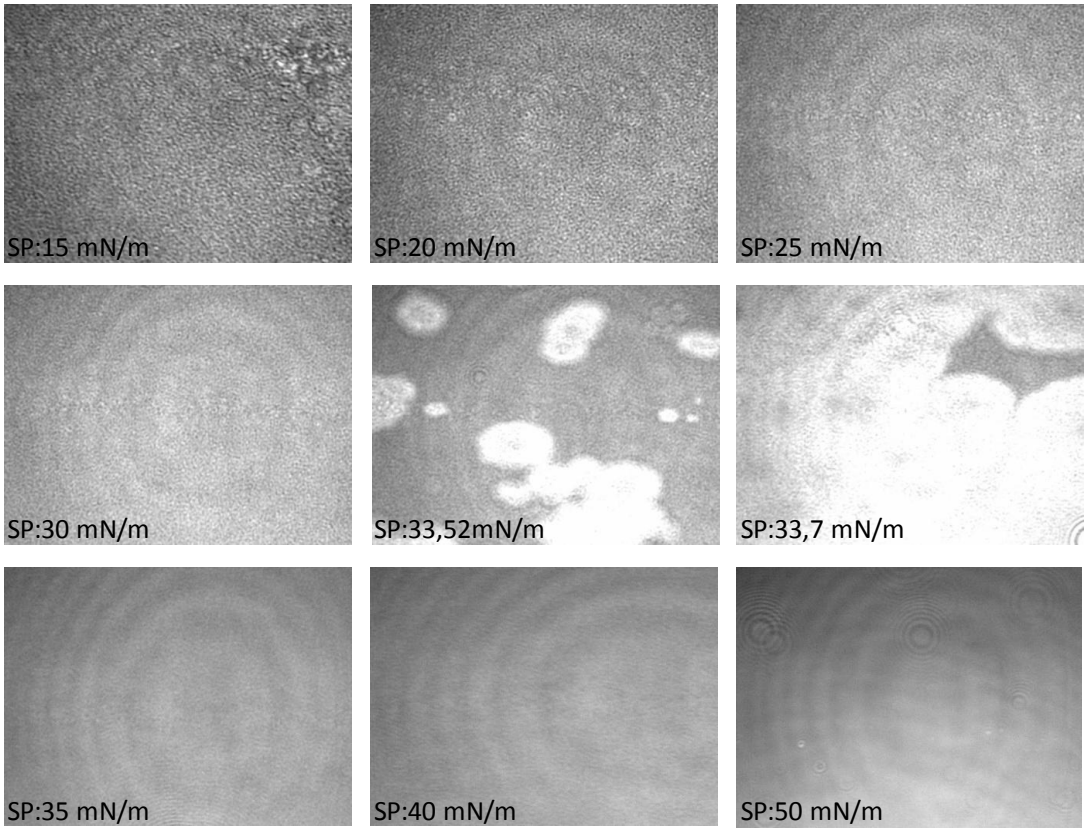

Figure 4.69. BAM images of 4:5:1 DSPC/PEG40 St/DSPE mixed monolayer at the air-water interface

Further analysis of the properties of the mixed monolayers was done based on BAM images taken for the studied mixed films. As seen in Figure 4.69, the images of DSPC/PEG40 St/DSPE mixed monolayer at 4:5:1 molar ratio exhibited almost homogenous surface up to 33 mN/m corresponding to surface pressure of plateau region noticed on the isotherm. After that bright circular domain appeared and at higher surface pressures these domain merged together and formed uniform film as observed for DSPC/PEG40 St/DSPG mixed monolayer at molar ratios of 4:5:1. Although homogenous film was detected for DSPC/PEG40 St/DSPE mixed monolayer at 2:5:3 molar ratio, molecular distance were large due to expansion effect of PEG chains at low surface pressures. At nearly 33 mN/m brightness increased at the surface like DSPC/PEG40 St/DSPG mixed monolayer at molar ratios of 2:5:3 then uniform film was observed up to collapse pressure (Figure 4.70). Similar results were found for 0:5:5 molar ratio as illustrated in Figure 4.71. The analysis of BAM images of these mixed monolayers indicated that no large separated phases were observed. However, at nearly 33 mN/m brightness appeared at the surfaces which were not seen in the BAM images

of DSPC/PEG40 St/DSPE mixtures of x_{DSPC}=0.7. The appearance of this brightness denoted that the transition of the molecules to more ordered phase were seen clearly from the BAM images of the mixtures composed of large amount of PEG40 St.

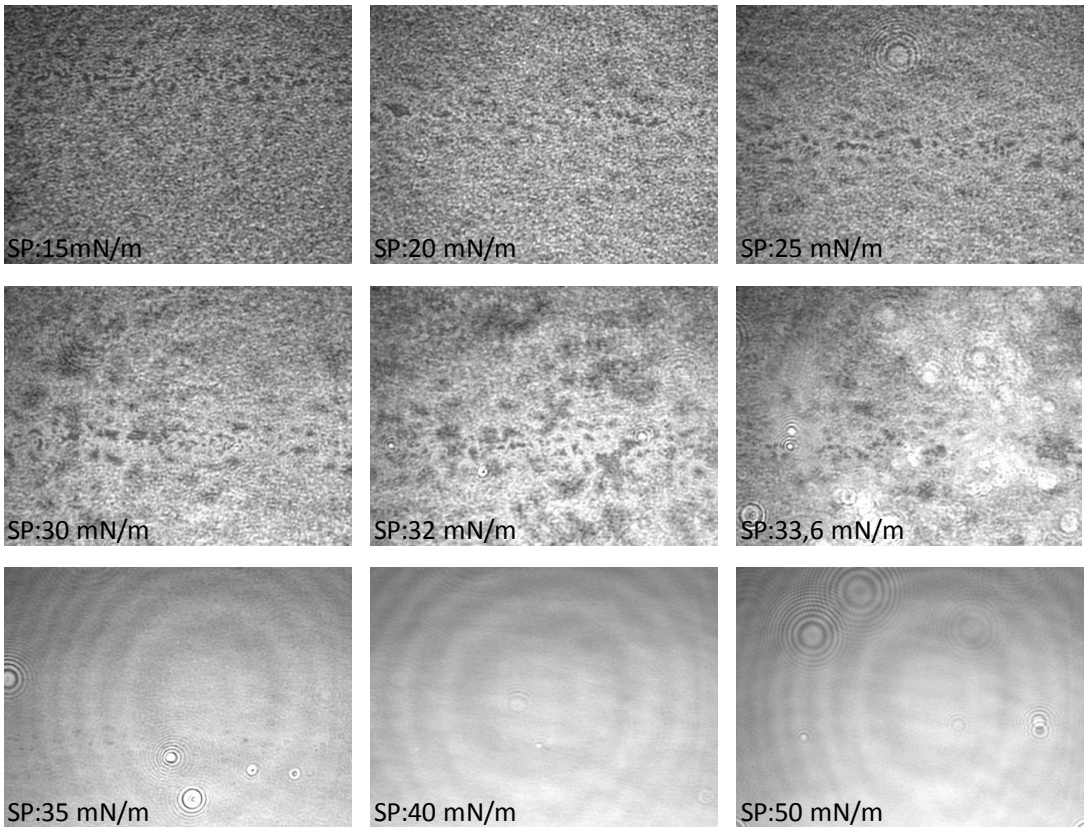

Figure 4.70. BAM images of 2:5:3 DSPC/PEG40 St/DSPE mixed monolayer at the air-water interface

The obtained results indicate that the addition of DSPE molecules into DSPC/PEG40 St monolayer increased the attractive forces between molecules due to close packing structure and hydrogen bonding capacity of DSPE. Also, the combination of analysis of surface pressure-molecular area isotherms and BAM experiments demonstrated that the interaction between molecules in the mixed film prepared with DSPC molar ratio kept at 0.7 were higher due to effect of the attractive forces.

In comparison with DSPC/PEG40 St/DSPG mixed monolayers, ΔG_{exc} of DSPC/PEG40 St/DSPE mixed films were more negative and uniform surface noticed in BAM images at higher surface pressures because hydrogen bond strength of glycerol was weaker (Garidel and Blume 2000).This situation might be referred that stability of

shell structure were enhanced with addition of DSPE molecules into DSPC/PEG40 St mixture.

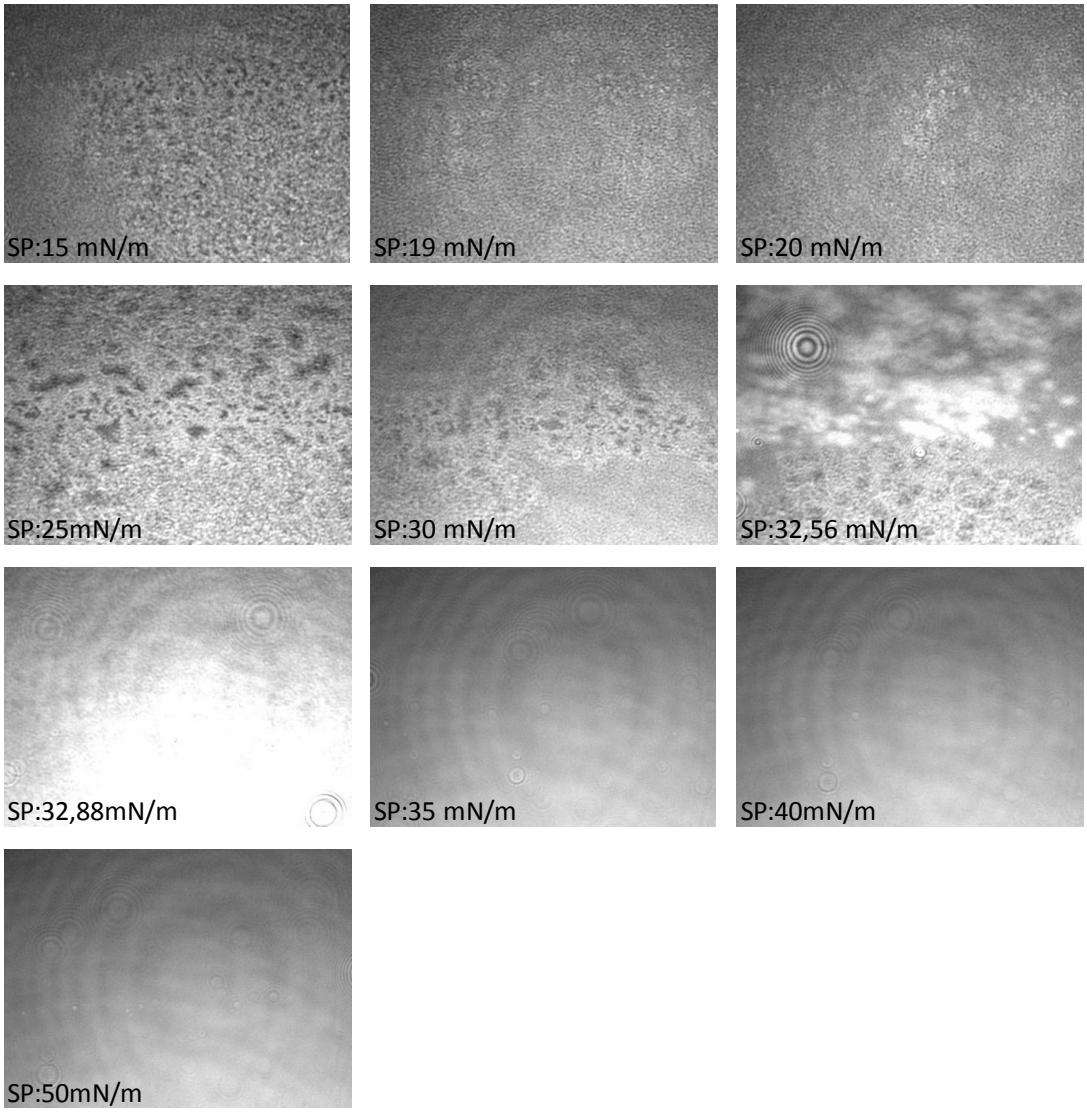

Figure 4.71. BAM images of 0:5:5 DSPC/PEG40 St/DSPE mixed monolayer at the air-water interface

4.2.3. The Phase Behavior and Morphology of DSPC/PEG40 St/DSPA Mixed Monolayers

In the literature, negatively charged PA (phosphate head group) based phospholipids are added to improve stabilization of MBs' shell structure. This type of shell component prevents contact between MBs due to repulsive forces (Hettiarachchi,

Talu et al. 2007). In this part of the study, the effect of PA based phospholipid on phase behavior and morphology of monolayers composed of DSPC and PEG40 St were investigated at varying molar ratio of DSPA in the mixtures.

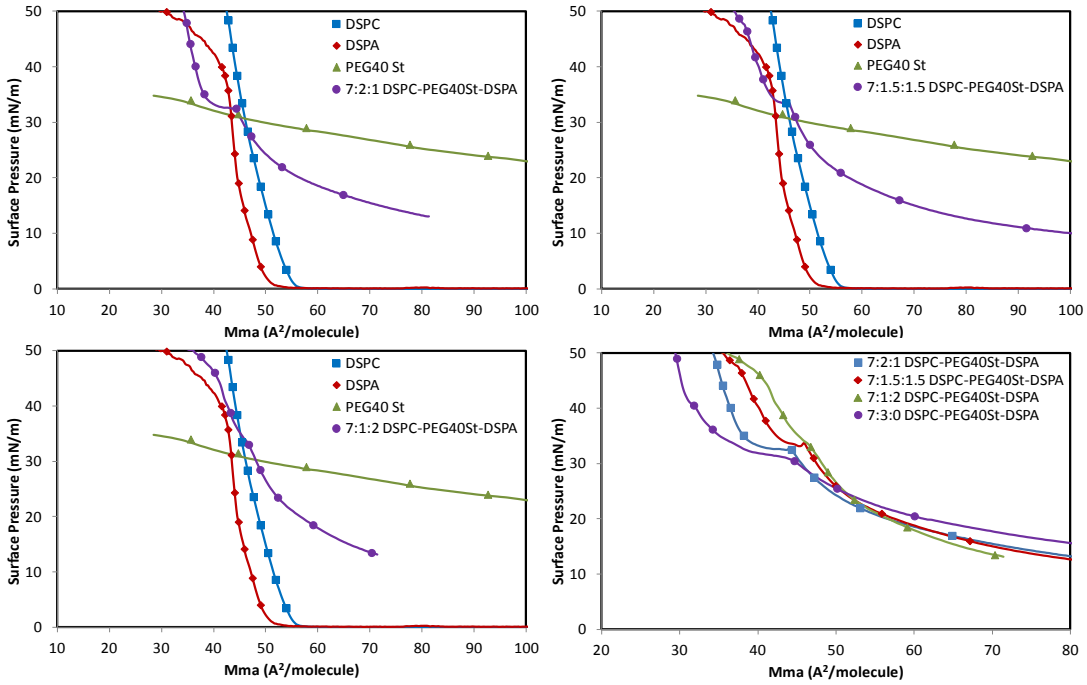

Figure 4.72. The surface pressure –mean molecular area (π-A) isotherms for pure and DSPC/PEG40 St/DSPA mixed monolayers at molar ratios of 7:2:1, 7:1.5:1.5, 7:1:2 at the air/water interface

Although, both DSPG and DSPA lipids have same chain length are negatively charged, the structure of their polar headgroup differs. DSPA has one hydroxyl hydrogen atom while DSPG has two hydroxyl hydrogen atoms, so they can easily form hydrogen bonds with neighboring molecules as well as themselves (Garidel and Blume 1998, Inoue and Nibu 1999, Dickey and Faller 2008).The differences between polar headgroups may affect the MBs' shell stability. For that reason, the mixtures consisting of DSPC, PEG40 St and DSPA were prepared at various molar ratios to examine the effect of DSPA amount on molecular interaction. The surface pressures (π) - mean area per molecule (A) isotherms recorded for pure DSPA and DSPC/PEG40 St/DSPA mixed monolayers with x_{DSPC}=0.7 were given in Figure 4.72. The isotherms of pure DSPA formed high ordered film at the air/water interface as observed for DSPC, DSPG and DSPE in a good agreement with previous result (Yoon, Lee et al. 2010).

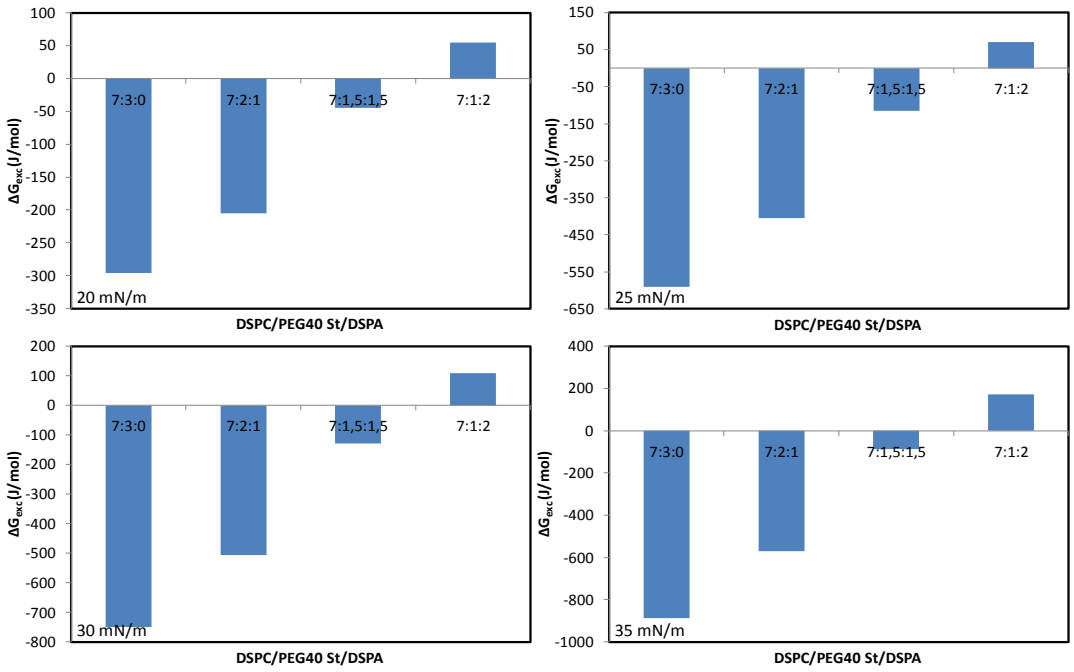

Figure 4.73. The excess free energy of mixing (ΔG_{exc}) values of DSPC/PEG40 St/DSPA mixed monolayers at molar ratios of 7:2:1, 7:1.5:1.5, 7:1:2 at different surface pressure

Also, as seen in Figure 4.72, molecules in the DSPA monolayer were packed densely and showed more condensed phase as compared to DSPC, due to differences in headgroup size. It is well known that attractive headgroup interactions can be occurred between PA molecules than PCs because of smaller headgroup of PAs (Bos and Nylander 1996, Garidel and Blume 1998, Estrela-Lopis, Brezesinski et al. 2004, Lee, Lin et al. 2006, Dickey and Faller 2008). Therefore, the molecular area of DSPA monolayer was significantly smaller than that of DSPC (Dickey and Faller 2008). For low surface pressures, the isotherms of mixed monolayers shown in Figure 4.72 exhibited that liquid-expanded (LE) phase behavior unlike pure DSPC and DSPA monolayers. In addition, a plateau was noticed at nearly 35 mN/m after that liquid-condensed phase behavior was observed as detected for other mixtures. Similar to DSPC/PEG40 St/DSPG mixed monolayer with x_{DSPC}=0.7, the addition of large amount of DSPA into DSPC/PEG40 St/DSPA mixtures affected the monolayer properties and the isotherms shifted to large area per molecule (Garidel, Johann et al. 1997, Cambrea, Haque et al. 2007).

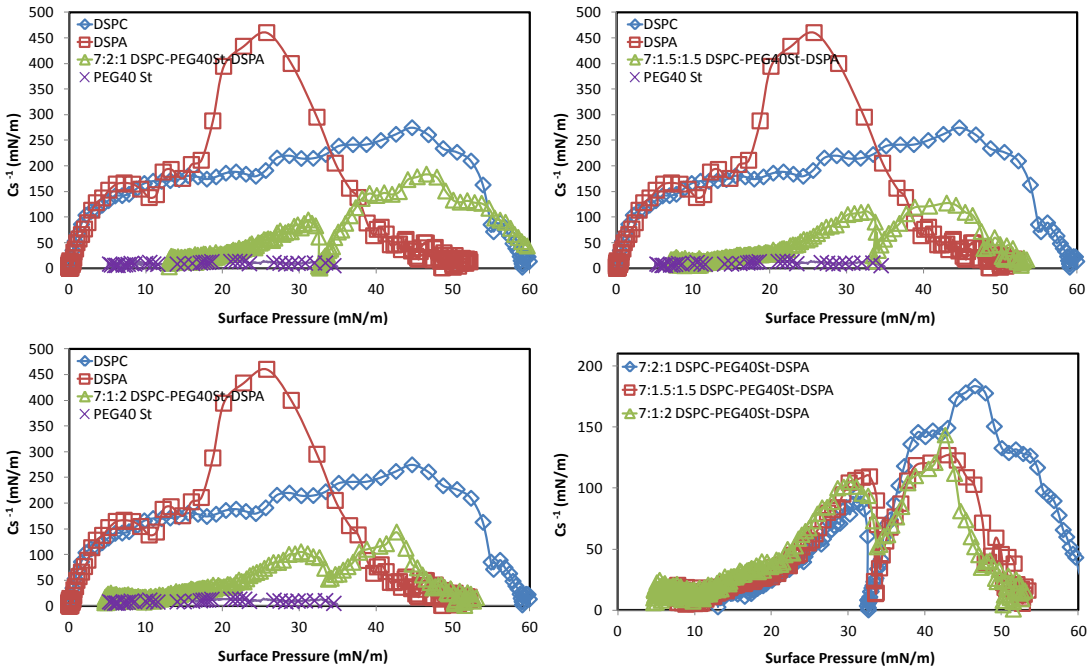

Figure 4.74. The compression modulus (C_s^{-1}) values of DSPC/PEG40 St/DSPA mixed monolayers at 7:2:1, 7:1.5:1.5, 7:1:2 molar ratios

The interactions between the components in the mixed monolayers were analyzed in terms of their the excess Gibbs energies (ΔG_{exc}). The negative values of ΔG_{exc} observed in Figure 4.73 suggested that attractive interactions were available between molecules in the mixed monolayers for 7:2:1 and 7:1.5:1.5 molar ratios. This results is similar to earlier investigation of DPPC/DPPA mixed monolayers showing that attractive forces between the molecules (Lee, Lin et al. 2006), so DSPC could interact strongly with both PEG40 St and DSPA molecules. However, ΔG_{exc} values of DSPC/PEG40 St/DSPA mixed monolayer at 7:1:2 molar ratio were positive at all surface pressures due to repulsive forces derived from large amount of negatively charged headgroup of DSPA and PEG chains. For each plots showing the variation of ΔG_{exc} values of the compositions at specific surface pressure, the minimum value occurred at x_{DSPA}=0.1.The occurrence of a minimum indicates that the influence of molecular interaction on the monolayer thermodynamic stability was most significant at this composition. It was also found that the negative value of G_{exc} increased with increasing surface pressure. Such a result implied that the molecular interactions became significant at higher surface pressures where the monolayer was in ordered state. Moreover, in Figure 4.74 the compressional modulus (C_s^{-1}) of pure and mixed

monolayers were presented. C_s^{-1} values of pure DSPA was higher than DSPC because of more condensed behavior of DSPA. Similar to results obtained for the other investigated mixed monolayers composed of the phospholipids having different headgroup, PEG chains in the mixed monolayers showing expanded behavior at the air/water interface decreased C_s^{-1} values compared to pure DSPC and DSPA and a minimum point at nearly 35 mN/m was noticed in these plots. These low C_s^{-1} values of the mixed monolayers suggest that the monolayer is in more elastic state (Quiroga, Monzón et al. 2011).

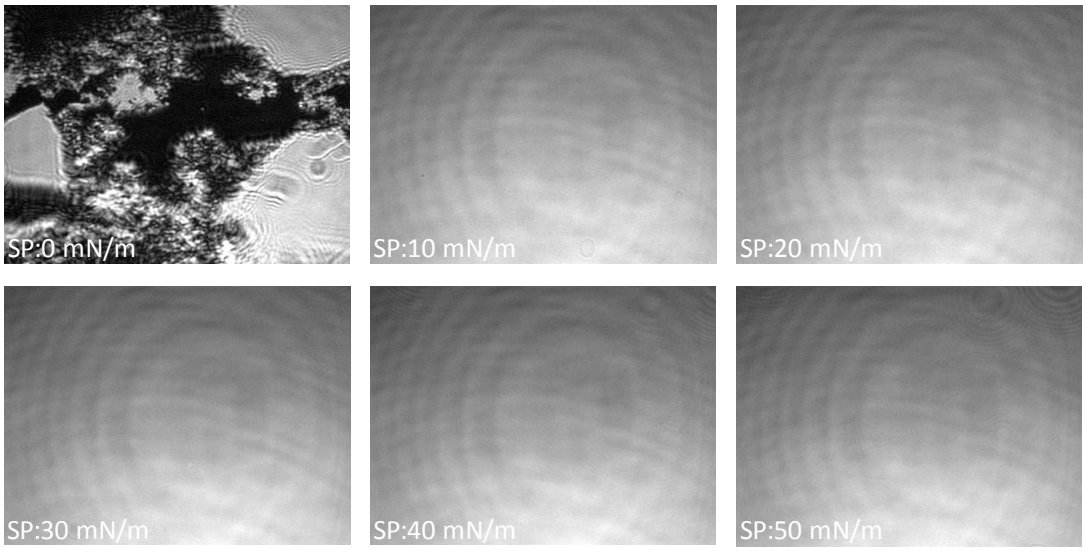

Figure 4.75. BAM images of pure DSPA monolayer at the air-water interface

BAM images of pure DSPA taken during compression were illustrated in Figure 4.75. Like pure DSPC and pure DSPG, for pure DSPA monolayer at low surface pressures condensed patches were detected and with increasing surface pressure these patches came together and formed uniform film which covered the surface completely. As seen in Figure 4.76, BAM images of DSPC/PEG40 St/DSPA mixed monolayer at 7:2:1 molar ratio demonstrated more homogeneous surface than that of other mixed monolayers at 7:1.5:1.5 and 7:1:2 molar ratios given in Figure 4.77 and in Figure 4.78 respectively.

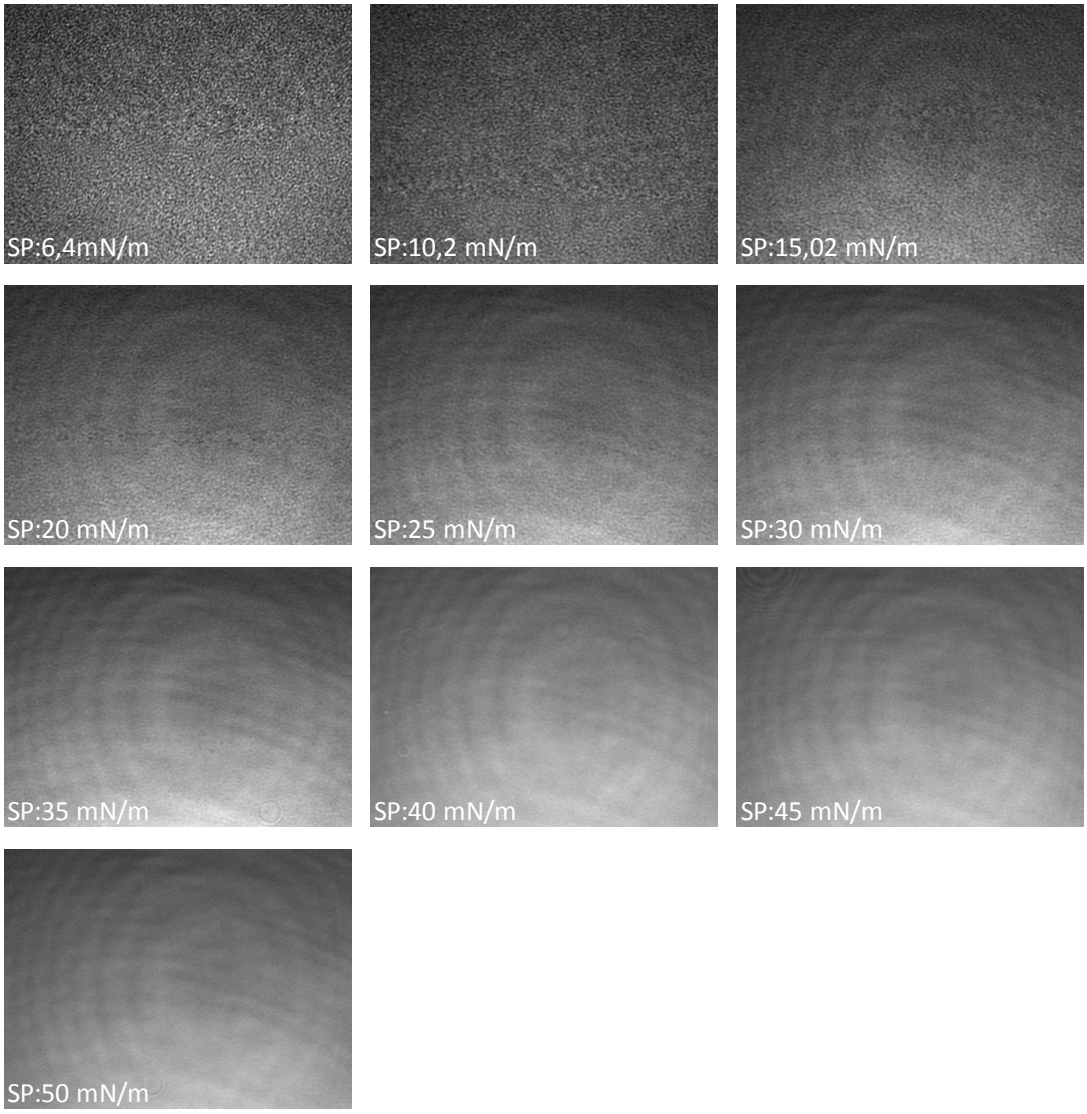

Figure 4.76. BAM images of 7:2:1 DSPC/PEG40 St/DSPA mixed monolayer at the air-water interface

At low surface pressures, large molecular distance and small bright condensed structures at some regions were detected for 7:1.5:1.5 molar ratio. Also, small separated circular bright domains were noticed at nearly 5 mN/m and 10 mN/m in BAM images of DSPC/PEG40 St/DSPA mixed monolayer at molar ratios of 7:1:2. The BAM images recorded for DSPC/PEG40 St/DSPA mixed monolayer with x_{DSPC}=0.7 showed more homogenous film compared to DSPC/PEG40 St/DSPG and DSPC/PEG40 St/DSPE mixed monolayers with x_{DSPC}=0.7. These results suggest that charge and size of phospholipids' headgroup are important parameters affecting the molecular interactions and morphology.

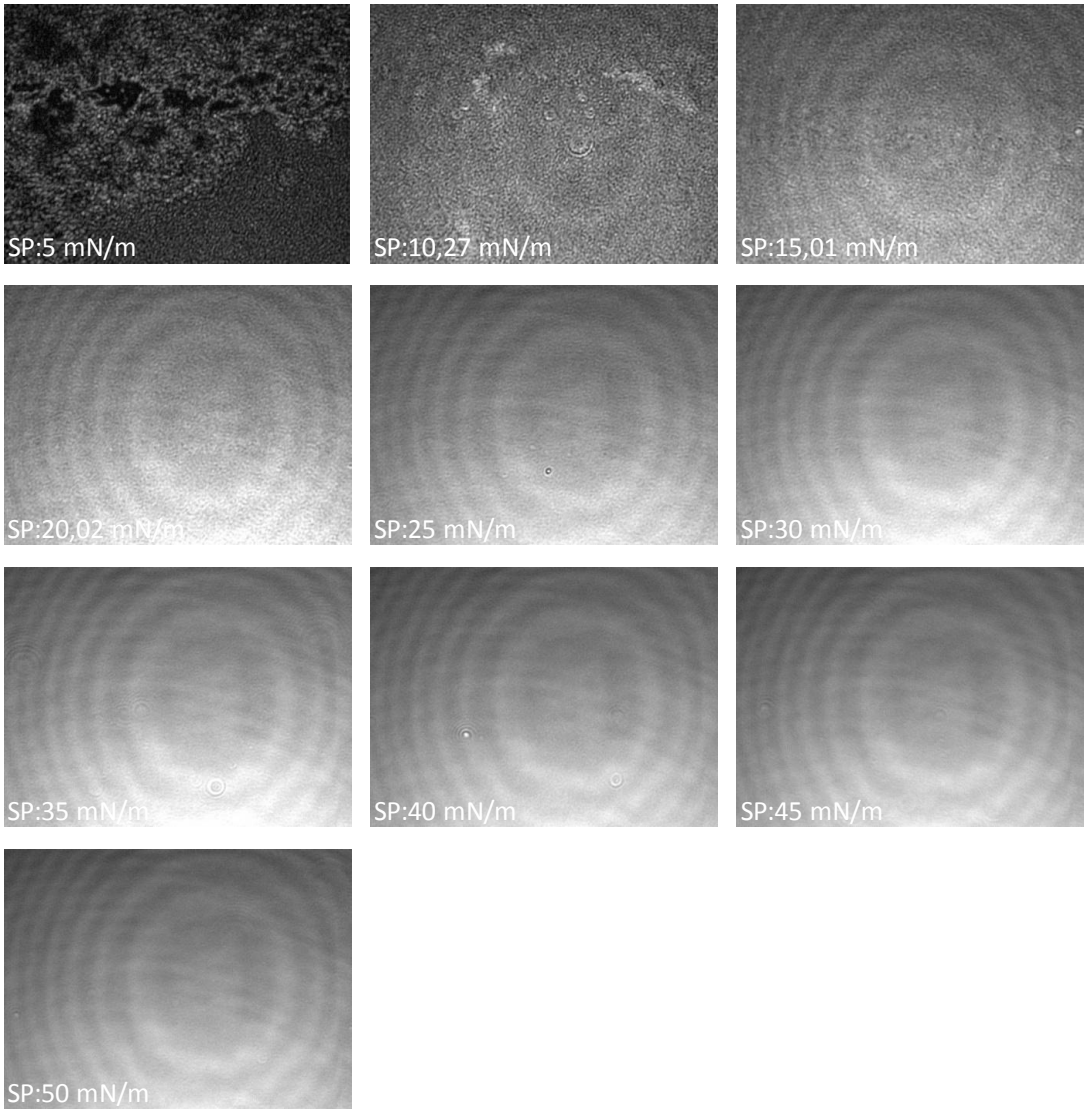

Figure 4.77. BAM images of 7:1.5:1.5 DSPC/PEG40 St/DSPA mixed monolayer at the air-water interface

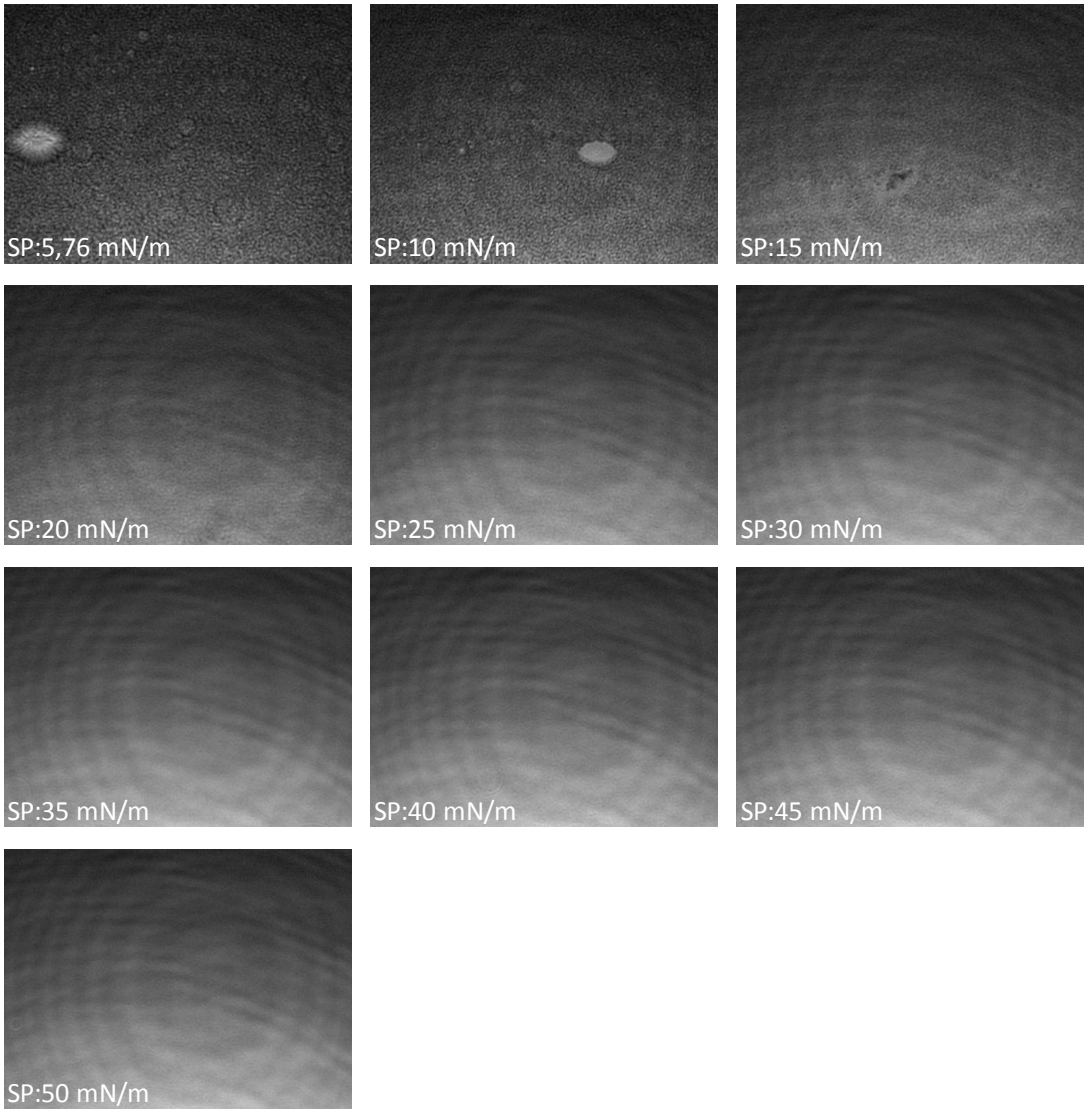

Figure 4.78. BAM images of 7:1:2 DSPC/PEG40 St/DSPA mixed monolayer at the air-water interface

The surface pressure (π) versus mean area per molecule (A) isotherms of DSPC/PEG40 St/DSPA mixtures at 4:5:1, 2:5:3, 0:5:5 molar ratios were shown in Figure 4.79. If the mixed monolayer at 4:5:1 and at 2:5:3 molar ratios are compared, it can be seen that area per molecule shifted to the left with increasing content of DSPA and the molecule in the mixed molar at molar ratio of 2:5:3 occupied very small area due to small headgroup of DSPA molecules and attractive forces between the components in these mixture. DSPC/PEG40 St/DSPA mixed monolayer at molar ratio of 0:5:5 disturbed this behavior due to absence of DSPC molecules. It suggested that DSPC molecules having zwitterionic character affected the interaction between DSPA

and PEG40 St. Moreover, plateau regions at nearly 35 mN/m were noticed on these isotherms as in the other investigated mixed monolayers.

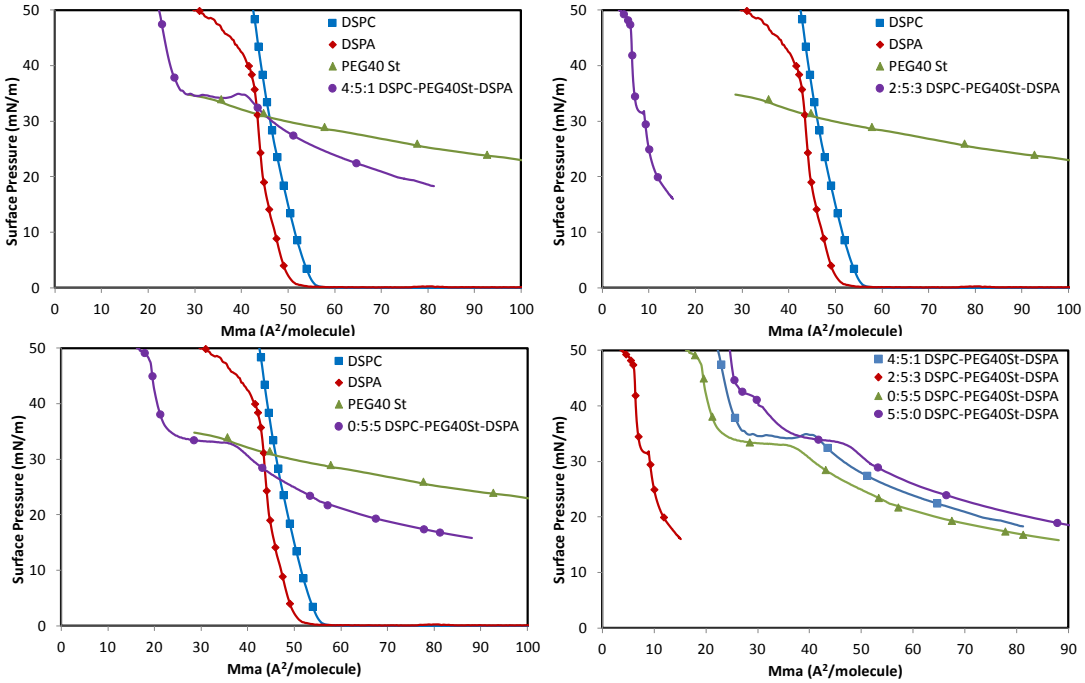

Figure 4.79. The surface pressure –mean molecular area (π-A) isotherms for pure and DSPC/PEG40 St/DSPA mixed monolayers at molar ratios of 4:5:1, 2:5:3, 0:5:5 at the air/water interface

As shown in Figure 4.80 that the values of the excess free energy of mixing were negative in the whole range of the monolayer composition. Therefore, attractive forces were dominant between the molecules in the DSPC/PEG40 St/DSPA mixed monolayer at these molar ratios. The minimum ΔG_{exc} observed at the x_{DSPA}=0.3 for DSPC/PEG40 St/DSPA mixed monolayers similar to DSPC/PEG40 St/DSPE mixed monolayers. The distance between molecules in these mixed monolayers was enlarged owing to large amount of PEG chains. The large amount of DSPA increased the attractive interactions between molecules in the mixed monolayers with $x_{PEG40\ St}$ =0.5, because DSPA molecules can easily form hydrogen bonds with neighboring molecules (Garidel and Blume 1998, Inoue and Nibu 1999, Dickey and Faller 2008). However, DSPC/PEG40 St/DSPG mixed monolayers at 4:5:1 molar ratio showed minimum ΔG_{exc} values. Although hydrogen bonding capacities of DSPG molecules were high, negative charge on the phosphate and two hydroxyl groups might cause more repulsive effect than DSPA molecules (Inoue and Nibu 1999, Watry, Tarbuck et al. 2003, Dickey and

Faller 2008, Maniti, Cheniour et al. 2009, Wydro and Witkowska 2009). Therefore, adding of large content of DSPG molecules in the mixtures might not be good for attractive interactions. In addition to this, Cs^{-1} values of these mixed monolayers were presented in Figure 4.81. As seen from Figure 4.81, a minimum point was detected for these mixed monolayers at nearly 35 mN/m corresponding to surface pressure of plateau region on the isotherms. Also, the Cs^{-1} values of the mixtures were smaller than the ones of pure DSPC and pure DSPA due to expansion effect of PEG chains. Same results were found for DSPC/PEG40 St/DSPG and DSPC/PEG40 St/DSPE mixed monolayers which denoted that PEG40 St molecules in the mixtures increased the elasticity.

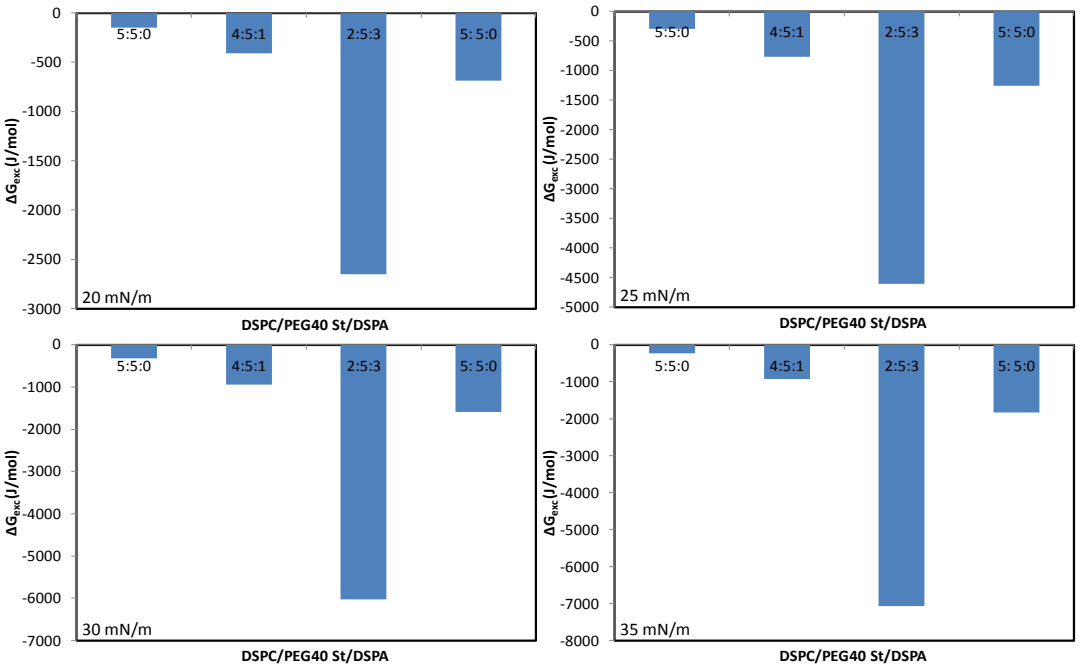

Figure 4.80. The excess free energy of mixing (ΔG_{exc}) values of DSPC/PEG40 St/DSPA mixed monolayers at molar ratios of 4:5:1, 2:5:3, 0:5:5 at different surface pressure

Figure 4.82, Figure 4.83 and Figure 4.84 show morphological information of the mixed monolayers for 4:5:1, 2:5:3, 0:5:5 molar ratios at various compression states respectively. As shown in the BAM images of DSPC/PEG40 St/DSPA mixed monolayer at 4:5:1 molar ratio, generally homogenous surface was noticed up to 34 mN/m, though at ≈ 19 mN/m large molecular distance (dark region) was detected .At nearly 34 mN/m, small bright circular domains occurred and they got together with

compression. Finally, uniform film was formed up to collapse pressure. Similar circular domains and uniform surface were noticed in BAM images of DSPC/PEG40 St/DSPG and DSPC/PEG40 St/DSPE mixed monolayers at 4:5:1 molar ratio. Dark expanded region seen in BAM image of DSPC/PEG40 St/DSPA mixed monolayer at molar ratios of 2:5:3 enlarged the molecular distance at low surface pressure similarly previous investigated BAM images of DPPA/DPPC mixed monolayer by Lee *et al* (Lee, Lin et al. 2006) and brightness appeared at ≈ 31 mN/m.. As can be seen in Figure 4.84, there were separated phases condensed and less condensed phase at low surface pressure. Similar to other mixed monolayers nearly 34 mN/m, brightness was observed. The surface pressure in which brightness appeared corresponded to nearly plateau regions on π-A isotherms of the mixed monolayers. These differences at the surfaces indicated that conformational changes of the molecules in the mixtures.

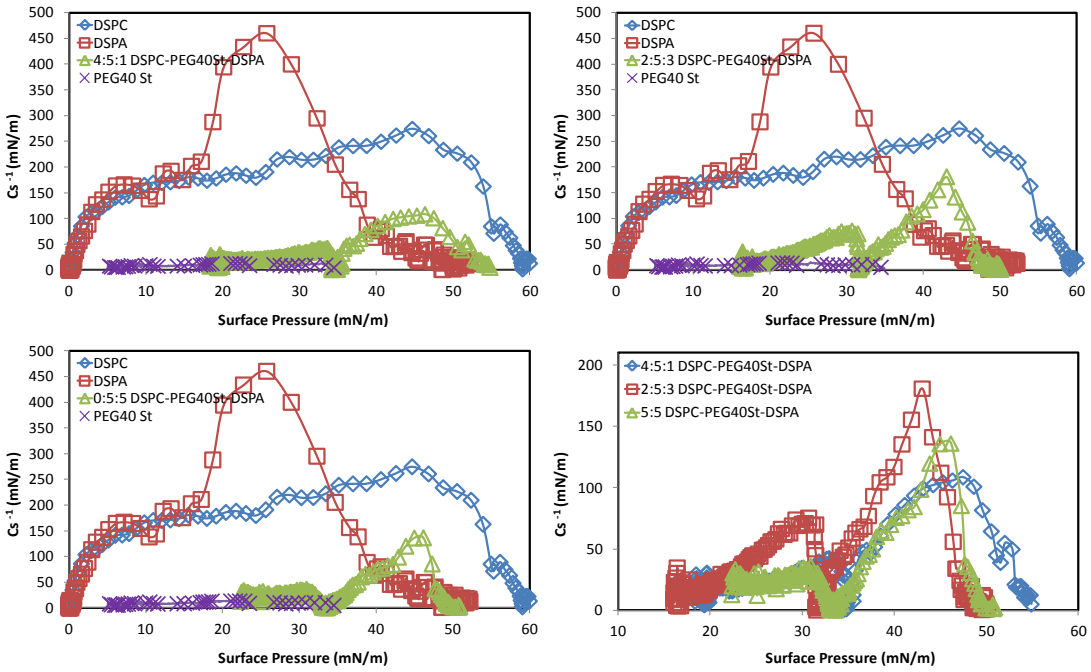

Figure 4.81. The compression modulus (C_s^{-1}) values of DSPC/PEG40 St/DSPA mixed monolayers at 4:5:1, 2:5:3, 0:5:5 molar ratios

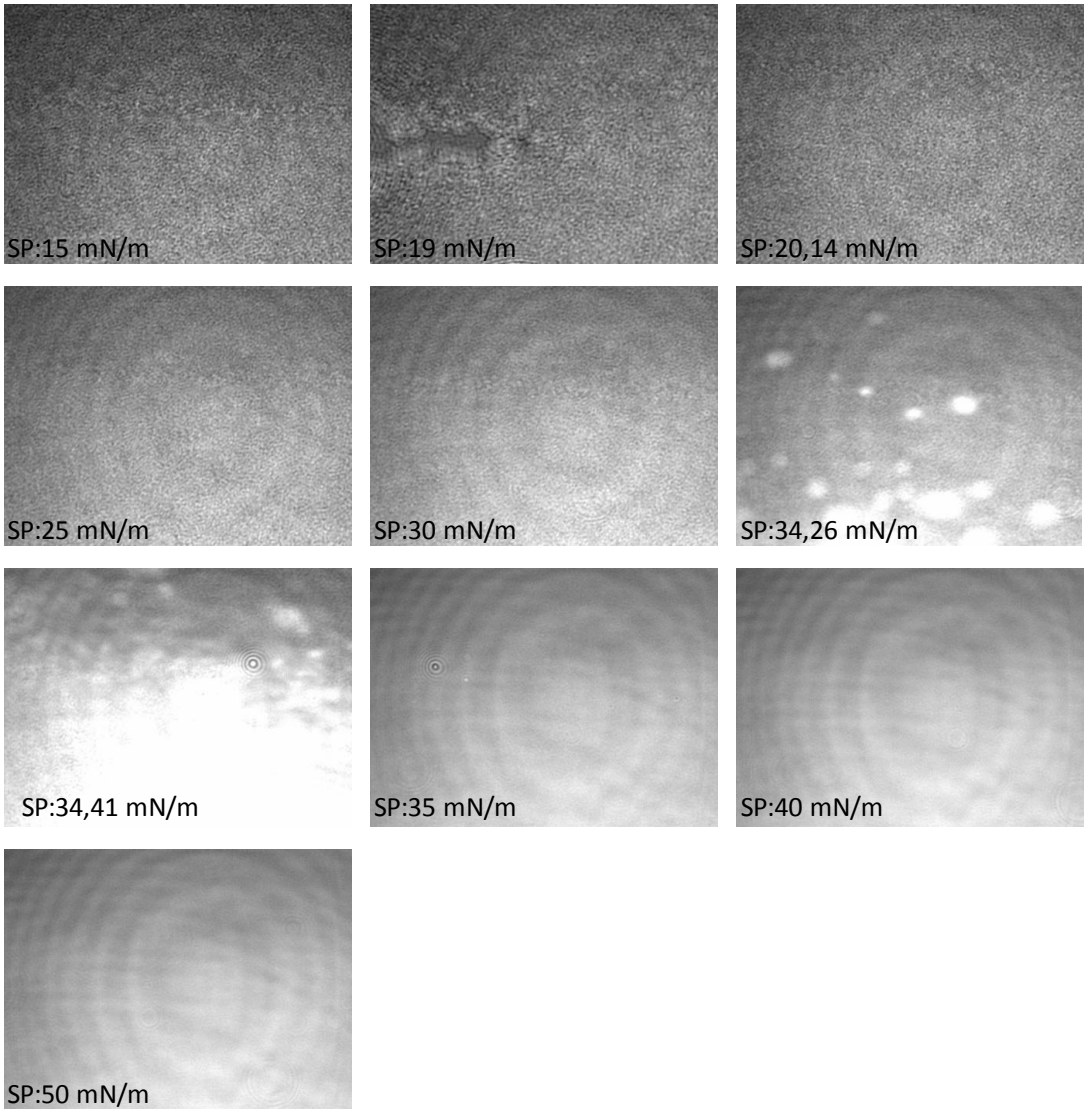

Figure 4.82. BAM images of 4:5:1 DSPC/PEG40 St/DSPA mixed monolayer at the air-water interface

The results obtained for DSPC/PEG40 St/DSPA mixed monolayers at various molar ratios signified that incorporation of DSPA molecule exhibited attractive interaction between molecules for mixed monolayers with x_{DSPC}=0.7 consisting a small amount of DSPA and for all compositions of mixed monolayers with $x_{PEG40\ St}$=0.5 thanks to close packing structure and hydrogen bonding capacity of DSPA. However, as seen from their BAM images separated phases and brightness were detected at some regions. In this situation, addition of DSPA molecules as a third component into MBs' shell formulation may improve shell stability and appropriate composition can be chosen with the help of combination of π-A isotherm analysis and BAM images outcomes.

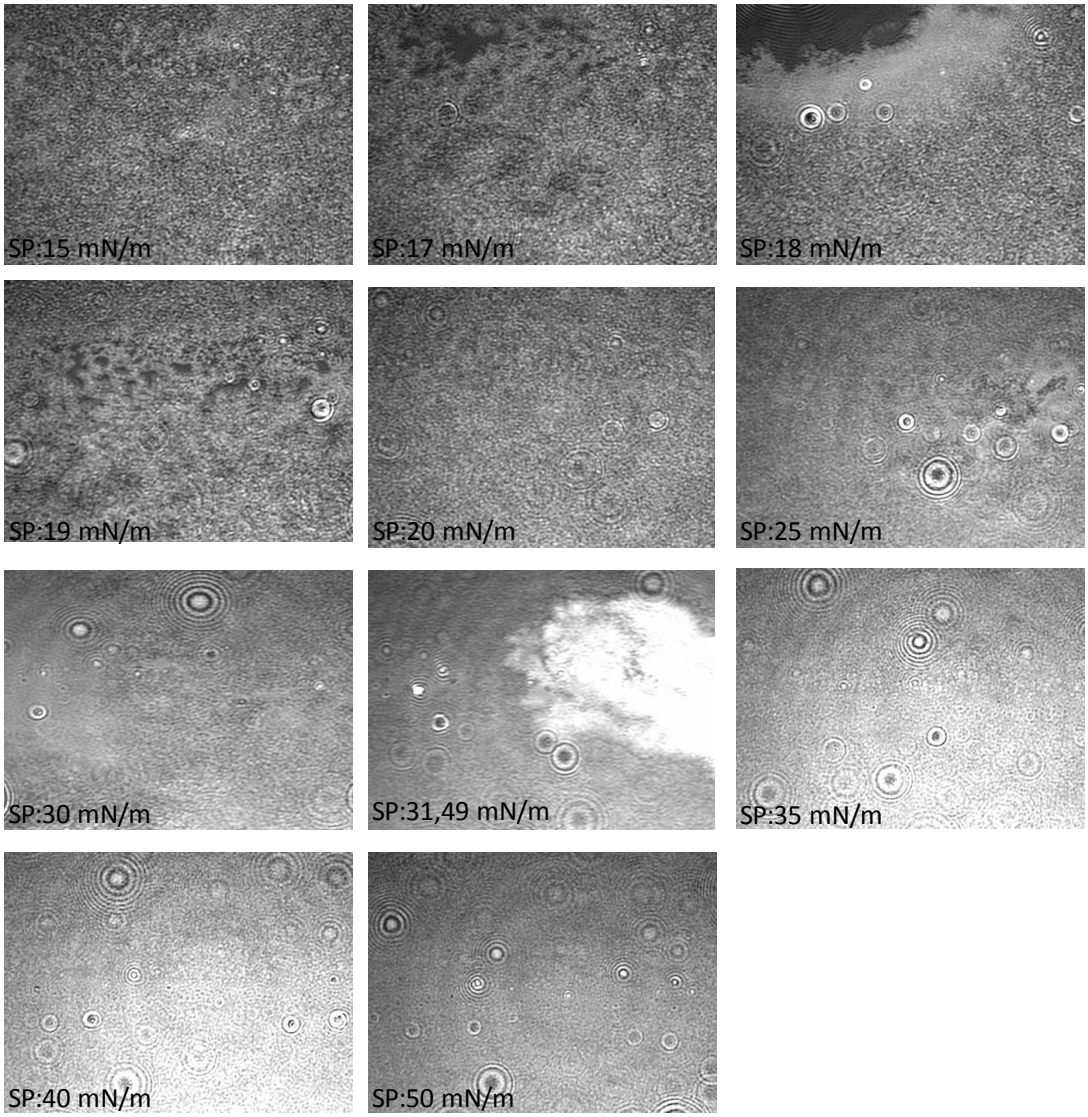

Figure 4.83. BAM images of 2:5:3 DSPC/PEG40 St/DSPA mixed monolayer at the air-water interface

In this section, several combinations of phospholipids having same acyl chain but different head group (DSPG, DSPE, DSPA, DSPC) and PEG40 St species were examined. The influence of the polar head structure on the intermolecular forces between the components of the mixed monolayers was investigated at various surface pressures by the analysis of the interactions between molecules and BAM images. As shown in Figure 4.85, the effects of polar headgroups on the π-A isotherms can be seen clearly by keeping the composition constant. The molecular areas were changed due to differences between the headgroups. DSPA includes the smallest headgroup, so the isotherm of DSPA/PEG40 St monolayer at 5:5 molar ratio was located at smaller molecular area than that of the others. It was also determined that the monolayer

behavior at the air/water interface was affected by the incorporation of DSPG, DSPE and DSPA as an additional component into DSPC/PEG40 St monolayer because of the specific interactions between these molecules.

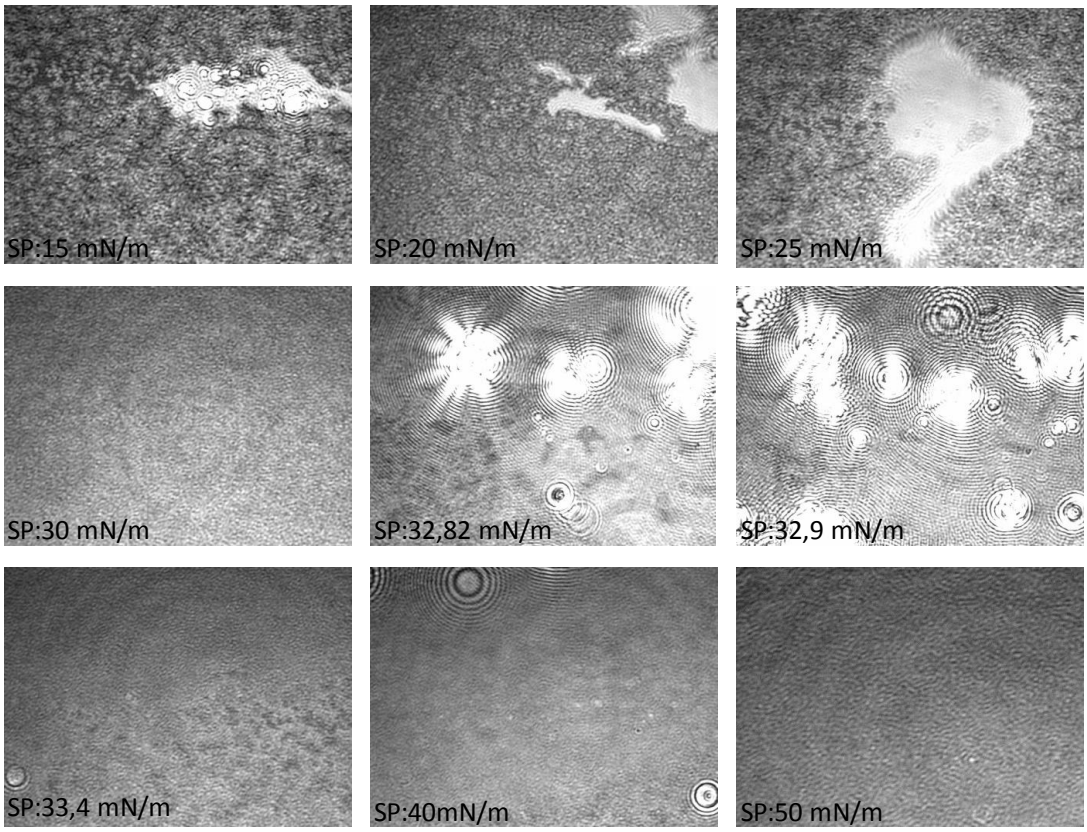

Figure 4.84. BAM images of 0:5:5 DSPC/PEG40 St/DSPA mixed monolayer at the air-water interface

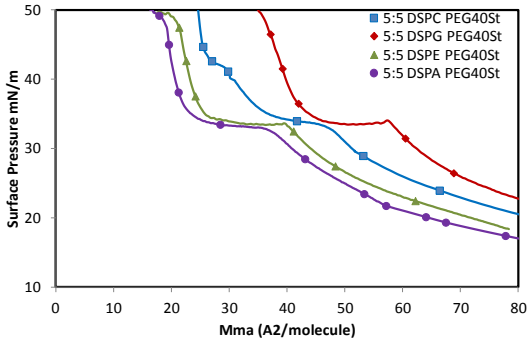

Figure 4.85. The surface pressure–mean molecular area (π-A) isotherms for DSPC/PEG40 St, DSPG/PEG40 St, DSPE/PEG40 St, DSPA/PEG40 St mixed monolayers at molar ratios of 5:5 at the air/water interface

Related to differences in the polar headgroup regions, effects of addition of these molecules were different. High hydrogen bonding capacity of DSPE molecules created strong attractive forces between the molecules. Therefore, DSPC/PEG40 St/DSPE mixed monolayers had the most minimum ΔG_{exc} values which can exhibit more stable shell structure than DSPC/PEG40 St/DSPG and DSPC/PEG40 St/DSPA mixed monolayers for the ternary mixtures with x_{DSPC}=0.7. As known that DSPA and DSPG molecules can form hydrogen bond with themselves and other molecules. However, repulsive forces derived from negatively charged headgroup weakened the attractive forces. This trend was observed for mixed monolayers with x_{DSPC}=0.7 disturbed for the mixed monolayers with $x_{PEG40\ St}$=0.5 due to expansion effect of PEG chains. The distance between the molecules was enlarged by the PEG chains so repulsive forces between DSPA-DSPA and DSPG-DSPG molecules were reduced. The DSPC/PEG40 St/DSPA mixed monolayers were more compressible and showed more negative ΔG_{exc} than others due to very small head group of DSPA molecules. Also, BAM and AFM results of ternary mixtures showed that there are separated phases at some regions. In addition to these, morphological differences at nearly 35 mN/m corresponding to plateau region on the π-A isotherms were observed that indicated possible conformational change of molecules in the mixture systems to form condensed phase at the air/water interface.

CHAPTER 5

CONCLUSIONS

In this study, shell structure of MBs was redesigned and characterized by Langmuir Blodgett (LB) method, Brewster Angle Microscopy (BAM) and Atomic Force Microscopy (AFM). For this purpose, phospholipids having same acyl chain length but different headgroup (DSPC, DSPG, DSPA, DSPE), PEG40 St and PEG-grafted phospholipids were used as shell components. The interactions between the shell components in the mixed monolayers prepared at different compositions were investigated.

Thermodynamically analysis of DSPC/PEG40 St binary systems at various molar ratios signified that miscibility of the two components increased with increasing PEG40St content, resulting in attractive forces between the components and thus more stable monolayers. However, separated phases were detected in BAM and AFM images of the mixed films. It is possible that in some regions of mixed monolayers PEG40 St molecules mixed with DSPC molecules, resulting in some regions composed of the condensed lipid-rich phase and some regions less condensed emulsifier-rich phase.

The mixed monolayers at different molar ratios of lipopolymers (DSPE-PEG350, DSPE-PEG1000, DSPE-PEG2000) and DSPC, were found to be miscible and attractive forces between the molecules were dominant as evidenced from the results of compression isotherm of the mixed systems. It was determined that mean molecular areas increase with increasing length of PEG chain due to steric repulsion between the polymer chains. Also, the attractive forces between the molecules became stronger with increasing PEG content for DSPC/DSPE-PEG1000 and DSPC/DSPE-PEG350 mixed monolayers unlike DSPC/DSPE-PEG2000 mixed monolayers since the PEG2000 chain length is longer than the lengths of PEG1000 and PEG350 chains. Therefore, repulsive forces between PEG2000 molecules were higher and they prevented strong interaction between molecules in mixture. BAM studies of these mixtures indicated that phase separations existed at some low and high surface pressure regions. The two phases in the mixed monolayers could be interpreted as a single-component DSPC phase and a mixed DSPC/lipopolymer phase. The phase separations at these regions were detected

for DSPC/DSPE-PEG2000 mixed monolayers consisting of 10% DSPE-PEG2000. However, DSPC/DSPE-PEG1000 mixed monolayer at 9:1 molar ratio exhibits difference only at low surface pressure region, whereas DSPC/DSPE-PEG350 mixed monolayer at this ratio do not reveal any difference because the length of PEG chain of DSPE-PEG350 molecule is shorter than DSPE-PEG2000 and DSPE-PEG1000 molecules' and molecules in this mixture can get close to each other and create homogenous surface. According to these, the repulsive and attractive interaction between binary molecules was influenced by the composition of mixed monolayer and the distribution of lipopolymers in DSPC varies depending not only on the surface pressure but also on the lipopoymer content.

The mixtures composed of several combinations of phospholipids having the same acyl chain lenght but different head group (DSPG, DSPE, DSPA, DSPC) and PEG40 St species were also concerned. The analysis of the interactions between the molecules and BAM images taken at various surface pressures allowed to examine the influence of the polar head structure on the intermolecular forces between the components of the mixed monolayers. It was found that the incorporation of DSPG, DSPE and DSPA as an additional component into DSPC/PEG40 St mixture differently affected the monolayer behavior at the air/water interface due to differences in the polar headgroup regions and the specific interactions between these molecules. For combinations of the ternary mixtures with x_{DSPC}=0.7, DSPC/PEG40 St/DSPE mixed monolayers having minimum ΔG_{exc} values can exhibit more stable shell structure than DSPC/PEG40 St/DSPG and DSPC/PEG40 St/DSPA mixed monolayers, because high hydrogen bonding capacity of DSPE molecules created strong attractive forces between the molecules in the mixtures. However, this trend was not the same for the mixed monolayers with $x_{PEG40\ St}$=0.5 because of expansion effect of PEG chains. The DSPC/PEG40 St/DSPA mixed monolayers were more compressible owing to very small head group of DSPA molecules and showed more negative ΔG_{exc} than the others. In addition to these results, BAM images of the mixed monolayers demonstrated that at some regions separated phases and morphological differences at nearly 35 mN/m corresponding to plateau region observed on the π-A isotherms which suggested that a possibility of conformational change of molecules in the investigated mixture systems.

This study suggests that in order to obtain more stable monolayer formation for microbubble shell structure, different molar ratios of phosphatidylcholine and PEG40 St should be considered. In addition, although phosphatidylcholine and PEG40 St are the

most common and most studied components for preparation of microbubbles, PEG-grafted phospholipids can be used instead of PEG40 St. Also, the use of other types of phospholipids as an additional component in a DSPC/PEG40 St mixture could be a good choice for microbubble formulations. Therefore, the analysis of the isotherms, AFM and BAM images of their mixtures at various molar ratios can give valuable information on the design of microbubble shell structure.

REFERENCES

Albrecht, T. and J. Hohmann (2004). "Contrast agents in sonography." Toshiba VISIONS 6: 3-25.

Anglin, T. C. and J. C. Conboy (2009). "Kinetics and thermodynamics of flip-flop in binary phospholipid membranes measured by sum-frequency vibrational spectroscopy." Biochemistry 48(43): 10220-10234.

Arnold, A., I. Cloutier, A. M. Ritcey and M. Auger (2005). "Temperature and pressure dependent growth and morphology of DMPC/DSPC domains studied by Brewster angle microscopy." Chemistry and physics of lipids 133(2): 165-179.

Baekmark, T. R., G. Elender, D. D. Lasic and E. Sackmann (1995). "Conformational transitions of mixed monolayers of phospholipids and polyethylene oxide lipopolymers and interaction forces with solid surfaces." Langmuir 11(10): 3975-3987.

Baekmark, T. R., T. Wiesenthal, P. Kuhn, A. Albersdörfer, O. Nuyken and R. Merkel (1999). "A systematic infrared reflection-absorption spectroscopy and film balance study of the phase behavior of lipopolymer monolayers at the air-water interface." Langmuir 15(10): 3616-3626.

Bianco-Peled, H., Y. Dori, J. Schneider, L. P. Sung, S. Satija and M. Tirrell (2001). "Structural study of langmuir monolayers containing lipidated poly (ethylene glycol) and peptides." Langmuir 17(22): 6931-6937.

Bjerknes, K., J. Braenden, J. Braenden, R. Skurtveit, G. Smistad and I. Agerkvist (2001). "Air-filled polymeric microcapsules from emulsions containing different organic phases." Journal of microencapsulation 18(2): 159-171.

Borden, M. A., J. A. Feshitan, C. C. Chen and J. J. Kwan (2009). "Microbubble size isolation by differential centrifugation." Journal of Colloid and Interface Science 329(2): 316-324.

Borden, M. A., D. E. Kruse, C. F. Caskey, S. Zhao, P. A. Dayton and K. W. Ferrara (2005). "Influence of lipid shell physicochemical properties on ultrasound-induced microbubble destruction." Ultrasonics, Ferroelectrics and Frequency Control, IEEE Transactions on 52(11): 1992-2002.

Borden, M. A. and M. L. Longo (2002). "Dissolution behavior of lipid monolayer-coated, air-filled microbubbles: Effect of lipid hydrophobic chain length." Langmuir 18(24): 9225-9233.

Borden, M. A. and M. L. Longo (2004). "Oxygen permeability of fully condensed lipid monolayers." The Journal of Physical Chemistry B 108(19): 6009-6016.

Borden, M. A., G. V. Martinez, J. Ricker, N. Tsvetkova, M. Longo, R. J. Gillies, P. A. Dayton and K. W. Ferrara (2006). "Lateral phase separation in lipid-coated microbubbles." Langmuir 22(9): 4291-4297.

Borden, M. A., G. Pu, G. J. Runner and M. L. Longo (2004). "Surface phase behavior and microstructure of lipid/PEG-emulsifier monolayer-coated microbubbles." Colloids and Surfaces B: Biointerfaces 35(3-4): 209-223.

Borden, M. A., S. Qin and K. W. Ferrara (2010). "Ultrasound contrast agents." Molecular imaging (ed. Weissleder R.): 425-444.

Bos, M. A. and T. Nylander (1996). "Interaction between β-lactoglobulin and phospholipids at the air/water interface." Langmuir 12(11): 2791-2797.

Brandal, Ø., T. Viitala and P. J. Sjöblom (2007). "Compression isotherms and morphological characteristics of pure and mixed langmuir monolayers of C80 isoprenoid tetraacids and a C18 monoacid." Journal of dispersion science and technology 28(1): 95-106.

Cambrea, L. R., F. Haque, J. L. Schieler, J. C. Rochet and J. S. Hovis (2007). "Effect of ions on the organization of phosphatidylcholine/phosphatidic acid bilayers." Biophysical journal 93(5): 1630-1638.

Cannan, S., J. Zhang, F. Grunfeld and P. R. Unwin (2004). "Scanning electrochemical microscopy (SECM) studies of oxygen transfer across phospholipid monolayers under surface pressure control: comparison of monolayers at air/water and oil/water interfaces." Langmuir 20(3): 701-707.

Cavalieri, F., M. Ashokkumar, F. Grieser and F. Caruso (2008). "Ultrasonic synthesis of stable, functional lysozyme microbubbles." Langmuir 24(18): 10078-10083.

Chatterji, D. and P. Rajdev (2008). "Macromolecular recognition at the air—water interface: application of Langmuir—Blodgett." Current Science 95(9): l0.

Chlon, C., C. Guédon, B. Verhaagen, W. T. Shi, C. S. Hall, J. Lub and M. R. Böhmer (2009). "Effect of molecular weight, crystallinity, and hydrophobicity on the acoustic activation of polymer-shelled ultrasound contrast agents." Biomacromolecules 10(5): 1025-1031.

Chou, T. H. and I. Chu (2002). "Behavior of DSPC/DSPE-PEG2000 mixed monolayers at the air/water interface." Colloids and Surfaces A: Physicochemical and Engineering Aspects 211(2-3): 267-274.

Chou, T. H. and I. Chu (2003). "Thermodynamic characteristics of DSPC/DSPE-PEG2000 mixed monolayers on the water subphase at different temperatures." Colloids and Surfaces B: Biointerfaces 27(4): 333-344.

Connell, S. D. and D. A. Smith (2006). "The atomic force microscope as a tool for studying phase separation in lipid membranes (Review)." Molecular membrane biology 23(1): 17-28.

Cox, D. J. and J. L. Thomas (2010). "Ultrasound-induced dissolution of lipid-coated and uncoated gas bubbles." Langmuir.

Cui, W., J. Bei, S. Wang, G. Zhi, Y. Zhao, X. Zhou, H. Zhang and Y. Xu (2005). "Preparation and evaluation of poly (L-lactide-co-glycolide)(PLGA) microbubbles as a contrast agent for myocardial contrast echocardiography." Journal of Biomedical Materials Research Part B: Applied Biomaterials 73(1): 171-178.

De Jong, N., L. Hoff, T. Skotland and N. Bom (1992). "Absorption and scatter of encapsulated gas filled microspheres: theoretical considerations and some measurements." Ultrasonics 30(2): 95-103.

Degen, P., H. Rehage, F. G. Klärner and J. Polkowska (2005). "Characterization of Langmuir-monolayers of molecular clips by means of Brewster-angle-microscopy." Colloid & Polymer Science 284(1): 44-50.

Deleu, M., K. Nott, R. Brasseur, P. Jacques, P. Thonart and Y. F. Dufrêne (2001). "Imaging mixed lipid monolayers by dynamic atomic force microscopy." Biochimica et Biophysica Acta (BBA)-Biomembranes 1513(1): 55-62.

Deleu, M., M. Paquot, P. Jacques, P. Thonart, Y. Adriaensen and Y. F. Dufrêne (1999). "Nanometer scale organization of mixed surfactin/phosphatidylcholine monolayers." Biophysical journal 77(4): 2304-2310.

Dickey, A. and R. Faller (2008). "Examining the contributions of lipid shape and headgroup charge on bilayer behavior." Biophysical journal 95(6): 2636-2646.

Dijkmans, P., L. Juffermans, R. Musters, A. Van Wamel, F. Ten Cate, W. Van Gilst, C. Visser, N. De Jong and O. Kamp (2004). "Microbubbles and ultrasound: from diagnosis to therapy." European Journal of Echocardiography 5(4): 245-246.

Doménech, Ò., J. Torrent-Burgues, S. Merino, F. Sanz, M. T. Montero and J. Hernández-Borrell (2005). "Surface thermodynamics study of monolayers formed with heteroacid phospholipids of biological interest." Colloids and Surfaces B: Biointerfaces 41(4): 233-238.

Dori, Y., H. Bianco-Peled, S. K. Satija, G. B. Fields, J. B. McCarthy and M. Tirrell (2000). "Ligand accessibility as means to control cell response to bioactive bilayer membranes." Journal of biomedical materials research 50(1): 75-81.

Dressaire, E., R. Bee, D. C. Bell, A. Lips and H. A. Stone (2008). "Interfacial polygonal nanopatterning of stable microbubbles." Science 320(5880): 1198-1201.

Dufrêne, Y. F., W. R. Barger, J. B. D. Green and G. U. Lee (1997). "Nanometer-scale surface properties of mixed phospholipid monolayers and bilayers." Langmuir 13(18): 4779-4784.

Estrela-Lopis, I., G. Brezesinski and H. Möhwald (2004). "Miscibility of DPPC and DPPA in monolayers at the air/water interface." Chemistry and physics of lipids 131(1): 71-80.

Feigenbaum, H., J. M. Stone, D. O. N. A. Lee, W. K. Nasser and S. Chang (1970). "Identification of ultrasound echoes from the left ventricle by use of intracardiac injections of indocyanine green." Circulation 41(4): 615-621.

Fuller, G. G. (2003). "Rheology of mobile interfaces." Rheology Reviews: 77-124.

Gaines, G. L. (1966). Insoluble Monolayers at Liquid/gas Interface. New York, Wiley-Interscience.

Garidel, P. and A. Blume (1998). "Miscibility of phospholipids with identical headgroups and acyl chain lengths differing by two methylene units: effects of headgroup structure and headgroup charge." Biochimica et Biophysica Acta (BBA)-Biomembranes 1371(1): 83-95.

Garidel, P. and A. Blume (2000). "Miscibility of phosphatidylethanolamine-phosphatidylglycerol mixtures as a function of pH and acyl chain length." European Biophysics Journal 28(8): 629-638.

Garidel, P., C. Johann and A. Blume (1997). "Nonideal mixing and phase separation in phosphatidylcholine-phosphatidic acid mixtures as a function of acyl chain length and pH." Biophysical journal 72(5): 2196-2210.

Greenough, K. P. and G. Blanchard (2009). "Lipid headgroups mediate organization and dynamics in bilayers." Spectrochimica Acta Part A: Molecular and Biomolecular Spectroscopy 71(5): 2050-2056.

Hąc-Wydro, K., M. Flasiński, P. Wydro and P. Dynarowicz-Łątka (2012). "Towards the understanding of the behavior of single-chained ether phospholipids in model biomembranes. Interactions with phosphatidylethanolamines in Langmuir monolayers." Colloids and Surfaces B: Biointerfaces.

Hac-Wydro, K., J. Kapusta, A. Jagoda, P. Wydro and P. Dynarowicz-Latka (2007). "The influence of phospholipid structure on the interactions with nystatin, a polyene antifungal antibiotic:: A Langmuir monolayer study." Chemistry and physics of lipids 150(2): 125-135.

Hénon, S. and J. Meunier (1991). "Microscope at the Brewster angle: Direct observation of first-order phase transitions in monolayers." Review of scientific instruments 62(4): 936-939.

Hernández, M. R. S. (2010). Spectroscopic Studies of Atmospheric Relevant Air-Aqueous Interfaces, The Ohio State University.

Hernot, S. and A. L. Klibanov (2008). "Microbubbles in ultrasound-triggered drug and gene delivery." Advanced drug delivery reviews 60(10): 1153-1166.

Hettiarachchi, K., E. Talu, M. L. Longo, P. A. Dayton and A. P. Lee (2007). "On-chip generation of microbubbles as a practical technology for manufacturing contrast agents for ultrasonic imaging." Lab Chip 7(4): 463-468.

Hoenig, D. and D. Moebius (1991). "Direct visualization of monolayers at the air-water interface by Brewster angle microscopy." The Journal of Physical Chemistry 95(12): 4590-4592.

Hollinshead, C. M., R. D. Harvey, D. J. Barlow, J. R. P. Webster, A. V. Hughes, A. Weston and M. J. Lawrence (2009). "Effects of Surface Pressure on the Structure of Distearoylphosphatidylcholine Monolayers Formed at the Air/Water Interface†." Langmuir 25(7): 4070-4077.

Inoue, T. and Y. Nibu (1999). "Phase behavior of hydrated lipid bilayer composed of binary mixture of phospholipids with different head groups." Chemistry and physics of lipids 100(1-2): 139-150.

Jebrail, M., R. Schmidt, C. DeWolf and V. Tsoukanova (2008). "Effect of aliphatic chain length on stability of poly (ethylene glycol)-grafted phospholipid monolayers at the air/water interface." Colloids and Surfaces A: Physicochemical and Engineering Aspects 321(1): 168-174.

Keller, S. L. (2003). "Miscibility transitions and lateral compressibility in liquid phases of lipid monolayers." Langmuir 19(5): 1451-1456.

Kim, K., C. Kim and Y. Byun (2000). "Preparation of a PEG-grafted phospholipid Langmuir-Blodgett monolayer for blood-compatible material." Journal of biomedical materials research 52(4): 836-840.

Kim, K., C. Kim and Y. Byun (2004). "Biostability and biocompatibility of a surface-grafted phospholipid monolayer on a solid substrate." Biomaterials 25(1): 33-41.

Klibanov, A. L. (1999). "Targeted delivery of gas-filled microspheres, contrast agents for ultrasound imaging." Advanced drug delivery reviews 37(1-3): 139-157.

Korpanty, G., P. A. Grayburn, R. V. Shohet and R. A. Brekken (2005). "Targeting vascular endothelium with avidin microbubbles." Ultrasound in medicine & biology 31(9): 1279-1283.

Kubo, I., S. Adachi, H. Maeda and A. Seki (2001). "Phosphatidylcholine monolayers observed with Brewster angle microscopy and π-A isotherms." Thin Solid Films 393(1): 80-85.

Kyun Kim, H., K. Kim and Y. Byun (2005). "Preparation of a chemically anchored phospholipid monolayer on an acrylated polymer substrate." Biomaterials 26(17): 3435-3444.

Lee, Y. L., J. Y. Lin and C. H. Chang (2006). "Thermodynamic characteristics and Langmuir–Blodgett deposition behavior of mixed DPPA/DPPC monolayers at air/liquid interfaces." Journal of colloid and interface science 296(2): 647-654.

Lentacker, I., S. C. De Smedt and N. N. Sanders (2009). "Drug loaded microbubble design for ultrasound triggered delivery." Soft Matter 5(11): 2161-2170.

Lipp, M., K. Lee, D. Takamoto, J. Zasadzinski and A. Waring (1998). "Coexistence of buckled and flat monolayers." Physical review letters 81(8): 1650-1653.

Liu, Y., H. Miyoshi and M. Nakamura (2006). "Encapsulated ultrasound microbubbles: therapeutic application in drug/gene delivery." Journal of controlled release 114(1): 89-99.

Lozano, M. M. and M. L. Longo (2009). "Complex formation and other phase transformations mapped in saturated phosphatidylcholine/DSPE-PEG2000 monolayers." Soft Matter 5(9): 1822-1834.

Lozano, M. M. and M. L. Longo (2009). "Microbubbles coated with disaturated lipids and DSPE-PEG2000: phase behavior, collapse transitions, and permeability." Langmuir 25(6): 3705-3712.

Lucero, A., M. Rodríguez Nino, A. Gunning, V. Morris, P. Wilde and J. Rodríguez Patino (2008). "Effect of hydrocarbon chain and pH on structural and topographical characteristics of phospholipid monolayers." The Journal of Physical Chemistry B 112(25): 7651-7661.

Luna, D., E. Falcão, S. Melo and C. Andrade (2011). "Interfacial properties of a novel pyrimidine derivative and poly (ethylene glycol)-grafted phospholipid floating monolayers." Colloids and Surfaces A: Physicochemical and Engineering Aspects 373(1): 22-28.

Majewski, J., T. Kuhl, M. Gerstenberg, J. Israelachvili and G. Smith (1997). "Structure of phospholipid monolayers containing poly (ethylene glycol) lipids at the air-water interface." The Journal of Physical Chemistry B 101(16): 3122-3129.

Maniti, O., M. Cheniour, O. Marcillat, C. Vial and T. Granjon (2009). "Morphology modifications in negatively charged lipid monolayers upon mitochondrial creatine kinase binding." Molecular membrane biology 26(3): 171-185.

Mansour, H. M. and G. Zografi (2007). "Relationships between equilibrium spreading pressure and phase equilibria of phospholipid bilayers and monolayers at the air-water interface." Langmuir 23(7): 3809-3819.

Mathe, G., C. Gege, K. R. Neumaier, R. R. Schmidt and E. Sackmann (2000). "Equilibrium swelling behavior of solid supported poly (ethylene glycol) lipid monolayers. Effects of short chain lengths." Langmuir 16(8): 3835-3845.

Meunier, J. (2000). "Why a Brewster angle microscope?" Colloids and Surfaces A: Physicochemical and Engineering Aspects 171(1-3): 33-40.

Minones, J., J. Rodríguez Patino, O. Conde, C. Carrera and R. Seoane (2002). "The effect of polar groups on structural characteristics of phospholipid monolayers spread at the air-water interface." Colloids and Surfaces A: Physicochemical and Engineering Aspects 203(1-3): 273-286.

Moghaddam, B., M. H. Ali, J. Wilkhu, D. J. Kirby, A. R. Mohammed, Q. Zheng and Y. Perrie (2011). "The application of monolayer studies in the understanding of liposomal formulations." International journal of pharmaceutics.

Mulvana, H., E. Stride, J. V. Hajnal and R. J. Eckersley (2010). "Temperature dependent behavior of ultrasound contrast agents." Ultrasound in medicine & biology 36(6): 925-934.

Nakahara, H., M. P. Krafft, A. Shibata and O. Shibata (2011). "Interaction of a partially fluorinated alcohol (F8H11OH) with biomembrane constituents in two-component monolayers." Soft Matter 7(16): 7325-7333.

Nakamura, S., H. Nakahara, M. P. Krafft and O. Shibata (2007). "Two-component Langmuir monolayers of single-chain partially fluorinated amphiphiles with dipalmitoylphosphatidylcholine (DPPC)." Langmuir 23(25): 12634-12644.

Naumann, C., C. Brooks, G. Fuller, W. Knoll and C. Frank (1999). "Viscoelastic properties of lipopolymers at the air-water interface: a combined interfacial stress rheometer and film balance study." Langmuir 15(22): 7752-7761.

Oguchi, T., K. Sakai, H. Sakai and M. Abe (2010). "AFM surface morphology and friction force studies of microscale domain structures of binary phospholipids." Colloids and Surfaces B: Biointerfaces 79(1): 205-209.

Pancholi, K., U. Farook, R. Moaleji, E. Stride and M. Edirisinghe (2008). "Novel methods for preparing phospholipid coated microbubbles." European Biophysics Journal 37(4): 515-520.

Pavinatto, F. J., L. Caseli, A. Pavinatto, D. S. dos Santos Jr, T. M. Nobre, M. E. D. Zaniquelli, H. S. Silva, P. B. Miranda and O. N. de Oliveira Jr (2007). "Probing chitosan and phospholipid interactions using Langmuir and Langmuir-Blodgett films as cell membrane models." Langmuir 23(14): 7666-7671.

Petty, M. (1996). Langmuir-Blodgett Films: An introduction, Cambridge University Press.

Pu, G., M. A. Borden and M. L. Longo (2006). "Collapse and shedding transitions in binary lipid monolayers coating microbubbles." Langmuir 22(7): 2993-2999.

Pu, G., M. L. Longo and M. A. Borden (2005). "Effect of microstructure on molecular oxygen permeation through condensed phospholipid monolayers." Journal of the American Chemical Society 127(18): 6524-6525.

Quiroga, C., L. Monzón and L. Yudi (2011). "Voltammetric study and surface pressure isotherms describing Flunitrazepam incorporation into a distearoylphosphatidic acid film adsorbed at air/water and water/1, 2-dichloroethane interfaces." Electrochimica Acta.

Risovic, D., S. Frka and Z. Kozarac (2011). "Application of Brewster angle microscopy and fractal analysis in investigations of compressibility of Langmuir monolayers." Journal of Chemical Physics 134(2): 24701.

Saad, S. M. I., Z. Policova, E. J. Acosta, M. L. Hair and A. W. Neumann (2009). "Mixed DPPC/DPPG Monolayers at Very High Film Compression." Langmuir 25(18): 10907-10912.

Sánchez-González, J., M. Cabrerizo-Vilchez and M. Gálvez-Ruiz (1998). "Chain dependence in phospholipid interactions: A thermodynamic study of mixed monolayers." Colloid & Polymer Science 276(3): 239-246.

Sanchez, J. and A. Badia (2008). "Spatial variation in the molecular tilt orientational order within the solid domains of phase-separated, mixed dialkylphosphatidylcholine monolayers." Chemistry and physics of lipids 152(1): 24-37.

Schneider, J., Y. F. Dufrêne, W. R. Barger Jr and G. U. Lee (2000). "Atomic force microscope image contrast mechanisms on supported lipid bilayers." Biophysical journal 79(2): 1107-1118.

Schutt, E. G., D. H. Klein, R. M. Mattrey and J. G. Riess (2003). "Injectable microbubbles as contrast agents for diagnostic ultrasound imaging: the key role of perfluorochemicals." Angewandte Chemie International Edition 42(28): 3218-3235.

Shen, Y., R. L. Powell and M. L. Longo (2008). "Interfacial and stability study of microbubbles coated with a monostearin/monopalmitin-rich food emulsifier and PEG40 stearate." Journal of colloid and interface science 321(1): 186-194.

Singhal, S., C. Moser and M. Wheatley (1993). "Surfactant-stabilized microbubbles as ultrasound contrast agents: stability study of Span 60 and Tween 80 mixtures using a Langmuir trough." Langmuir 9(9): 2426-2429.

Sirsi, S. and M. Borden (2009). "Microbubble compositions, properties and biomedical applications." Bubble science engineering and technology 1(1-2): 3.

Stepniewski, M., M. Pasenkiewicz-Gierula, T. Róg, R. Danne, A. Orlowski, M. Karttunen, A. Urtti, M. Yliperttula, E. Vuorimaa and A. Bunker (2011). "Study of PEGylated Lipid Layers as a Model for PEGylated Liposome Surfaces: Molecular Dynamics Simulation and Langmuir Monolayer Studies." Langmuir.

Stride, E. and M. Edirisinghe (2008). "Novel microbubble preparation technologies." Soft Matter 4(12): 2350-2359.

Swanson, E. J., V. Mohan, J. Kheir and M. A. Borden (2010). "Phospholipid-Stabilized Microbubble Foam for Injectable Oxygen Delivery." Langmuir.

Takamoto, D., M. Lipp, A. Von Nahmen, K. Y. C. Lee, A. Waring and J. Zasadzinski (2001). "Interaction of lung surfactant proteins with anionic phospholipids." Biophysical journal 81(1): 153-169.

Talu, E., M. M. Lozano, R. L. Powell, P. A. Dayton and M. L. Longo (2006). "Long-term stability by lipid coating monodisperse microbubbles formed by a flow-focusing device." Langmuir 22(23): 9487-9490.

Tanwir, K. and V. Tsoukanova (2008). "Lateral distribution of a poly (ethylene glycol)-grafted phospholipid in phosphocholine monolayers studied by epifluorescence microscopy." Langmuir 24(24): 14078-14087.

Thurmond, R. L., S. W. Dodd and M. F. Brown (1991). "Molecular areas of phospholipids as determined by 2H NMR spectroscopy. Comparison of phosphatidylethanolamines and phosphatidylcholines." Biophysical journal 59(1): 108-113.

Tinkov, S., R. Bekeredjian, G. Winter and C. Coester (2009). "Microbubbles as ultrasound triggered drug carriers." Journal of pharmaceutical sciences 98(6): 1935-1961.

Tinkov, S., C. Coester, R. Bekeredjian and G. Winter (2010). "Drug Targeting by Diagnostic Ultrasound Contrast."

Tsukanova, V. and C. Salesse (2003). "High-pressure transition of a poly (ethylene glycol)-grafted phospholipid monolayer at the air/water interface." Macromolecules 36(19): 7227-7235.

Tsukanova, V. and C. Salesse (2004). "On the nature of conformational transition in poly (ethylene glycol) chains grafted onto phospholipid monolayers." The Journal of Physical Chemistry B 108(30): 10754-10764.

Unger, E. C., T. Porter, W. Culp, R. Labell, T. Matsunaga and R. Zutshi (2004). "Therapeutic applications of lipid-coated microbubbles." Advanced drug delivery reviews 56(9): 1291-1314.

Wang, W., C. C. Moser and M. A. Wheatley (1996). "Langmuir trough study of surfactant mixtures used in the production of a new ultrasound contrast agent consisting of stabilized microbubbles." The Journal of Physical Chemistry 100(32): 13815-13821.

Watry, M. R., T. L. Tarbuck and G. L. Richmond (2003). "Vibrational sum-frequency studies of a series of phospholipid monolayers and the associated water structure at the vapor/water interface." The Journal of Physical Chemistry B 107(2): 512-518.

Wheatley, M. A., B. Schrope and P. Shen (1990). "Contrast agents for diagnostic ultrasound: development and evaluation of polymer-coated microbubbles." Biomaterials 11(9): 713-717.

Winterhalter, M., H. Bürner, S. Marzinka, R. Benz and J. Kasianowicz (1995). "Interaction of poly (ethylene-glycols) with air-water interfaces and lipid monolayers: investigations on surface pressure and surface potential." Biophysical journal 69(4): 1372-1381.

Wydro, P., M. Flasiński and M. Broniatowski (2012). "Molecular organization of bacterial membranes lipids in mixed systems–A comprehensive monolayer study combined with Grazing Incidence X-ray Diffraction and Brewster Angle Microscopy experiments." Biochimica et Biophysica Acta (BBA)-Biomembranes.

Wydro, P., S. Knapczyk and M. Łapczyńska (2011). "Variations in the Condensing Effect of Cholesterol on Saturated versus Unsaturated Phosphatidylcholines at Low and High Sterol Concentration." Langmuir.

Wydro, P. and K. Witkowska (2009). "The interactions between phosphatidylglycerol and phosphatidylethanolamines in model bacterial membranes:: The effect of the acyl chain length and saturation." Colloids and Surfaces B: Biointerfaces 72(1): 32-39.

Xing, Z., H. Ke, J. Wang, B. Zhao, X. Yue, Z. Dai and J. Liu (2010). "Novel ultrasound contrast agent based on microbubbles generated from surfactant mixtures of Span 60 and polyoxyethylene 40 stearate." Acta Biomaterialia 6(9): 3542-3549.

Xu, Z., N. B. Holland and R. E. Marchant (2001). "Conformations of short-chain poly (ethylene oxide) lipopolymers at the air-water interface: a combined film balance and surface tension study." Langmuir 17(2): 377-383.

Yoon, J. H., K. S. Lee, J. E. Yang, M. S. Won and Y. B. Shim (2010). "Electron transfer kinetics and morphology of cytochrome< i> c</i> at the biomimetic phospholipid layers." Journal of Electroanalytical Chemistry 644(1): 36-43.

Zasadzinski, J., R. Viswanathan, L. Madsen, J. Garnaes and D. Schwartz (1994). "Langmuir-Blodgett films." Science 263(5154): 1726.